

The Reality of Subcritical Neutron Measurements and How They Can Differ with What Your Favorite Neutron Physics Code Is Telling You

William L Myers

*Advanced Nuclear Technology Group (N-2), Los Alamos National Laboratory
PO Box 1663, MS B228, Los Alamos, New Mexico 87545 USA.*

bmyers@lanl.gov

INTRODUCTION

The Nuclear Criticality Safety Program (NCSP) has supported the execution of benchmark quality experiments (measurements of critical and subcritical neutron chain reacting systems) and the execution of compilation and modeling of these same experiments. One application of this effort is to evaluate, by comparison with experimental results, the performance of neutron physics codes and the usage of associated input data. The products of this effort are well documented in the Nuclear Energy Agency (NEA) Nuclear Science Committee's International Handbook of Evaluated Criticality Safety Benchmark Experiments which is used by criticality safety professionals to help evaluate criticality safety related risks or biases associated with the computational analysis tools they use to support their customers.

Recently, the utility of supporting benchmark subcritical measurements as part of this evaluation process has come into question because of differences observed between experimentally derived results and computational results. The purpose of this summary is to present to the NCSP community in a quick, concise, and non-all inclusive manner the process for performing and analyzing data taken on a subcritical neutron chain reacting system and how the inferred results can differ from what is calculated using your favorite neutron physics code.

SUPERCRITICAL VERSUS CRITICAL VERSUS SUBCRITICAL

The quantity (or state) $K_{\text{eff}} = 1.0$, a standard nuclear engineering definition for delayed critical, can be directly determined by experiment by observing how the measured neutron population behaves as a function of time. To determine the K_{eff} value for a system that is either supercritical or subcritical requires the measurement of a set of experimental observables and the use of an inference model to estimate the quantity (or state) K_{eff} (i.e. a measure of the reactor period and use of the inhour equation for the supercritical case or some statistical measure of the neutron count rate for a source driven subcritical system and use of your favorite

subcritical analysis technique). Note: most of the data in the International Handbook of Evaluated Criticality Safety Benchmark Experiments are evaluated critical experiments.

INFERENCE MODELS

The inference model used to relate experimentally measured observables to K_{eff} in a subcritical neutron chain reacting system most likely plays the major contributing role in causing differences from computational results. One needs to evaluate all the parameters that can affect the measurement and decide how much of the true physics to incorporate into the inference model. In general, the following steps¹ represent one method to systematically construct an inference model to estimate K_{eff} for a subcritical neutron chain reacting system:

- 1. By choosing what to include in the model for the neutron chain reacting system and treating the evolution process as being Markovian, the probability balance equation will be derived.**
- 2. Using the generating function technique, the probability balance equation will be transformed into a first-order partial differential equation in the generating function.**
- 3. Equations for moments of the generating function can be found by performing various differentiations on the original first-order partial differential equation derived in step two.**
- 4. The desired parameters are then extracted from solutions of the generating function and its moments.**

When executing Step 1, one incorporates as much of the physics of the process as possible (including effects from detectors, the environment, etc.) and compiles a list of assumptions about the process and model. The following is a partial list of assumptions² commonly used

for constructing an inference model for analyzing subcritical neutron measurements:

- **Space-independent model**
- **Neutrons are treated as classical particles.**
- **There are no neutron-neutron interactions.**
- **One-Energy Group Model.**
- **A minimum of zero and a maximum of 6 prompt neutrons are born per fission**
- **Delayed neutrons are ignored.**
- **All neutrons are detected with equal probability.**

Terms in the probability balance equation can contain constants or functions that are related to physical data. For simplified inference models, processing all the available data to get it in a compatible form to use in the inference model can cause differences too. Sometimes multiple inference models (or multiple transformations) are needed to get an estimate of K_{eff} (i.e. data and model infer subcritical neutron leakage multiplication factor which needs to be converted to total subcritical neutron multiplication factor to estimate K_{eff}).



Fig. 1. A Subcritical Neutron Measurement Being Performed on the Los Alamos Thor Core.

EXPERIMENTAL SUBCRITICAL NEUTRON MEASUREMENTS

The "irony" of using critical benchmarks to validate codes and input data for use to ensure processes and configurations remain subcritical within established margins has never really been emphasized or debated by the NCSP community. The wording most often used to explain differences is "the system is not behaving in normal-mode", hence the comparison differences.

Fig. 1 shows a subcritical neutron measurement being performed on the Los Alamos Thor Core. A subcritical

measurement can directly provide data to the criticality safety professional to validate that a configuration or process is subcritical (assuming it is representative of the process they are analyzing). For the investment, multiple subcritical data points (k_{eff} values measured at different intervals (K_{eff} states) up to the most reactive configuration) can be obtained and used as separate but similar benchmarks.

In the best case scenario, one can report all the geometric and physical property information about the measurement with the caveat that the different pieces of information important for putting together a computational model can only be reported to a finite number of decimal places. For a measurement, one needs to account for background noise or other interferences that can increase the error bars on the measured observables one collects. The effects of the environment or correction of background interferences are not always easily accounted for when reporting results. Sometimes operational characteristics or variances in the operational characteristics of the data collection equipment used to perform the measurement can add some uncertainties to the final reported results (i.e. detector dead-time corrections, etc.).

COMPUTATIONAL MODELLING OF A SUBCRITICAL OBJECT

It is fairly straight forward to construct a computational model of a subcritical object and perform a K_{eff} calculation. The only major decision involves how many decimal places to use for data input parameters and how much of the external environment (items that through some sort of interaction with the subcritical object of concern may affect the computed K_{eff} value) to include as part of the model. One can easily perform a parameter sensitivity study to investigate what affects the computational results by removing items or by varying the magnitudes of input data. These results would be considered more qualitative than quantitative until directly compared to experimentally measured data. As noted above, only the delayed critical configurations ($K_{\text{eff}} = 1.0$) can be directly compared. For supercritical or subcritical configurations, an inference model is needed to estimate K_{eff} ; hence an alternative process for better utilizing subcritical benchmark data is presented below.

CURRENT RECOMMENDATION FOR UTILIZING SUBCRITICAL BENCHMARK NEUTRON MEASUREMENTS

From the discussion above, the use of the inference model for processing the experimental data to estimate K_{eff} is most likely the main cause for differences in experimentally estimated K_{eff} and directly computed K_{eff} . To eliminate this bias, we recommend the following:

- A. Construct a computational model of the experimental setup that includes the subcritical object being measured, the detection equipment that is used to collect data, and as much of the room or external environment that is practical.
 - B. The neutron physics code that performs the computations must be enabled to calculate the time-dependent observables that are being collected by the experimental detection system.
 - C. The outcome of a successful execution of the previous step would be the generation of a time-dependent list-mode data set that can be analyzed by performing the same corrections and by using the same inference model to estimate K_{eff} as was performed on the real experimental data. Both the measured and computed data sets were analyzed similarly, hence estimating K_{eff} similarly (essentially exposing both data sets to the same biases introduced by the inference model).
 - D. Differences in “estimated” K_{eff} from both cases can be used to debate about deficiencies in the input model or data and the reported experimental information used to construct the computational model (normal benchmark community arguments).
 - E. If the inferred K_{eff} is consistent between the computed and measured cases, then the bias introduced by the inference model can be quantified and studied. This may lead to a determination of a better inference model.
3. G. P. Estes and C.A. Goulding, “Subcritical Multiplication Determination Studies”, Proceedings of the 5th International Conference on Nuclear Criticality Safety, Albuquerque, New Mexico, September 17–21, Volume 2, Chapter 11, pp. 146-151, (1995).
 4. J.T. Mihalczko and T.E. Valentine, “Bias in Calculated K_{eff} From Subcritical Measurements By The ^{252}Cf -Source-Driven Noise Analysis Method,” Proceedings of the 5th International Conference on Nuclear Criticality Safety, Albuquerque, New Mexico, September 17–21, Volume 2, Chapter 13, pp. 42-50 (1995).
 5. W. L. Myers, C. A. Goulding, C. L. Hollas, and C. E. Moss, “Photon and Neutron Active Interrogation of Highly Enriched Uranium,” Proc. Int. Conf. on Nuclear Data for Science and Technology, ND2004, Santa Fe, New Mexico, USA, Sept 26-Oct 1, pp. 1688-1692 (2004).

The ideas presented in steps A, B, and C were first put into practical use for studying subcritical neutron measurements by Estes and Goulding³ in their research efforts at Los Alamos National Laboratory and by Mihalczko and Valentine⁴ at Oak Ridge National Laboratory. These ideas again were reiterated as a practical way for utilizing subcritical neutron measurements for use as a benchmarking tool for codes and data by Myers, Goulding, Hollas, and Moss⁵.

REFERENCES

1. W. L. MYERS, "A Stochastic, Four Energy Group Model of a Nuclear Assembly", PhD Thesis, University of Illinois (1995)
2. M.M.R. WILLIAMS, *Random Processes in Nuclear Reactors*, Pergamon Press, Ltd., Cambridge (1974)

The Reality of Subcritical Neutron Measurements and How They Can Differ with What Your Favorite Neutron Physics Code Is Telling You

William L Myers
Los Alamos National Laboratory
Advanced Nuclear Technology Group (N-2)

SUPERCritical VS. CRITICAL VS. SUBCRITICAL

CRITICAL $K_{eff} = 1.0$

State is Defined as *Delayed Critical* and Can Be Directly Observed During Measurement

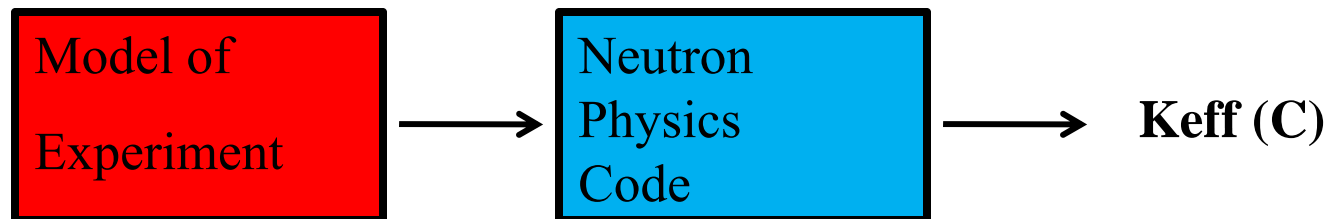
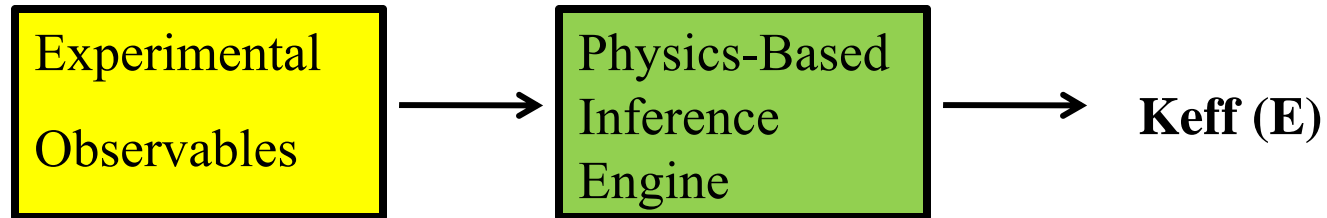
SUPERCritical $K_{eff} > 1.0$

State Can Be Quantitatively Determined By Using an Inference Model With Measurement Data such as: Inhour Formula with Measured Reactor Period data

SUBCRITICAL $K_{eff} < 1.0$

State Can Be Quantitatively Determined By Using Inference Model With Measurement Data such as: Time Dependent Statistical analysis of Neutron Counts with Your Favorite Subcritical Neutron Analysis Technique

Information Transformation



Experimental Realities

Variances in experimental observables caused by background interferences, environmental effects, and operational settings of data collection equipment can affect results

Results obtained from processing data thru the inference engine is affected by how much real physics is used to construct the inference model

Can only report physical and geometric information to a finite number of decimal points

Inference Engine (“Under the Hood” Example)

Hage-Cifarelli Formalism of Feynman’s Variance-To-Mean Technique

$$R2/R1 = (\varepsilon) * [M_L * \{ (M_L - 1) * v_{I2} / (v_{I1} - 1) \}]$$

$$R3/R1 = (\varepsilon^2) * M_L^2 * \{ (M_L - 1) / (v_{I1} - 1) * [v_{I3} + 2 * (M_L - 1) * v_{I2}^2 / (v_{I1} - 1)] \}$$

$$M_T = (M_L * v - 1 - \alpha) / (v - 1 - \alpha) \text{ Serber’s formula}$$

Model construction assumptions: Space-independent model, One-Energy Group, delayed neutrons are ignored, all neutron detected with equal probability, etc...

Processing of physical Data for usage in the inference model can affect results

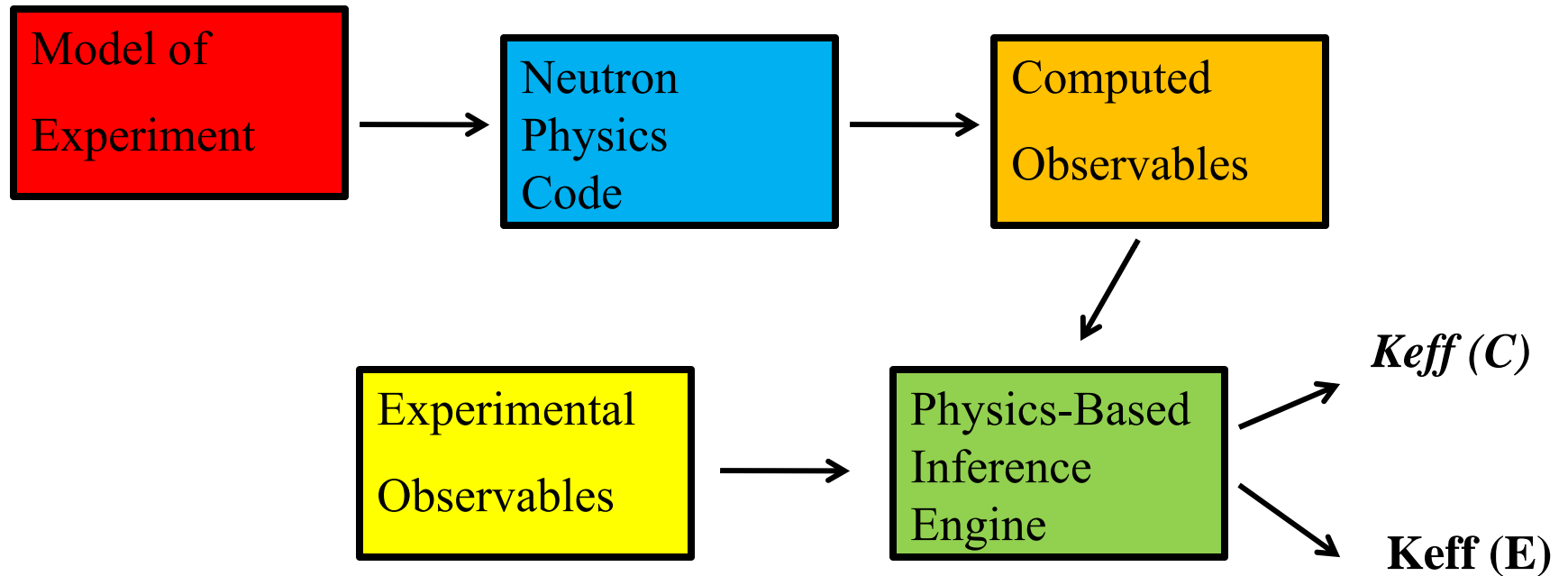
Code Realities

Difficult at times to account for background interferences and environmental effects

Code results are affected by how much real physics is used to construct the code

Processing of physical Data for usage in the neutron physics code can affect results

Best of Both Worlds



Utilization of Subcritical Benchmark Data

Multiple data points for the same Money

If the experiment is design properly, the actual data would be the first choice of the Criticality Safety Analyst to justify controls on the process being supported

Subcritical regime measurements used to directly justify subcritical controls and risk assessment

Payback on investment has been demonstrated at times to be 10 to 1

Can perform a measurement in the absence of enough material to build an assembly that can reach delayed critical

Characterization of Cf-252 Source CF-52 for use in Subcritical Measurements

J. Hutchinson, G. Arnone, S. Melton, W. Myers, A. Sood

Los Alamos National Laboratory, MS-B228, Los Alamos, New Mexico 87545

INTRODUCTION

Measurements were conducted with the ^{252}Cf source ionization chamber (SIC) provided by ORNL in 2009 (referred to as CF-52) for subcritical experiments in support of the NCSP. Measurements with the source with and without the BERP ball were conducted. Measurements with two different detector systems were used. These measurements are compared with previous data using the same measurement techniques.

DESCRIPTION OF WORK

ORNL has constructed many neutron sources contained inside ionization chambers. Placing the source inside an ionization chamber allows for the timing of the source decays to be measured, which can be utilized for several applications. The ^{252}Cf is located at a height of approximately 0.0993 inches from the bottom of the SIC cladding and is centered in the other two planes as shown in Fig. 1.

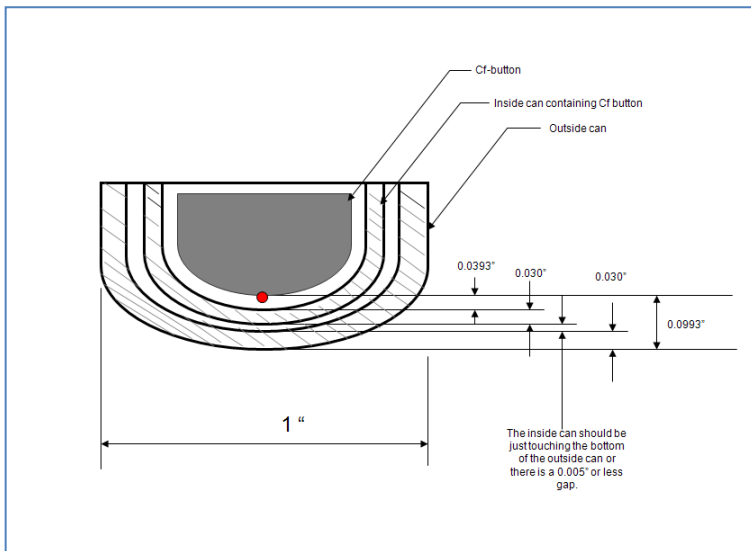


Fig. 1. ^{252}Cf source CF-52.

The ^{252}Cf source ionization chamber works by producing a pulse whenever a charged particle passes through the ionization gas. Since the ionization gas is nearly hemispherical as shown in Fig. 1, slightly more than $\frac{1}{2}$ of the decays should generally be recorded. Since nearly two fission products are born during each fission event and they generally travel 180° from each other,

slightly more than half of the spontaneous fission events should be recorded. The isotope ^{252}Cf decays with a half-life of 2.645 years and decays by alpha decay (96.91%) and spontaneous fission (3.09%)¹. Both the alpha particles and the fission fragments create a pulse in the ionization chamber. The mass of the fission fragments is much larger than that of an alpha particle, so the energy deposited by a single fission fragment is greater than that of an alpha particle. For this reason, the energy deposited is also larger for the fission fragments, which results in the voltage of the pulse produced by the fission fragments to be larger than those created by alpha decays. As a result of this, a discriminator can be used to remove the alpha decays from the signal and calculate only the spontaneous fission events.

The source CF-52 had a mass of 1.918 micro-grams on 11/20/2008 as provided by ORNL². This can be converted to $1.17\text{e}6$ spontaneous fissions per second (sf/s) using a conversion of $2.3\text{e}6$ n/s per micro-gram of ^{252}Cf and an average of 3.77 neutrons per ^{252}Cf fission^{3,4}. To discriminate against the alpha decays and count as many of the spontaneous fission events as possible, a pulse height curve is generally produced. This curve shows the number of counts as a function of the discriminator level. These curves generally have three regions, each with distinctive features. In the first region (low discriminator levels), there is a sharp decrease in counts (less alpha particles are being counted). In the middle region the counts are relatively flat (here nearly all of the fission events are being counted and few of the alpha decays are recorded). As the discriminator level increases, the last region shows a sharp decrease in counts (less of the fission products are being counted). Generally, the discriminator level which gives the smallest variation in count rate is chosen. More information regarding pulse height curves has been published previously^{3,5}. From the pulse height curve performed on 12/18/2008 as provided by ORNL², the emission rate was estimated to be $8.20\text{e}5$ sf/s. Given the emission rate on 11/20/2008, the ^{252}Cf emission rate can easily be calculated for 12/18/2008 (which has a 2.645 year half-life¹) to be $1.15\text{e}6$ sf/s. This means that around 71% of the fission events were recorded. Previous sources (CF-43 and CF-49) have generally always measured 95%-105% of the calculated strength which makes these data questionable. Implications from this will be discussed further.

The measurements performed from May to August 2010 showed that even less of the spontaneous fission events were recorded. It is currently unknown why the measured efficiency of the SIC is so low (about 48% at LANL in 2010 compared to the 71% measured by ORNL

in 2008). An electronic issue (either the SIC preamp, bias supply, discriminator, counter or in the SIC itself) is a possible explanation. It is interesting to note that for ^{252}Cf source CF-49 (which used the same SIC preamp, bias supply, discriminator, and counter) the measured emission rate was only 3%-5% lower than the calculated spontaneous fission rate as shown in Table 1.

Table 1. Measured SIC Count Rates

| CF-52 | | | CF-49 | | | | |
|-----------|----------|------------|--------|-----------|----------|------------|--------|
| Date | Measured | Calculated | % Diff | Date | Measured | Calculated | % Diff |
| 5/17/2010 | 410525 | 791998 | 48.17% | 5/22/2010 | 100071 | 103479 | 3.29% |
| 5/18/2010 | 410673 | 791430 | 48.11% | 6/22/2010 | 96862 | 101203 | 4.29% |
| 5/19/2010 | 412890 | 790863 | 47.79% | 6/23/2010 | 96076 | 101131 | 5.00% |
| 5/21/2010 | 412283 | 789729 | 47.79% | 6/24/2010 | 97560 | 101058 | 3.46% |
| 6/07/2010 | 407735 | 780154 | 47.74% | 6/30/2010 | 96620 | 100624 | 3.98% |
| 6/08/2010 | 408221 | 779595 | 47.64% | 7/01/2010 | 96478 | 100552 | 4.05% |
| 6/25/2010 | 405395 | 770144 | 47.36% | 8/02/2010 | 94547 | 98269 | 3.79% |
| 6/30/2010 | 403884 | 767386 | 47.37% | 8/03/2010 | 94507 | 98199 | 3.76% |
| 7/01/2010 | 403175 | 766835 | 47.42% | 8/05/2010 | 93718 | 98058 | 4.43% |
| 8/04/2010 | 393904 | 748355 | 47.36% | | | | |
| 8/05/2010 | 393723 | 747818 | 47.35% | | | | |

Measurements were taken for analysis using the Californium Source-Driven Analysis Method (CSDNA) for both CF-49 and CF-52 as shown in Fig. 2. For CF-49, the average percent difference between the measured and simulated (from MCNP-DSP) was 13.6%. For CF-52 this value was similar (13.4%) when the measured spontaneous fission rate ($3.94\text{e}5$ sf/s) was input into MCNP-DSP but was 38.7% different when the calculated spontaneous fission value was used ($7.48\text{e}5$ sf/s).

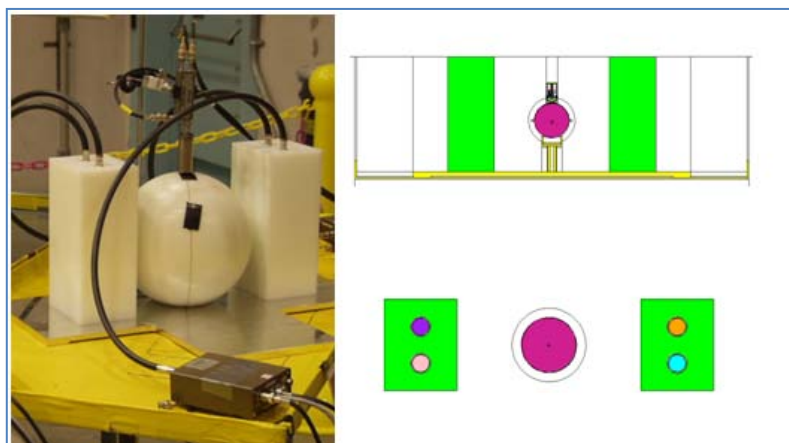


Fig. 2. CSDNA Measurements with the BERP Ball reflected by polyethylene.

Measurements were also made with several sources and detectors to attempt to calculate the detection efficiency for these detectors. The measured efficiency (measured count rate divided by the calculated emission rate) for all of the detectors used was different for CF-52 than for the other sources investigated. The average efficiency values were then used to calculate the emission

rate of CF-52 to be near $5.6\text{e}5$ n/s (as opposed to the calculated value of $7.5\text{e}5$ n/s on 8/5/2010).

CONCLUSIONS

Both the measured data performed at ORNL in 2008 and at LANL in 2010 provided questionable results for ^{252}Cf source CF-52. The measured source emission rate was only about 70% of the calculated strength from the ORNL measurements and about 48% for the LANL measurements. It is still unknown if this percentage will decrease even further as time progresses. If subcritical benchmark measurements are to use the CSDNA method in the future, additional work must be performed to resolve these issues with the source.

REFERENCES

- ¹ BNL Chart of Nuclides, <http://www.nndc.bnl.gov/chart/reCenter.jsp?z=98&n=154>, accessed on 8/27/10.
- ² Personal communication with Joseph Williams, Ronald Brunson, and Curtis Porter, ORNL, 8/23/10.
- ³ G. Knoll, "Radiation Detection and Measurement, Third Edition," 2000.
- ⁴ T. Valentine, "MCNP-DSP User's Manual," ORNL/TM-13334, R2, 2001.
- ⁵ T. Valentine, "Review of Subcritical Source-Driven Noise Analysis Measurements."

Characterization of Cf-252 Source CF-52 for use in Subcritical Measurements

J. Hutchinson, G. Arnone, S. Melton,
W. Myers, A. Sood

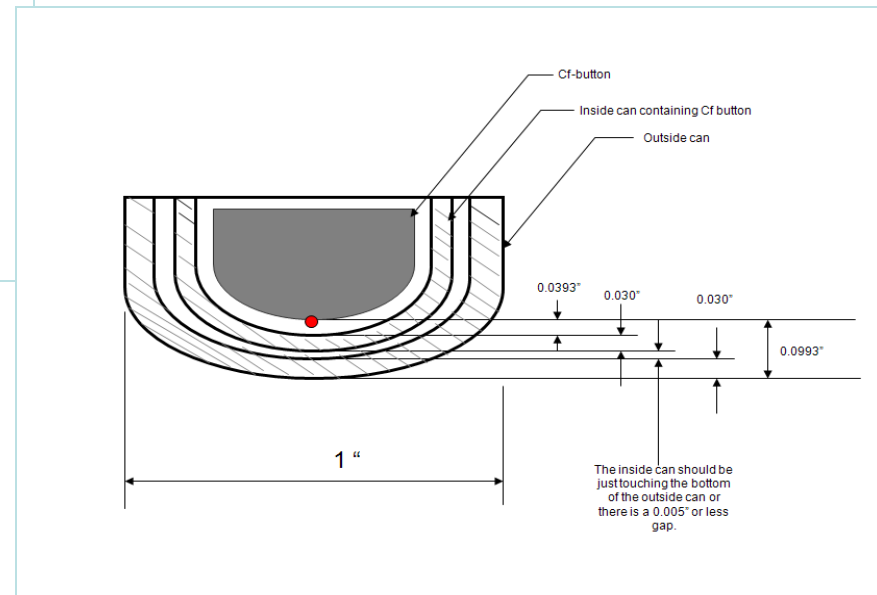
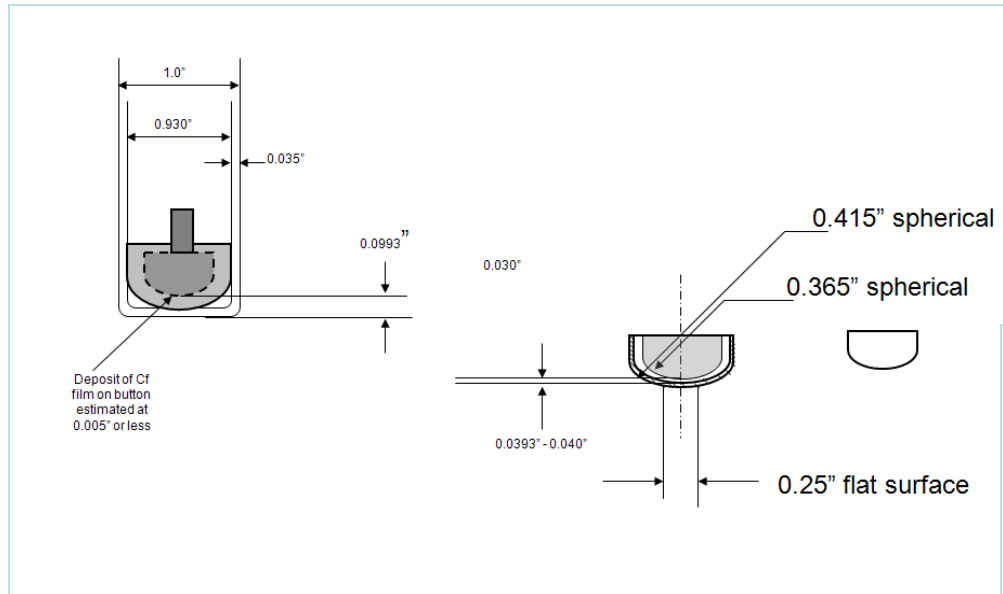
Los Alamos National Laboratory
N-2 (Advanced Nuclear Technology) and
XCP-7 (Transport Applications)

Introduction

- Measurements were conducted to characterize the ^{252}Cf source ionization chamber (SIC) provided by ORNL in 2009 (referred to as CF-52).
- Measured data included 4 ^{252}Cf sources and the BERP ball reflected by polyethylene with several detector systems.

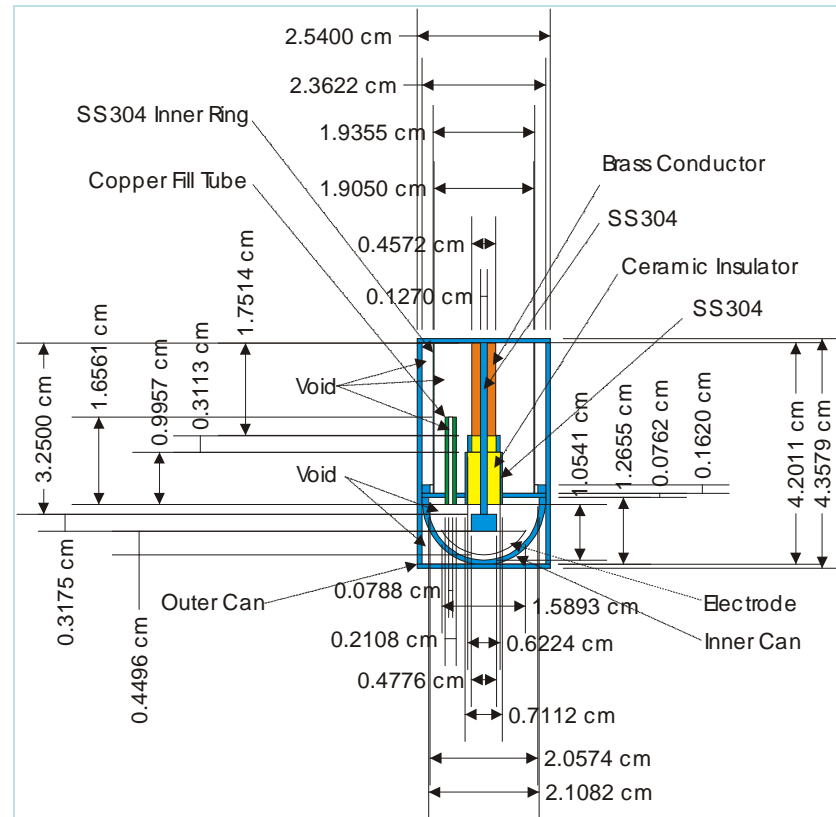
Source Drawings

- ^{252}Cf source CF-52



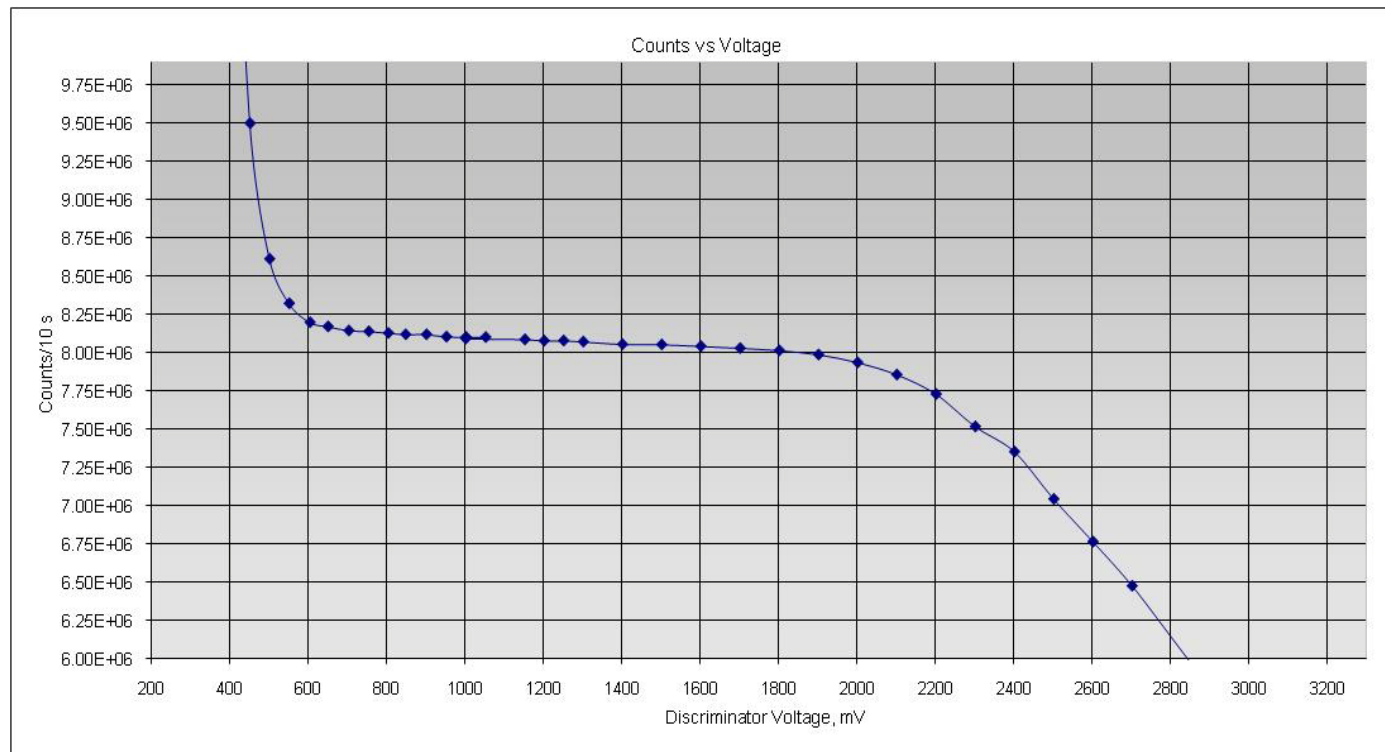
Source Drawings

- CF-49



Pulse Height Curves

- ORNL measured data: 12/18/2008

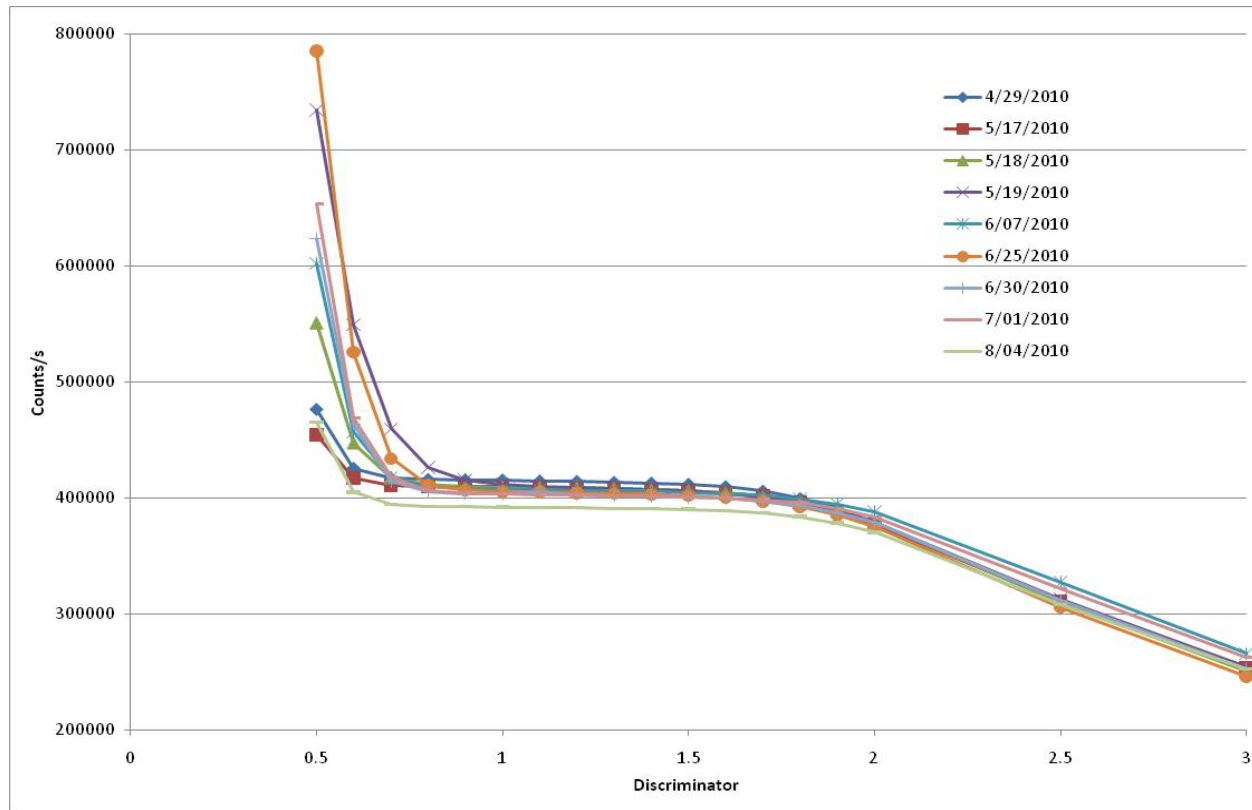


Pulse Height Curves

- Measured emission rate: 8.20×10^5 sf/s
- Calculated emission rate: 1.15×10^6 sf/s (from 1.918 micro-grams on 11/20/2008 using conversion factors of 2.3×10^6 n/s per micro-gram and $\bar{\nu}$ of 3.77).
- So only 71% of the spontaneous fission events are being recorded by the SIC.
- This is very disturbing since previous measurements with ^{252}Cf sources CF-43 and CF-49 have been within 5% of the calculated value.

Pulse Height Curves

- Pulse height curves produced at LANL



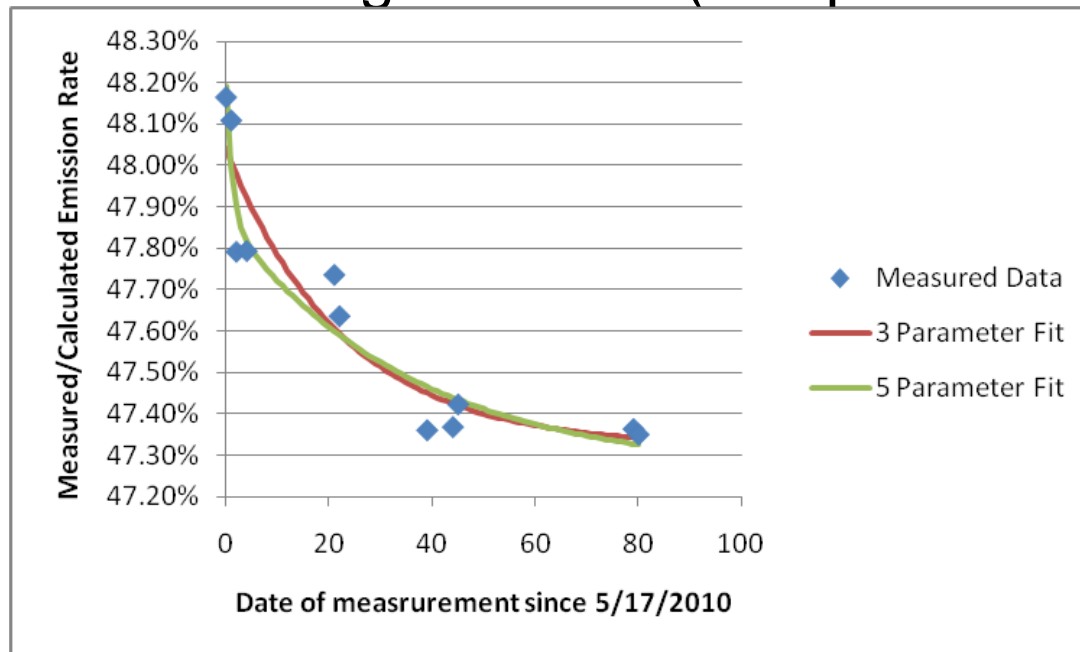
Pulse Height Curves

- The same electronics were used for both sources.

| CF-52 | | | | CF-49 | | | |
|-----------|----------|------------|--------|-----------|----------|------------|--------|
| Date | Measured | Calculated | % Diff | Date | Measured | Calculated | % Diff |
| 5/17/2010 | 410525 | 791998 | 48.17% | 5/22/2010 | 100071 | 103479 | 3.29% |
| 5/18/2010 | 410673 | 791430 | 48.11% | 6/22/2010 | 96862 | 101203 | 4.29% |
| 5/19/2010 | 412890 | 790863 | 47.79% | 6/23/2010 | 96076 | 101131 | 5.00% |
| 5/21/2010 | 412283 | 789729 | 47.79% | 6/24/2010 | 97560 | 101058 | 3.46% |
| 6/07/2010 | 407735 | 780154 | 47.74% | 6/30/2010 | 96620 | 100624 | 3.98% |
| 6/08/2010 | 408221 | 779595 | 47.64% | 7/01/2010 | 96478 | 100552 | 4.05% |
| 6/25/2010 | 405395 | 770144 | 47.36% | 8/02/2010 | 94547 | 98269 | 3.79% |
| 6/30/2010 | 403884 | 767386 | 47.37% | 8/03/2010 | 94507 | 98199 | 3.76% |
| 7/01/2010 | 403175 | 766835 | 47.42% | 8/05/2010 | 93718 | 98058 | 4.43% |
| 8/04/2010 | 393904 | 748355 | 47.36% | | | | |
| 8/05/2010 | 393723 | 747818 | 47.35% | | | | |

Pulse Height Curves

- The measured/calculated ratio was much worse for the LANL measurements in 2010 than the ORNL measurements in 2008.
- Is this ratio decreasing with time (see plot below).



UNCLASSIFIED

CSDNA Measurements Compared to MCNP-DSP

| Source | Poly thickness (inches) | R23 | R24 | R25 | R34 | R35 | R45 | Ravg |
|--|-------------------------|---------|---------|---------|---------|---------|---------|---------|
| CF-52 (calculated activity 7.48e5 sf/s) | 0 | -32.24% | -33.75% | -35.25% | -37.35% | -37.04% | -27.67% | -33.88% |
| | 0.5 | -35.94% | -35.94% | -38.67% | -43.69% | -36.33% | -34.27% | -37.53% |
| | 1 | -36.82% | -32.13% | -42.34% | -43.10% | -38.78% | -37.17% | -38.42% |
| | 1.5 | -42.32% | -45.94% | -42.51% | -42.78% | -44.42% | -34.29% | -42.09% |
| | 3 | -42.12% | -42.10% | -31.94% | -51.64% | -42.65% | -37.07% | -41.34% |
| CF-52 (measured activity 3.94e5 sf/s) | 0 | -20.02% | -19.11% | -21.64% | -24.50% | -24.09% | -13.51% | -20.58% |
| | 0.5 | -13.57% | -13.99% | -20.30% | -24.51% | -16.17% | -13.58% | -17.08% |
| | 1 | -12.19% | -3.23% | -17.63% | -19.37% | -14.61% | -10.23% | -12.92% |
| | 1.5 | -13.66% | -17.19% | -13.57% | -13.25% | -16.21% | 0.76% | -12.27% |
| | 3 | -4.27% | -5.33% | 8.75% | -20.11% | -3.82% | 1.67% | -3.90% |
| CF-49 | 0 | 4.25% | 5.54% | 8.70% | -11.48% | -1.17% | 8.12% | 2.25% |
| | 0.5 | 11.69% | 7.95% | -1.20% | 3.48% | 10.41% | 13.02% | 7.50% |
| | 1 | 8.50% | 10.81% | 28.61% | -15.83% | 5.05% | 10.51% | 7.91% |
| | 1.5 | 27.76% | 9.26% | 44.45% | -9.92% | 30.36% | 17.04% | 19.61% |
| | 3 | 30.65% | 26.59% | 40.14% | 16.94% | 35.52% | 32.60% | 30.44% |

Efficiency Measurements 8/05/10

(counts rate/spontaneous fission rate)

| Detector | | CF-52 | CF-49 | G5-089 | G3-106 |
|--|-------------------------------|-----------|-----------|-----------|-----------|
| SIC | Date | 8/5/2010 | 8/5/2010 | | |
| | Calculated (sf/s) | 747840 | 98058 | | |
| | Ct rate (cts/s) | 393813 | 93718 | | |
| | Efficiency | 5.27E-01 | 9.56E-01 | | |
| 4 He-3 tube system | Date | 6/25/2010 | 6/24/2010 | 6/25/2010 | 6/25/2010 |
| | Calculated (sf/s) | 770144 | 101058 | 476754 | 451777 |
| | Ct rate (cts/s) | 3776 | 738 | 2889 | 2971 |
| | Efficiency | 4.90E-03 | 7.31E-03 | 6.06E-03 | 6.58E-03 |
| | Predicted CF-52 emission rate | - | 5.17E+05 | 6.23E+05 | 5.74E+05 |
| 15 He-3 tube system | Date | 8/5/2010 | 8/5/2010 | | |
| | Calculated (sf/s) | 747818 | 98058 | | |
| | Ct rate (cts/s) | 51180 | 8231 | | |
| | Efficiency | 6.84E-02 | 8.39E-02 | | |
| | Predicted CF-52 emission rate | - | 6.10E+05 | | |
| Single He-3 tube system (contains poly & Cd) | Date | 8/5/2010 | 8/5/2010 | | |
| | Calculated (sf/s) | 747818 | 98058 | | |
| | Ct rate (cts/s) | 169 | 31 | | |
| | Efficiency | 2.26E-04 | 3.13E-04 | | |
| | Predicted CF-52 emission rate | - | 5.39E+05 | | |
| Average | Predicted CF-52 emission rate | 5.63E+05 | | | |

- An emission rate of $5.63e5$ would put the 2008 strength at $6e5$ which does not make sense.

Modified CSDNA Data

| Source | Poly thickness (inches) | R23 | R24 | R25 | R34 | R35 | R45 | Ravg |
|--|-------------------------|----------|----------|----------|----------|----------|----------|----------|
| MCNP-DSP (5.63e5 sf/s) | 0 | 2.09E-01 | 2.21E-01 | 2.20E-01 | 2.17E-01 | 2.21E-01 | 2.03E-01 | 2.15E-01 |
| | 0.5 | 1.12E-01 | 1.19E-01 | 1.13E-01 | 1.18E-01 | 1.17E-01 | 1.10E-01 | 1.15E-01 |
| | 1 | 5.31E-02 | 5.48E-02 | 5.54E-02 | 5.53E-02 | 5.56E-02 | 5.32E-02 | 5.46E-02 |
| | 1.5 | 2.55E-02 | 2.70E-02 | 2.61E-02 | 2.63E-02 | 2.62E-02 | 2.55E-02 | 2.61E-02 |
| | 3 | 3.86E-03 | 3.99E-03 | 3.87E-03 | 4.03E-03 | 3.88E-03 | 3.89E-03 | 3.92E-03 |
| Measured Data (Values divided by 0.70) | 0 | 2.12E-01 | 2.23E-01 | 2.18E-01 | 2.09E-01 | 2.14E-01 | 2.22E-01 | 2.16E-01 |
| | 0.5 | 1.14E-01 | 1.21E-01 | 1.09E-01 | 1.07E-01 | 1.18E-01 | 1.15E-01 | 1.14E-01 |
| | 1 | 5.42E-02 | 6.04E-02 | 5.19E-02 | 5.12E-02 | 5.53E-02 | 5.49E-02 | 5.47E-02 |
| | 1.5 | 2.47E-02 | 2.48E-02 | 2.53E-02 | 2.55E-02 | 2.47E-02 | 2.87E-02 | 2.56E-02 |
| | 3 | 3.95E-03 | 4.11E-03 | 4.66E-03 | 3.46E-03 | 3.93E-03 | 4.26E-03 | 4.06E-03 |
| Comparison | 0 | 1.51% | 1.00% | -1.22% | -3.43% | -3.26% | 9.09% | 0.50% |
| | 0.5 | 1.54% | 1.95% | -3.56% | -9.58% | 1.22% | 4.54% | -0.71% |
| | 1 | 2.08% | 10.25% | -6.36% | -7.28% | -0.45% | 3.04% | 0.17% |
| | 1.5 | -2.89% | -8.21% | -3.01% | -3.11% | -5.55% | 12.44% | -1.81% |
| | 3 | 2.41% | 3.00% | 20.51% | -14.17% | 1.30% | 9.64% | 3.66% |

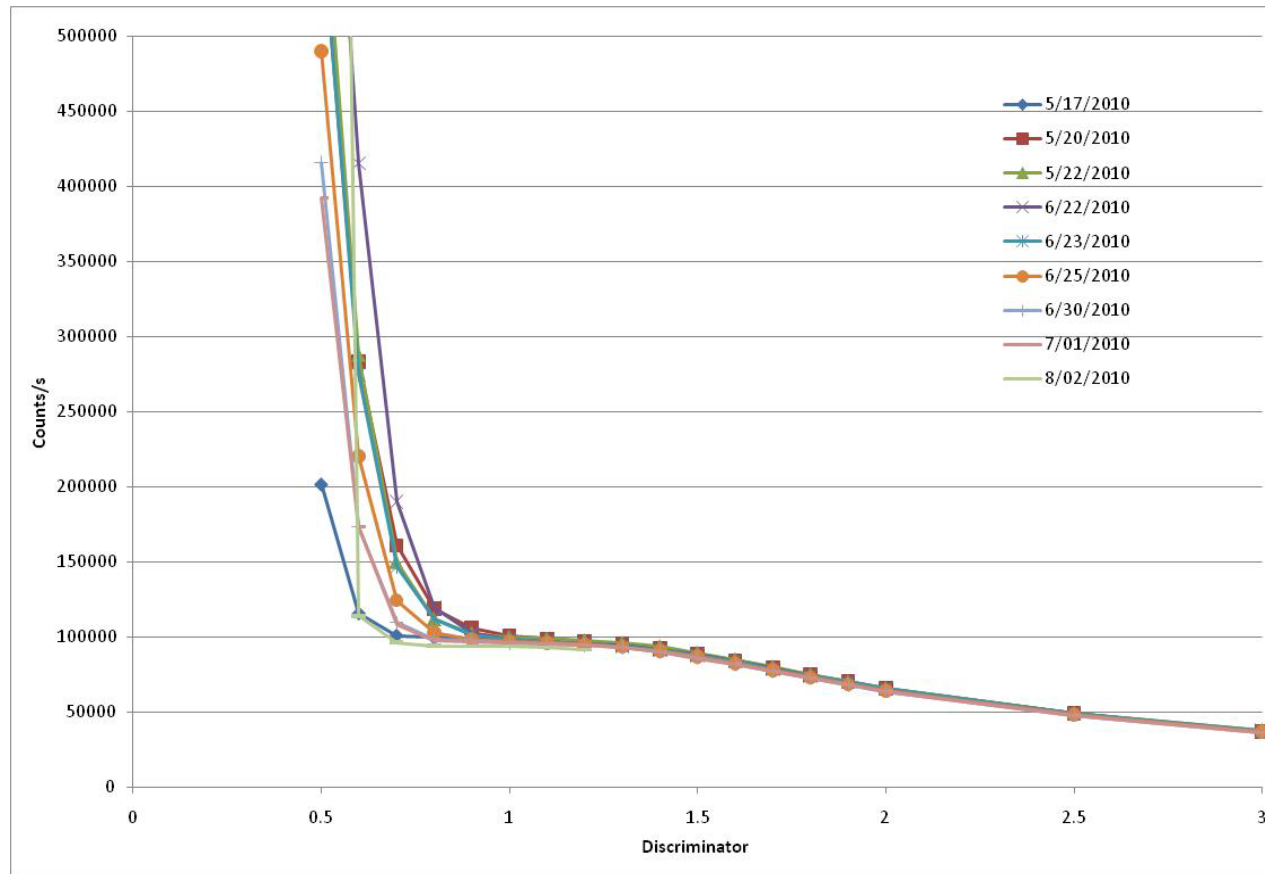
Conclusions

- ORNL 2008 measurements: Only 71% of the fissions were detected.
- LANL 2010 measurements: Only about 48% of the fissions were detected (and it seemed to decrease with time from May to August 2010).
- Detector efficiency measurements predicted the source strength to be around $5.63e5$ on 8/05/10 which is much lower than the calculated emission rate.
- Correlated neutron measurements were difficult to compare.

Extra Slides

Pulse Height Curves

- CF-49 pulse height curves



Detector Count Data

| Date | Source | Configuration | 2 | 3 | 4 | 5 | average |
|-----------|--------|---------------------------|------|------|------|------|---------|
| 5/17/2010 | CF-52 | Source only | 3897 | 3816 | 3802 | 3753 | 3817 |
| 5/18/2010 | CF-52 | Source only | 3750 | 3788 | 3845 | 3917 | 3825 |
| 5/19/2010 | CF-52 | Source only | 3842 | 3827 | 3895 | 3893 | 3864 |
| 5/21/2010 | CF-52 | Source only | 3833 | 3815 | 3905 | 3900 | 3863 |
| 6/07/2010 | CF-52 | Source only | 3794 | 3770 | 3867 | 3849 | 3820 |
| 6/08/2010 | CF-52 | Source only | 3802 | 3773 | 3861 | 3853 | 3822 |
| 6/25/2010 | CF-52 | Source only | 3761 | 3725 | 3815 | 3805 | 3776 |
| 6/30/2010 | CF-52 | Source only | 3752 | 3732 | 3795 | 3792 | 3768 |
| 7/01/2010 | CF-52 | Source only | 3736 | 3714 | 3799 | 3774 | 3756 |
| 8/05/2010 | CF-52 | BERP + Source | 9014 | 9132 | 8608 | 8634 | 8847 |
| 8/05/2010 | CF-52 | BERP + 0.5" Poly + Source | 8304 | 8417 | 8201 | 8225 | 8287 |
| 8/04/2010 | CF-52 | BERP + 1.0" Poly + Source | 8119 | 8279 | 8009 | 8055 | 8115 |
| 8/04/2010 | CF-52 | BERP + 1.5" Poly + Source | 7813 | 8016 | 7656 | 7672 | 7789 |
| 8/04/2010 | CF-52 | BERP + 3.0" Poly + Source | 5124 | 5286 | 4940 | 4951 | 5075 |
| 5/22/2010 | CF-49 | Source only | 743 | 732 | 756 | 753 | 746 |
| 6/22/2010 | CF-49 | Source only | 727 | 737 | 728 | 726 | 730 |
| 6/23/2010 | CF-49 | Source only | 732 | 726 | 723 | 729 | 728 |
| 6/24/2010 | CF-49 | Source only | 772 | 717 | 733 | 732 | 738 |
| 6/30/2010 | CF-49 | Source only | 718 | 710 | 785 | 730 | 736 |
| 7/01/2010 | CF-49 | Source only | 724 | 720 | 721 | 711 | 719 |
| 8/02/2010 | CF-49 | BERP + Source | 3435 | 3227 | 3163 | 3150 | 3244 |
| 8/02/2010 | CF-49 | BERP + 0.5" Poly + Source | 3727 | 3540 | 3448 | 3462 | 3544 |
| 8/02/2010 | CF-49 | BERP + 1.0" Poly + Source | 4312 | 4148 | 3738 | 3761 | 3990 |
| 8/02/2010 | CF-49 | BERP + 1.5" Poly + Source | 4615 | 4502 | 4089 | 4102 | 4327 |
| 8/02/2010 | CF-49 | BERP + 3.0" Poly + Source | 3827 | 3745 | 3608 | 3635 | 3704 |

Detector Count Data

| Tube # | CF-52 | BERP + Polyethylene (thickness in inches) | | | | |
|--------|-------------|---|--------|--------|--------|-------|
| | Source only | 0 | 0.5 | 1 | 1.5 | 3 |
| 0 | 1272 | 2649 | 3059 | 3452 | 3180 | 2333 |
| 1 | 1517 | 3563 | 3313 | 3990 | 3819 | 3046 |
| 2 | 1494 | 2861 | 3580 | 3709 | 3805 | 3121 |
| 3 | 1495 | 3258 | 3607 | 4112 | 4287 | 3175 |
| 4 | 1539 | 3285 | 3794 | 3977 | 4358 | 3046 |
| 5 | 1375 | 3391 | 3687 | 3928 | 3918 | 3359 |
| 6 | 1475 | 2980 | 3006 | 3405 | 4145 | 2992 |
| 7 | 1332 | 2795 | 2765 | 3210 | 3336 | 2614 |
| 8 | 1740 | 4106 | 3593 | 3563 | 4131 | 2603 |
| 9 | 1926 | 4185 | 3847 | 3917 | 3663 | 3186 |
| 10 | 1926 | 4331 | 4194 | 4066 | 3833 | 3175 |
| 11 | 2451 | 4199 | 4448 | 3880 | 3961 | 2657 |
| 12 | 1892 | 4119 | 3927 | 3758 | 3833 | 2959 |
| 13 | 1981 | 4106 | 3500 | 4144 | 4017 | 3089 |
| 14 | 1904 | 3973 | 3714 | 3841 | 3918 | 2549 |
| 15 | 1377 | 2596 | 2912 | 3233 | 3549 | 2570 |
| 16 | 1538 | 3391 | 3527 | 3416 | 4117 | 2981 |
| 17 | 1699 | 3550 | 3620 | 3928 | 3748 | 3024 |
| 18 | 1842 | 3775 | 3740 | 3965 | 4174 | 3445 |
| 19 | 1572 | 3788 | 3794 | 4135 | 4401 | 3272 |
| 20 | 1624 | 3497 | 3914 | 3685 | 4230 | 3326 |
| 21 | 1367 | 3271 | 3767 | 3952 | 4131 | 3110 |
| 22 | 1247 | 2967 | 2925 | 3147 | 3322 | 2884 |
| 23 | 1635 | 3775 | 3593 | 4048 | 3606 | 2873 |
| 24 | 2036 | 4503 | 3887 | 3843 | 3890 | 3035 |
| 25 | 1840 | 4159 | 4007 | 3706 | 3946 | 2808 |
| 26 | 1968 | 4199 | 4061 | 4099 | 4131 | 3164 |
| 27 | 2077 | 4013 | 4154 | 4087 | 4216 | 2916 |
| 28 | 2022 | 3973 | 4154 | 3615 | 3478 | 2786 |
| 29 | 2018 | 3682 | 3820 | 3656 | 3563 | 2938 |
| Total | 51180 | 108936 | 109911 | 113465 | 116705 | 89038 |

UNCLASSIFIED

Detector Count Data

| Tube # | CF-49 | BERP + Polyethylene (thickness in inches) | | | | |
|--------|-------------|---|-------|-------|-------|-------|
| | Source only | 0 | 0.5 | 1 | 1.5 | 3 |
| 0 | 216 | 848 | 1025 | 1380 | 1622 | 1354 |
| 1 | 212 | 945 | 1364 | 1607 | 1813 | 1365 |
| 2 | 238 | 1069 | 1419 | 1403 | 1919 | 1339 |
| 3 | 249 | 1095 | 1374 | 1881 | 1984 | 1566 |
| 4 | 262 | 1108 | 1359 | 1764 | 1997 | 1555 |
| 5 | 231 | 1272 | 1439 | 1607 | 1908 | 1504 |
| 6 | 251 | 1219 | 1359 | 1543 | 1853 | 1447 |
| 7 | 184 | 958 | 1035 | 1304 | 1615 | 1318 |
| 8 | 302 | 1285 | 1334 | 1537 | 1633 | 1390 |
| 9 | 302 | 1382 | 1488 | 1537 | 1692 | 1236 |
| 10 | 334 | 1369 | 1518 | 1729 | 1754 | 1370 |
| 11 | 350 | 1466 | 1414 | 1636 | 1771 | 1339 |
| 12 | 326 | 1431 | 1523 | 1718 | 1770 | 1478 |
| 13 | 308 | 1391 | 1444 | 1700 | 1673 | 1195 |
| 14 | 298 | 1241 | 1458 | 1427 | 1617 | 1262 |
| 15 | 228 | 1069 | 1234 | 1392 | 1666 | 1437 |
| 16 | 219 | 972 | 1279 | 1677 | 1823 | 1643 |
| 17 | 255 | 1232 | 1454 | 1846 | 1977 | 1689 |
| 18 | 260 | 1237 | 1259 | 1718 | 2032 | 1653 |
| 19 | 264 | 1161 | 1404 | 1758 | 2053 | 1586 |
| 20 | 241 | 1007 | 1259 | 1735 | 1980 | 1555 |
| 21 | 255 | 1073 | 1259 | 1659 | 1881 | 1354 |
| 22 | 204 | 958 | 1155 | 1427 | 1723 | 1380 |
| 23 | 287 | 1356 | 1304 | 1415 | 1604 | 1148 |
| 24 | 313 | 1400 | 1543 | 1776 | 1709 | 1293 |
| 25 | 333 | 1440 | 1468 | 1671 | 1778 | 1411 |
| 26 | 311 | 1382 | 1588 | 1718 | 1809 | 1504 |
| 27 | 347 | 1422 | 1493 | 1549 | 1766 | 1581 |
| 28 | 352 | 1356 | 1249 | 1520 | 1678 | 1277 |
| 29 | 299 | 1316 | 1563 | 1461 | 1608 | 1282 |
| Total | 8231 | 36459 | 41066 | 48095 | 53704 | 42513 |

UNCLASSIFIED

CSDNA Measurements – Sources only

| Source | Run | Time (min) | R23 | R24 | R25 | R34 | R35 | R45 | Ravg | |
|--------|----------|-----------------------|-----------|-----------|-----------|-----------|-----------|-----------|-----------|-----------|
| CF-52 | 0007 | 1 | 1.600E-01 | 3.241E-01 | 1.756E-01 | 2.289E-01 | 1.492E-01 | 1.317E-01 | 1.949E-01 | |
| | 0011 | 2 | 2.081E-01 | 3.005E-01 | 3.419E-01 | 2.056E-01 | 1.851E-01 | 2.160E-01 | 2.429E-01 | |
| | 0016 | 2 | 2.211E-01 | 2.702E-01 | 1.946E-01 | 2.510E-01 | 1.924E-01 | 3.553E-01 | 2.474E-01 | |
| | 0001 | 5 | 3.053E-01 | 3.557E-01 | 3.278E-01 | 3.971E-01 | 4.356E-01 | 3.844E-01 | 3.677E-01 | |
| | 0017 | 5 | 2.912E-01 | 3.390E-01 | 3.248E-01 | 4.502E-01 | 3.567E-01 | 4.420E-01 | 3.673E-01 | |
| | 0018 | 10 | 5.357E-01 | 5.377E-01 | 5.834E-01 | 4.550E-01 | 4.139E-01 | 5.353E-01 | 5.102E-01 | |
| | 0019 | 20 | 5.186E-01 | 4.833E-01 | 5.755E-01 | 6.297E-01 | 4.999E-01 | 4.073E-01 | 5.191E-01 | |
| | 0021 | 30 | 6.251E-01 | 1.036E+00 | 5.412E-01 | 6.631E-01 | 6.832E-01 | 5.407E-01 | 6.816E-01 | |
| | 0020 | 60 | 1.761E+00 | 4.715E-01 | 1.047E+00 | 5.890E-01 | 9.021E-01 | 3.429E-01 | 8.521E-01 | |
| | 0014 | 120 | 5.069E-01 | 9.749E-01 | 1.001E+00 | 4.876E-01 | 4.427E-01 | 6.566E-01 | 6.783E-01 | |
| | 0031 | 600 | 8.974E-01 | 7.519E-01 | 7.866E-01 | 7.055E-01 | 7.235E-01 | 8.982E-01 | 7.939E-01 | |
| | 0074 | 600 | 8.623E-01 | 8.139E-01 | 7.927E-01 | 8.074E-01 | 7.700E-01 | 7.675E-01 | 8.023E-01 | |
| | | average (10-600 min) | | 8.153E-01 | 7.242E-01 | 7.610E-01 | 6.196E-01 | 6.336E-01 | 5.927E-01 | 6.911E-01 |
| | | time-weighted average | | 8.665E-01 | 7.807E-01 | 8.032E-01 | 7.175E-01 | 7.167E-01 | 7.793E-01 | 7.773E-01 |
| CF-49 | 0035 | 1 | 3.088E-01 | 3.090E-01 | 2.498E-01 | 2.363E-01 | 1.440E-01 | 2.801E-01 | 2.547E-01 | |
| | 0005 | 2 | 4.217E-01 | 6.252E-01 | 6.062E-01 | 3.536E-01 | 3.247E-01 | 3.520E-01 | 4.472E-01 | |
| | 0002 | 5 | 3.272E-01 | 4.980E-01 | 5.166E-01 | 5.964E-01 | 4.717E-01 | 3.761E-01 | 4.643E-01 | |
| | 0038 | 5 | 8.897E-01 | 8.122E-01 | 7.199E-01 | 5.506E-01 | 3.177E-01 | 5.017E-01 | 6.320E-01 | |
| | 0039 | 10 | 1.010E+00 | 1.146E+00 | 1.140E+00 | 4.809E-01 | 5.135E-01 | 4.553E-01 | 7.910E-01 | |
| | 0049 | 10 | 7.132E-01 | 8.346E-01 | 7.246E-01 | 4.596E-01 | 5.203E-01 | 5.710E-01 | 6.372E-01 | |
| | 0048 | 20 | 8.791E-01 | 1.159E+00 | 7.154E-01 | 5.466E-01 | 6.775E-01 | 6.838E-01 | 7.770E-01 | |
| | 0047 | 30 | 6.743E-01 | 7.638E-01 | 6.430E-01 | 8.987E-01 | 7.914E-01 | 7.829E-01 | 7.590E-01 | |
| | 0046 | 60 | 7.737E-01 | 8.225E-01 | 6.968E-01 | 8.394E-01 | 7.538E-01 | 9.276E-01 | 8.023E-01 | |
| | 0045 | 120 | 1.068E+00 | 7.708E-01 | 7.918E-01 | 8.245E-01 | 7.837E-01 | 9.131E-01 | 8.587E-01 | |
| | 0116 | 600 | 1.057E+00 | 8.331E-01 | 8.496E-01 | 9.950E-01 | 1.002E+00 | 9.724E-01 | 9.515E-01 | |
| | | average (10-600 min) | | 8.822E-01 | 9.043E-01 | 7.945E-01 | 7.207E-01 | 7.203E-01 | 7.580E-01 | 7.967E-01 |
| | | time-weighted average | | 1.009E+00 | 8.293E-01 | 8.186E-01 | 9.273E-01 | 9.189E-01 | 9.287E-01 | 9.053E-01 |
| | MCNP-DSP | | | 6.845E-01 | 7.703E-01 | 7.498E-01 | 7.258E-01 | 7.574E-01 | 6.783E-01 | 7.277E-01 |

CSDNA Measurements – Berp Ball Reflected by Polyethylene

| Source | Poly thickness (inches) | Run | Time (min) | R23 | R24 | R25 | R34 | R35 | R45 | Ravg |
|--------|-------------------------|-----|------------|----------|----------|----------|----------|----------|----------|----------|
| CF-52 | 0 | 056 | 1 | 1.50E-01 | 1.50E-01 | 1.05E-01 | 1.21E-01 | 1.63E-01 | 1.50E-01 | 1.40E-01 |
| | | 057 | 20 | 1.48E-01 | 1.56E-01 | 1.52E-01 | 1.47E-01 | 1.50E-01 | 1.55E-01 | 1.51E-01 |
| | 0.5 | 051 | 1 | 8.23E-02 | 7.35E-02 | 5.61E-02 | 7.77E-02 | 8.00E-02 | 7.70E-02 | 7.45E-02 |
| | | 050 | 30 | 7.95E-02 | 8.47E-02 | 7.60E-02 | 7.50E-02 | 8.29E-02 | 8.03E-02 | 7.97E-02 |
| | 1 | 045 | 1 | 4.29E-02 | 4.20E-02 | 3.73E-02 | 3.99E-02 | 4.14E-02 | 4.85E-02 | 4.20E-02 |
| | | 046 | 30 | 3.79E-02 | 4.23E-02 | 3.63E-02 | 3.59E-02 | 3.87E-02 | 3.84E-02 | 3.83E-02 |
| | 1.5 | 049 | 13 | 1.73E-02 | 1.74E-02 | 1.77E-02 | 1.78E-02 | 1.73E-02 | 2.01E-02 | 1.79E-02 |
| | 3 | 038 | 1 | 4.92E-03 | 3.69E-03 | 5.40E-03 | 2.79E-03 | 3.64E-03 | 2.90E-03 | 3.89E-03 |
| | | 037 | 5 | 3.12E-03 | 3.16E-03 | 2.93E-03 | 2.78E-03 | 2.79E-03 | 2.93E-03 | 2.95E-03 |
| | | 036 | 30 | 2.77E-03 | 2.88E-03 | 3.26E-03 | 2.42E-03 | 2.75E-03 | 2.98E-03 | 2.84E-03 |
| CF-49 | 0 | 015 | 1 | 9.81E-02 | 8.69E-02 | 6.92E-02 | 7.55E-02 | 7.00E-02 | 8.30E-02 | 8.05E-02 |
| | | 001 | 5 | 9.61E-02 | 8.59E-02 | 8.00E-02 | 8.65E-02 | 8.91E-02 | 8.67E-02 | 8.74E-02 |
| | | 011 | 30 | 8.64E-02 | 9.21E-02 | 9.47E-02 | 7.82E-02 | 8.71E-02 | 9.15E-02 | 8.84E-02 |
| | 0.5 | 017 | 1 | 4.70E-02 | 3.51E-02 | 3.68E-02 | 3.23E-02 | 3.00E-02 | 3.48E-02 | 3.60E-02 |
| | | 010 | 30 | 3.88E-02 | 3.82E-02 | 3.49E-02 | 3.75E-02 | 4.00E-02 | 3.81E-02 | 3.79E-02 |
| | 1 | 023 | 1 | 1.45E-02 | 2.28E-02 | 1.78E-02 | 1.56E-02 | 1.26E-02 | 1.84E-02 | 1.70E-02 |
| | | 007 | 20 | 1.49E-02 | 1.54E-02 | 1.79E-02 | 1.20E-02 | 1.40E-02 | 1.50E-02 | 1.49E-02 |
| | | 008 | 20 | 1.55E-02 | 1.70E-02 | 2.09E-02 | 1.17E-02 | 1.59E-02 | 1.67E-02 | 1.63E-02 |
| | | 006 | 30 | 1.55E-02 | 1.55E-02 | 2.03E-02 | 1.13E-02 | 1.61E-02 | 1.53E-02 | 1.57E-02 |
| | | 024 | 60 | 1.54E-02 | 1.60E-02 | 1.57E-02 | 1.42E-02 | 1.50E-02 | 1.56E-02 | 1.53E-02 |
| | average (20-60 min) | | | 1.53E-02 | 1.60E-02 | 1.87E-02 | 1.23E-02 | 1.52E-02 | 1.57E-02 | 1.55E-02 |
| | 1.5 | 025 | 1 | 1.01E-02 | 8.60E-03 | 6.24E-03 | 1.21E-02 | 7.60E-03 | 6.56E-03 | 8.54E-03 |
| | | 002 | 5 | 8.12E-03 | 7.02E-03 | 9.11E-03 | 5.94E-03 | 8.33E-03 | 7.30E-03 | 7.64E-03 |
| | 3 | 032 | 1 | 2.55E-03 | 1.97E-03 | 1.27E-03 | 2.36E-03 | 1.87E-03 | 2.51E-03 | 2.09E-03 |
| | | 033 | 5 | 1.15E-03 | 9.80E-04 | 1.22E-03 | 1.50E-03 | 1.34E-03 | 1.40E-03 | 1.26E-03 |
| | | 004 | 5 | 9.29E-04 | 9.89E-04 | 1.31E-03 | 1.22E-03 | 1.66E-03 | 1.75E-03 | 1.31E-03 |
| 003 | | 30 | 9.92E-04 | 9.50E-04 | 1.08E-03 | 8.86E-04 | 1.04E-03 | 9.70E-04 | 9.86E-04 | |

MCNP-DSP – BERP Ball Reflected by Polyethylene

| Source | thickness (in) | R23 | R24 | R25 | R34 | R35 | R45 | Ravg |
|--|----------------|----------|----------|----------|----------|----------|----------|----------|
| CF-52 (calculated activity 7.48e5 sf/s) | 0 | 2.19E-01 | 2.36E-01 | 2.35E-01 | 2.34E-01 | 2.38E-01 | 2.15E-01 | 2.29E-01 |
| | 0.5 | 1.24E-01 | 1.32E-01 | 1.24E-01 | 1.33E-01 | 1.30E-01 | 1.22E-01 | 1.28E-01 |
| | 1 | 6.00E-02 | 6.23E-02 | 6.30E-02 | 6.30E-02 | 6.33E-02 | 6.11E-02 | 6.21E-02 |
| | 1.5 | 3.00E-02 | 3.21E-02 | 3.08E-02 | 3.12E-02 | 3.11E-02 | 3.05E-02 | 3.10E-02 |
| | 3 | 4.78E-03 | 4.97E-03 | 4.79E-03 | 5.00E-03 | 4.79E-03 | 4.74E-03 | 4.85E-03 |
| CF-52 (measured activity 3.94e5 sf/s) | 0 | 1.86E-01 | 1.93E-01 | 1.94E-01 | 1.94E-01 | 1.97E-01 | 1.79E-01 | 1.91E-01 |
| | 0.5 | 9.20E-02 | 9.84E-02 | 9.54E-02 | 9.93E-02 | 9.89E-02 | 9.29E-02 | 9.62E-02 |
| | 1 | 4.32E-02 | 4.37E-02 | 4.41E-02 | 4.45E-02 | 4.54E-02 | 4.28E-02 | 4.39E-02 |
| | 1.5 | 2.01E-02 | 2.10E-02 | 2.05E-02 | 2.06E-02 | 2.07E-02 | 1.99E-02 | 2.04E-02 |
| | 3 | 2.89E-03 | 3.04E-03 | 3.00E-03 | 3.03E-03 | 2.86E-03 | 2.93E-03 | 2.96E-03 |
| CF-49 | 0 | 8.29E-02 | 8.73E-02 | 8.71E-02 | 8.83E-02 | 8.82E-02 | 8.47E-02 | 8.64E-02 |
| | 0.5 | 3.47E-02 | 3.54E-02 | 3.54E-02 | 3.62E-02 | 3.62E-02 | 3.37E-02 | 3.53E-02 |
| | 1 | 1.41E-02 | 1.44E-02 | 1.46E-02 | 1.46E-02 | 1.45E-02 | 1.42E-02 | 1.44E-02 |
| | 1.5 | 6.35E-03 | 6.43E-03 | 6.31E-03 | 6.60E-03 | 6.39E-03 | 6.24E-03 | 6.39E-03 |
| | 3 | 7.59E-04 | 7.51E-04 | 7.68E-04 | 7.57E-04 | 7.70E-04 | 7.32E-04 | 7.56E-04 |

Comparison to DSP When Values are Divided by Measured/Calculated sf/s Ratio

| Source | Poly thickness (inches) | Run | Time (min) | R23 | R24 | R25 | R34 | R35 | R45 | Ravg |
|--------|-------------------------|----------|------------|----------|----------|----------|----------|----------|----------|----------|
| CF-52 | 0 | 057 | 20 | 2.82E-01 | 2.97E-01 | 2.89E-01 | 2.78E-01 | 2.84E-01 | 2.95E-01 | 2.88E-01 |
| | | MCNP-DSP | | 2.19E-01 | 2.36E-01 | 2.35E-01 | 2.34E-01 | 2.38E-01 | 2.15E-01 | 2.29E-01 |
| | | % Diff | | 28.68% | 25.81% | 22.96% | 18.98% | 19.56% | 37.35% | 25.34% |
| | 0.5 | 050 | 30 | 1.51E-01 | 1.61E-01 | 1.44E-01 | 1.42E-01 | 1.58E-01 | 1.52E-01 | 1.51E-01 |
| | | MCNP-DSP | | 1.24E-01 | 1.32E-01 | 1.24E-01 | 1.33E-01 | 1.30E-01 | 1.22E-01 | 1.28E-01 |
| | | % Diff | | 21.65% | 21.66% | 16.46% | 6.93% | 20.92% | 24.82% | 18.63% |
| | 1 | 046 | 30 | 7.20E-02 | 8.03E-02 | 6.90E-02 | 6.81E-02 | 7.36E-02 | 7.29E-02 | 7.27E-02 |
| | | MCNP-DSP | | 6.00E-02 | 6.23E-02 | 6.30E-02 | 6.30E-02 | 6.33E-02 | 6.11E-02 | 6.21E-02 |
| | | % Diff | | 19.98% | 28.88% | 9.49% | 8.04% | 16.25% | 19.30% | 16.93% |
| | 1.5 | 049 | 13 | 3.29E-02 | 3.30E-02 | 3.36E-02 | 3.39E-02 | 3.29E-02 | 3.81E-02 | 3.41E-02 |
| | | MCNP-DSP | | 3.00E-02 | 3.21E-02 | 3.08E-02 | 3.12E-02 | 3.11E-02 | 3.05E-02 | 3.10E-02 |
| | | % Diff | | 9.53% | 2.65% | 9.17% | 8.67% | 5.54% | 24.78% | 9.97% |
| | 3 | 036 | 30 | 5.25E-03 | 5.46E-03 | 6.20E-03 | 4.60E-03 | 5.22E-03 | 5.66E-03 | 5.40E-03 |
| | | MCNP-DSP | | 4.78E-03 | 4.97E-03 | 4.79E-03 | 5.00E-03 | 4.79E-03 | 4.74E-03 | 4.85E-03 |
| | | % Diff | | 9.91% | 9.94% | 29.25% | -8.16% | 8.91% | 19.50% | 11.39% |

Previous BERP Ball Data

| | Date | R23 | R24 | R25 | R34 | R35 | R45 | Ravg |
|----------|-----------|----------|----------|----------|----------|----------|----------|----------|
| Measured | 7/10/2007 | 1.40E-01 | 1.44E-01 | 1.46E-01 | 1.44E-01 | 1.45E-01 | 1.38E-01 | 1.43E-01 |
| MCNP-DSP | | 1.35E-01 | 1.43E-01 | 1.44E-01 | 1.45E-01 | 1.44E-01 | 1.36E-01 | 1.41E-01 |
| % Diff | | 3.44% | 0.33% | 1.36% | -0.56% | 1.14% | 1.90% | 1.24% |
| Measured | 1/13/2008 | 1.30E-01 | 1.46E-01 | 1.42E-01 | 1.41E-01 | 1.46E-01 | 1.39E-01 | 1.41E-01 |
| MCNP-DSP | | 1.32E-01 | 1.41E-01 | 1.39E-01 | 1.40E-01 | 1.41E-01 | 1.32E-01 | 1.38E-01 |
| % Diff | | -1.84% | 3.68% | 2.23% | 0.43% | 3.60% | 5.52% | 2.28% |
| Measured | 9/20/2008 | 1.22E-01 | 1.31E-01 | 1.43E-01 | 1.25E-01 | 1.32E-01 | 1.12E-01 | 1.27E-01 |
| MCNP-DSP | | 1.16E-01 | 1.26E-01 | 1.24E-01 | 1.24E-01 | 1.24E-01 | 1.17E-01 | 1.22E-01 |
| % Diff | | 4.91% | 4.13% | 14.99% | 0.96% | 5.89% | -4.31% | 4.51% |
| Measured | 6/6/2009 | 1.40E-01 | 1.49E-01 | 1.50E-01 | 1.50E-01 | 1.48E-01 | 1.40E-01 | 1.46E-01 |
| MCNP-DSP | | 1.17E-01 | 1.22E-01 | 1.26E-01 | 1.24E-01 | 1.24E-01 | 1.18E-01 | 1.22E-01 |
| % Diff | | 19.70% | 22.12% | 18.63% | 21.02% | 19.69% | 19.41% | 20.10% |

Previous BERP Ball Data (smaller run times)

| | Time (min) | Date | R23 | R24 | R25 | R34 | R35 | R45 | Ravg |
|----------|------------|-----------|----------|----------|----------|----------|----------|----------|----------|
| Measured | 30 | 7/10/2007 | 1.46E-01 | 1.46E-01 | 1.50E-01 | 1.43E-01 | 1.52E-01 | 1.36E-01 | 1.45E-01 |
| MCNP-DSP | | | 1.35E-01 | 1.43E-01 | 1.44E-01 | 1.45E-01 | 1.44E-01 | 1.36E-01 | 1.41E-01 |
| % Diff | | | 7.92% | 2.33% | 4.10% | -1.16% | 5.43% | -0.01% | 3.08% |
| Measured | 30 | 1/13/2008 | 1.24E-01 | 1.44E-01 | 1.43E-01 | 1.35E-01 | 1.45E-01 | 1.40E-01 | 1.39E-01 |
| MCNP-DSP | | | 1.32E-01 | 1.41E-01 | 1.39E-01 | 1.40E-01 | 1.41E-01 | 1.32E-01 | 1.38E-01 |
| % Diff | | | -6.21% | 2.32% | 3.06% | -3.71% | 2.61% | 6.28% | 0.73% |
| Measured | 30 | 9/20/2008 | 1.20E-01 | 1.29E-01 | 1.26E-01 | 1.18E-01 | 1.17E-01 | 1.01E-01 | 1.19E-01 |
| MCNP-DSP | | | 1.16E-01 | 1.26E-01 | 1.24E-01 | 1.24E-01 | 1.24E-01 | 1.17E-01 | 1.22E-01 |
| % Diff | | | 3.42% | 2.77% | 1.62% | -4.89% | -5.85% | -13.79% | -2.73% |
| Measured | 40 | 6/6/2009 | 1.40E-01 | 1.48E-01 | 1.56E-01 | 1.48E-01 | 1.48E-01 | 1.35E-01 | 1.46E-01 |
| MCNP-DSP | | | 1.17E-01 | 1.22E-01 | 1.26E-01 | 1.24E-01 | 1.24E-01 | 1.18E-01 | 1.22E-01 |
| % Diff | | | 20.13% | 20.93% | 23.92% | 19.93% | 19.68% | 14.51% | 19.90% |

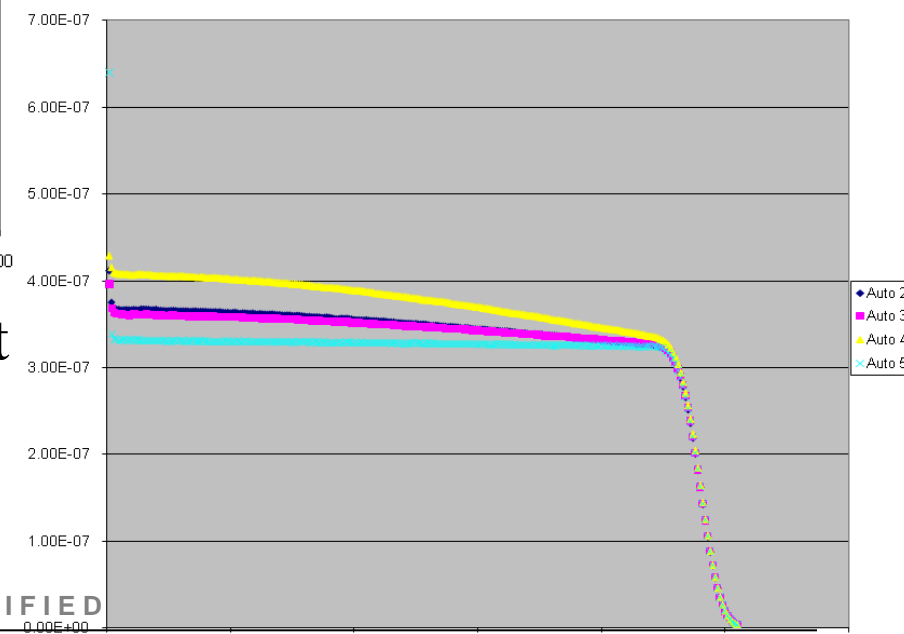
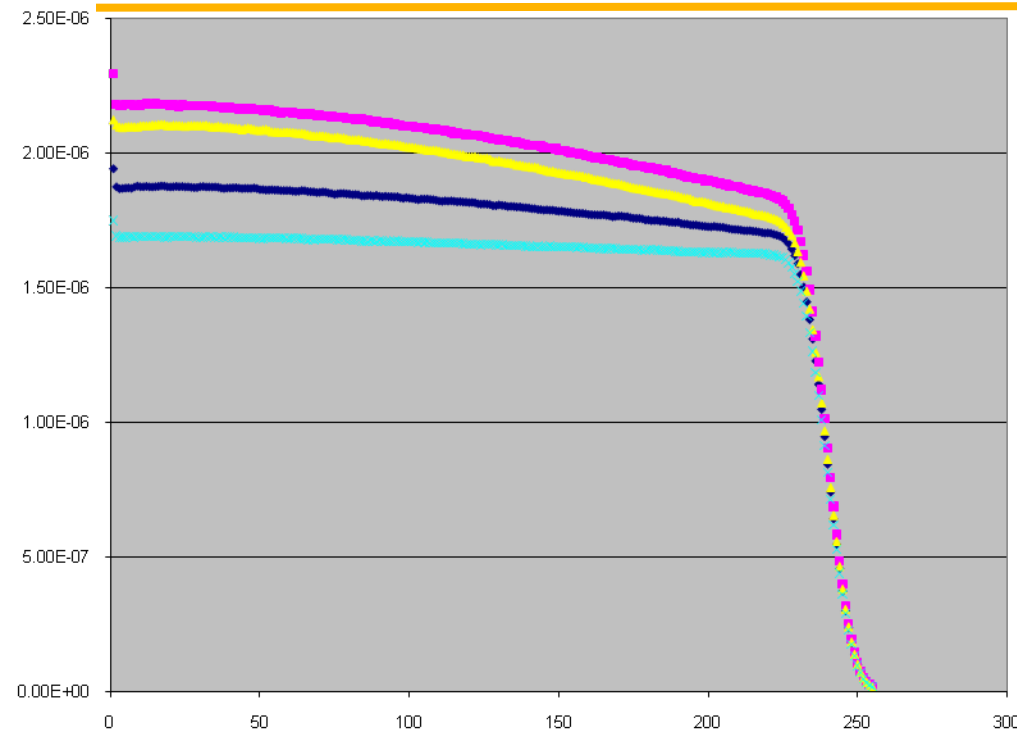
Previous BERP/Poly Data

| Poly Thickness (in) | | R23 | R24 | R25 | R34 | R35 | R45 | Ravg |
|---------------------|-----|----------|----------|----------|----------|----------|----------|----------|
| Measured | 0 | 1.40E-01 | 1.44E-01 | 1.46E-01 | 1.44E-01 | 1.45E-01 | 1.38E-01 | 1.43E-01 |
| MCNP-DSP | | 1.35E-01 | 1.43E-01 | 1.44E-01 | 1.45E-01 | 1.44E-01 | 1.36E-01 | 1.41E-01 |
| % Diff | | 3.44% | 0.33% | 1.36% | -0.56% | 1.14% | 1.90% | 1.24% |
| Measured | 0.5 | 6.35E-02 | 6.64E-02 | 6.57E-02 | 6.43E-02 | 6.47E-02 | 6.19E-02 | 6.44E-02 |
| MCNP-DSP | | 5.98E-02 | 6.26E-02 | 6.28E-02 | 6.20E-02 | 6.32E-02 | 5.95E-02 | 6.16E-02 |
| % Diff | | 6.19% | 6.04% | 4.59% | 3.70% | 2.40% | 4.12% | 4.50% |
| Measured | 1 | 2.73E-02 | 2.70E-02 | 2.68E-02 | 2.69E-02 | 2.72E-02 | 2.42E-02 | 2.66E-02 |
| MCNP-DSP | | 2.51E-02 | 2.62E-02 | 2.61E-02 | 2.59E-02 | 2.59E-02 | 2.51E-02 | 2.57E-02 |
| % Diff | | 8.67% | 2.70% | 2.73% | 3.63% | 5.14% | -3.79% | 3.19% |
| Measured | 1.5 | 1.06E-02 | 1.09E-02 | 1.09E-02 | 1.08E-02 | 1.08E-02 | 1.07E-02 | 1.08E-02 |
| MCNP-DSP | | 1.09E-02 | 1.11E-02 | 1.12E-02 | 1.12E-02 | 1.11E-02 | 1.09E-02 | 1.11E-02 |
| % Diff | | -2.85% | -2.10% | -3.40% | -3.55% | -2.47% | -1.97% | -2.73% |
| Measured | 3 | 1.29E-03 | 1.40E-03 | 1.46E-03 | 1.39E-03 | 1.38E-03 | 1.45E-03 | 1.39E-03 |
| MCNP-DSP | | 1.43E-03 | 1.46E-03 | 1.45E-03 | 1.46E-03 | 1.44E-03 | 1.47E-03 | 1.45E-03 |
| % Diff | | -9.90% | -4.61% | 0.48% | -4.71% | -4.32% | -0.89% | -3.97% |

Previous BERP/Poly Data (smaller run times)

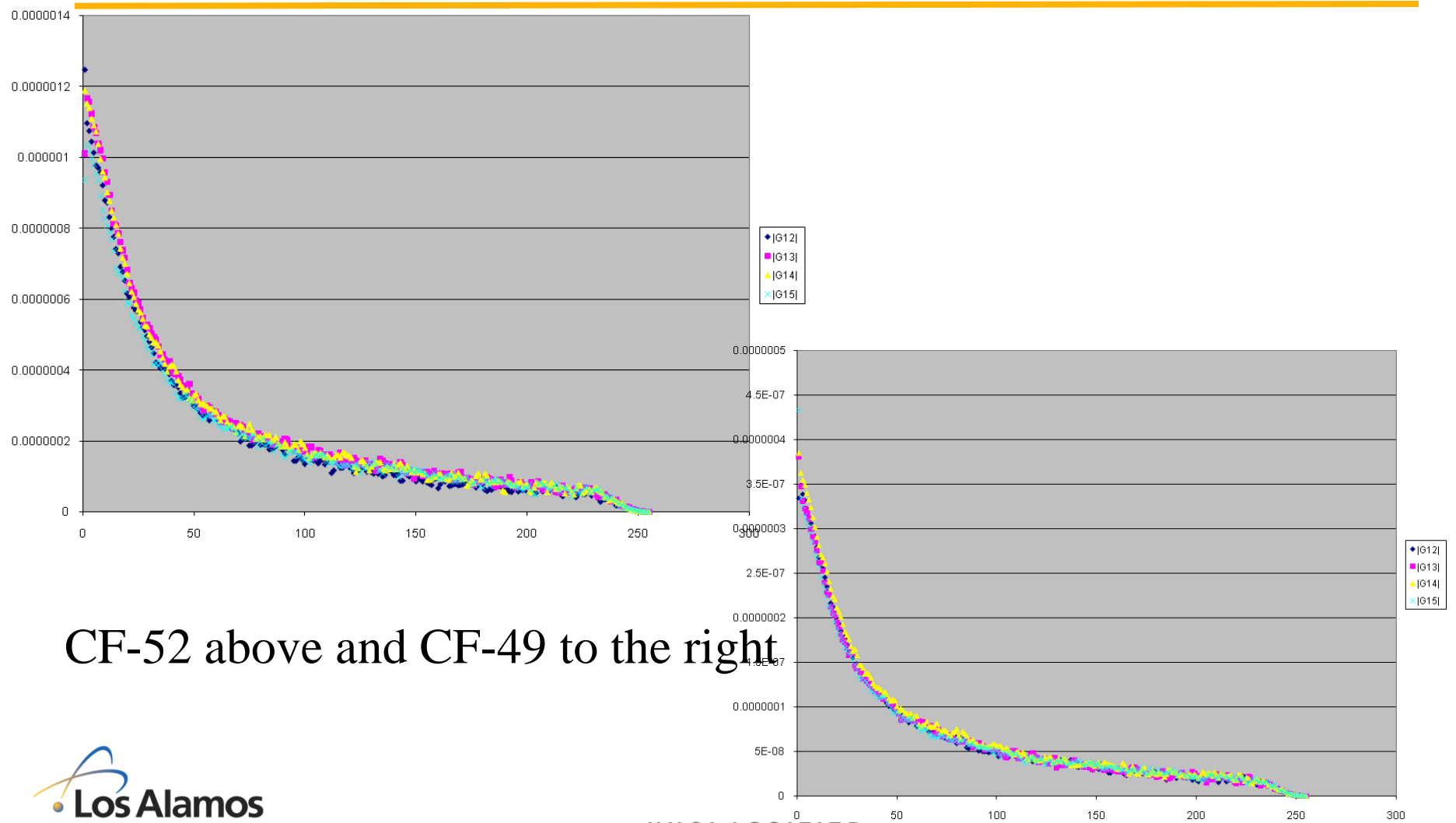
| | Configuration | Time (min) | R23 | R24 | R25 | R34 | R35 | R45 | Ravg |
|----------|---------------|------------|-----------|-----------|-----------|----------|-----------|----------|----------|
| Measured | 0 | 30 | 1.46E-01 | 1.46E-01 | 1.50E-01 | 1.43E-01 | 1.52E-01 | 1.36E-01 | 1.45E-01 |
| MCNP-DSP | | | 1.35E-01 | 1.43E-01 | 1.44E-01 | 1.45E-01 | 1.44E-01 | 1.36E-01 | 1.41E-01 |
| % Diff | | | 7.92% | 2.33% | 4.10% | -1.16% | 5.43% | -0.01% | 3.08% |
| Measured | 0.5 | 20 | 0.0621134 | 0.0657205 | 0.0665554 | 0.061851 | 0.0632787 | 0.062785 | 6.37E-02 |
| MCNP-DSP | | | 0.0597847 | 0.0625866 | 0.0628387 | 0.061986 | 0.0632081 | 0.05949 | 6.16E-02 |
| % Diff | | | 3.90% | 5.01% | 5.91% | -0.22% | 0.11% | 5.54% | 3.37% |
| Measured | 1 | 40 | 0.0275403 | 0.0256351 | 0.0261887 | 0.026492 | 0.0268792 | 0.023478 | 2.60E-02 |
| MCNP-DSP | | | 0.0251269 | 0.0262433 | 0.0260968 | 0.025915 | 0.0258855 | 0.025131 | 2.57E-02 |
| % Diff | | | 9.60% | -2.32% | 0.35% | 2.22% | 3.84% | -6.58% | 1.19% |
| Measured | 1.5 | 20 | 0.0104113 | 0.0102692 | 0.0105476 | 0.010142 | 0.0099596 | 0.009852 | 1.02E-02 |
| MCNP-DSP | | | 0.0108838 | 0.0111243 | 0.0112322 | 0.011179 | 0.011053 | 0.010883 | 1.11E-02 |
| % Diff | | | -4.34% | -7.69% | -6.10% | -9.28% | -9.89% | -9.47% | -7.79% |
| Measured | 3 | 30 | 0.0011623 | 0.000991 | 0.0012911 | 0.000931 | 0.0011436 | 0.000963 | 1.08E-03 |
| MCNP-DSP | | | 0.0014268 | 0.0014633 | 0.0014534 | 0.001461 | 0.0014442 | 0.001466 | 1.45E-03 |
| % Diff | | | -18.54% | -32.28% | -11.17% | -36.27% | -20.81% | -34.26% | -25.56% |

Measured frequency plots (frequency in Hz on the x-axis)



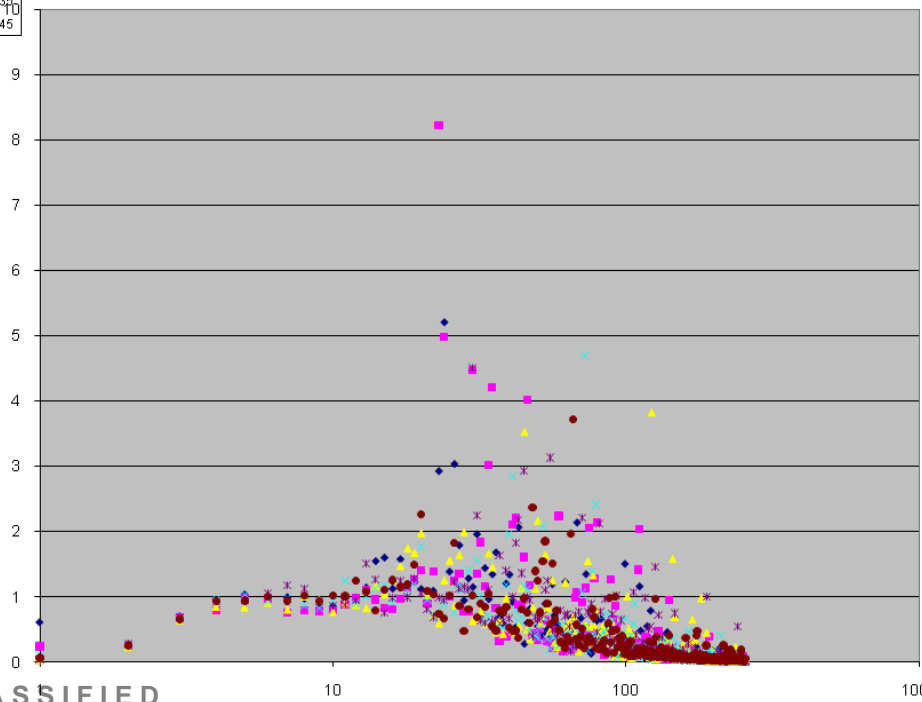
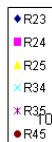
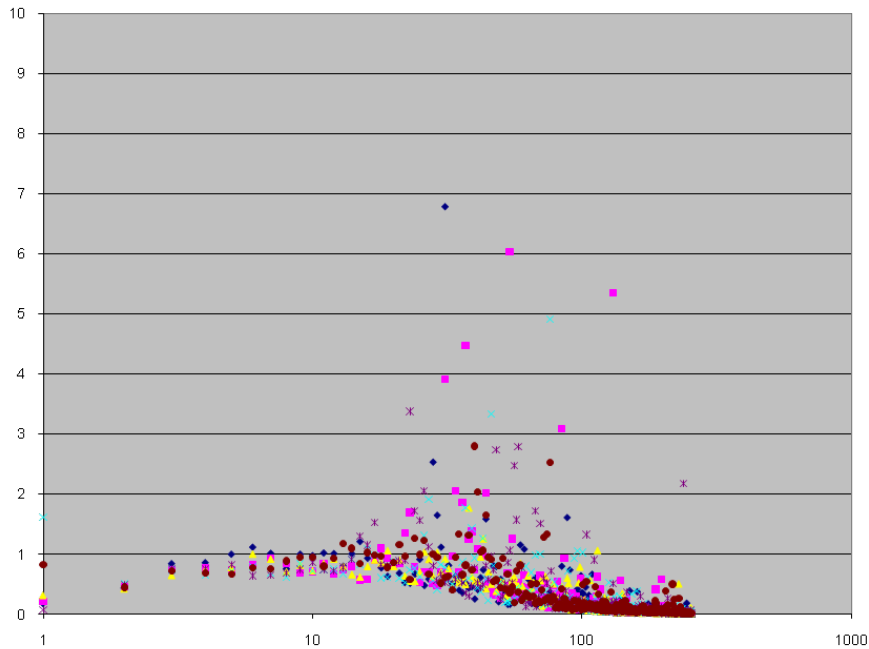
CF-52 above and CF-49 to the right

Detector Cross-Spectra



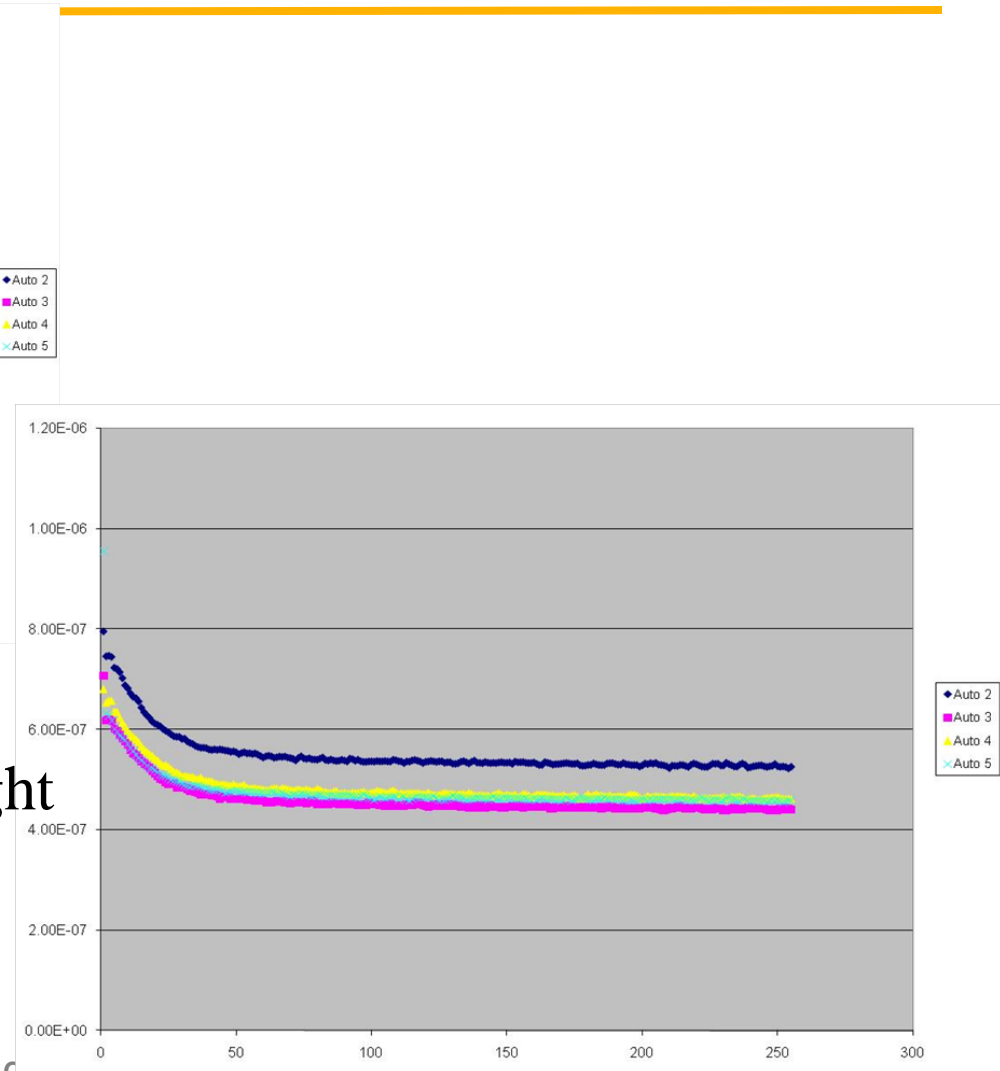
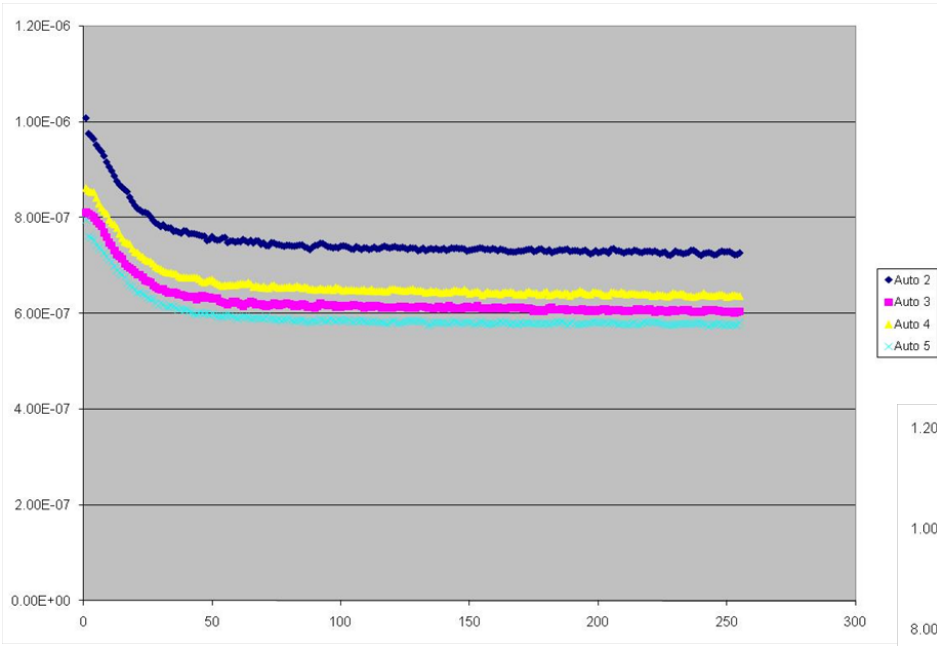
CF-52 above and CF-49 to the right

Spectral Ratio (R) Data



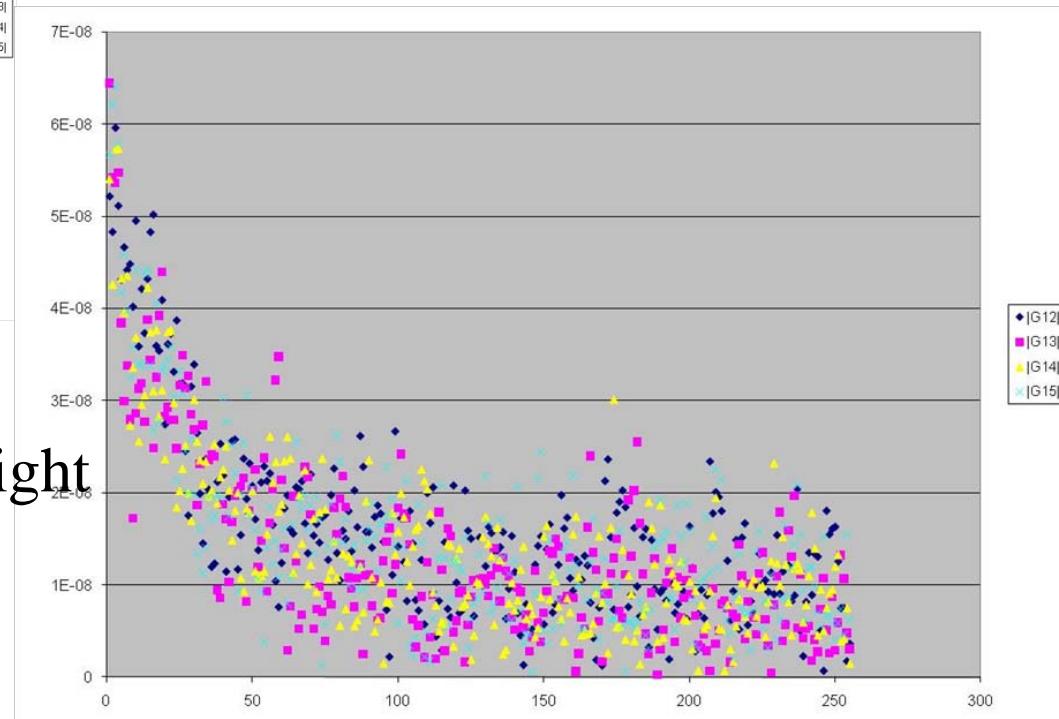
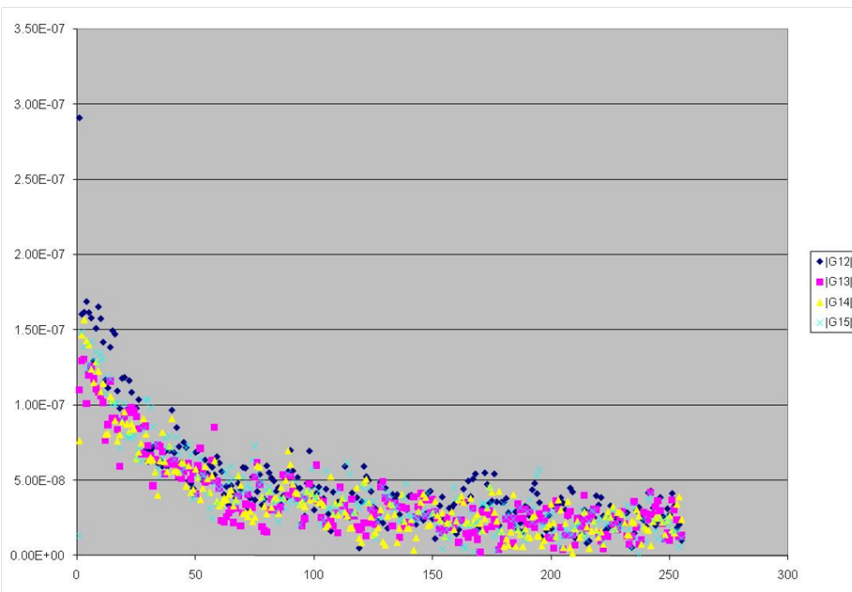
CF-52 above and CF-49 to the right

Detector Auto Spectra for BERP ball Reflected by 3 inch-thick Polyethylene



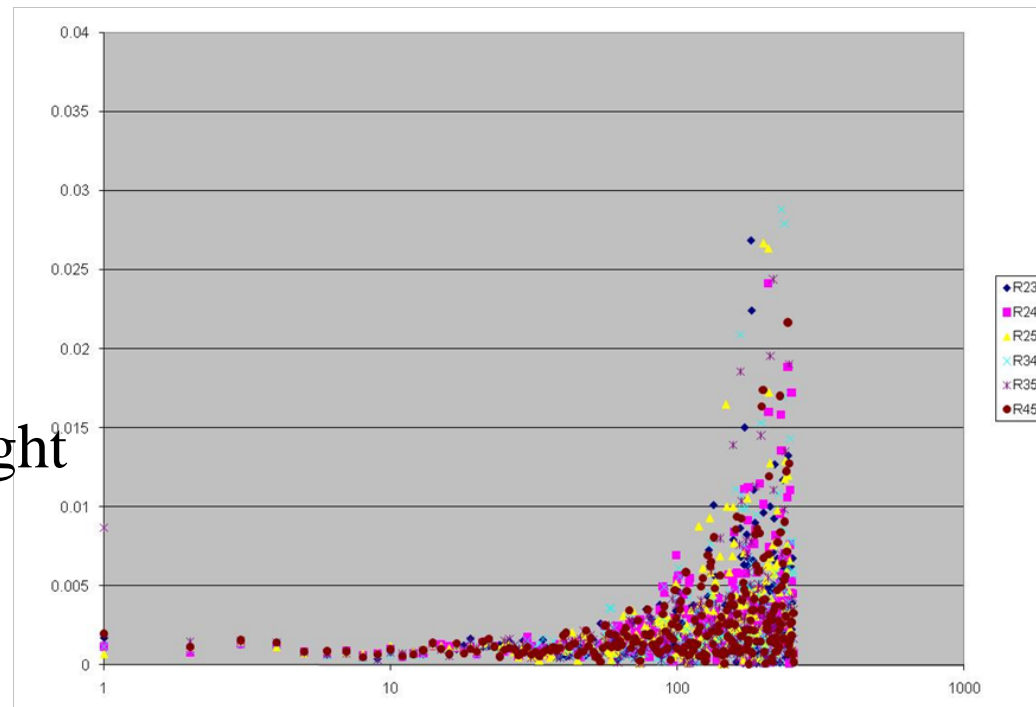
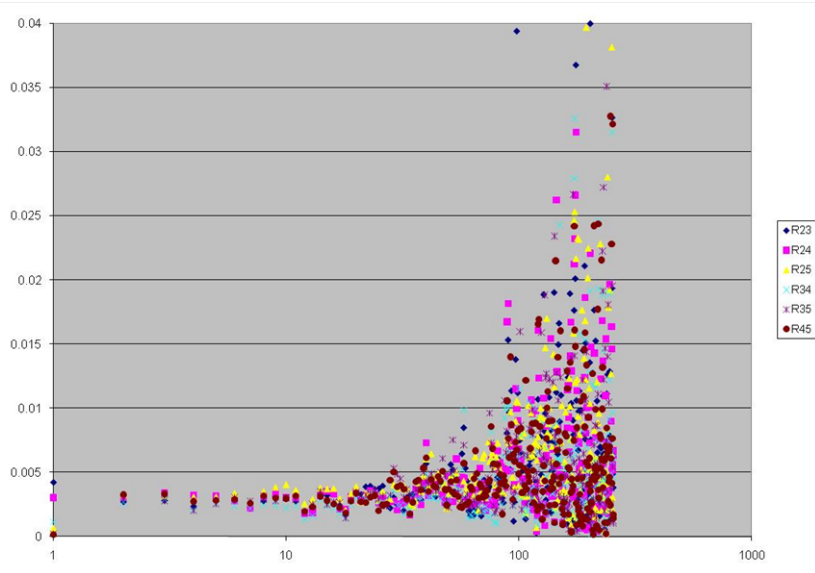
CF-52 above and CF-49 to the right

Source-Detector Cross Spectra for BERP ball Reflected by 3 inch-thick Polyethylene



CF-52 above and CF-49 to the right

Spectral Ratio (R) for BERP ball Reflected by 3 inch-thick Polyethylene



CF-52 above and CF-49 to the right

The Design and Application of the Pulse Arrival-Time Module for Passive and Active Subcritical Neutron Measurements

G. Arnone, J. Hutchinson, S. Melton, W. Myers, A. Sood

Los Alamos Nation Laboratory, MS-B228, Los Alamos, New Mexico 87545

INTRODUCTION

A data acquisition system was developed for making passive and active subcritical neutron measurements. This system is based on the LANL designed PATRM_PMC (Pulse Arrival Time Recording Module_PCI Mezzanine Card). We describe the data acquisition system along with the hardware and software design of the PATRM_PMC.

DESCRIPTION OF DATA ACQUISITION SYSTEM

The active interrogation data acquisition (DAQ) system, Fig. 1, consists of a tablet computer and a local computer connected by 100 feet of Gigabit Ethernet cable. The tablet computer runs the remote desktop program allowing the operator to control the local data acquisition computer from a remote location.

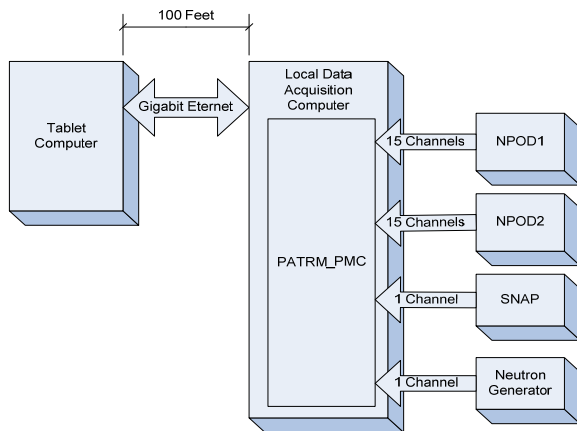


Fig. 1. Data Acquisition System Block Diagram

The main DAQ component located in the local data acquisition computer is the PATRM_PMC (Pulse Arrival-Time Recording Module / (PCI Mezzanine Card). This card allows the 31 signals from two NPODS and one SNAP detector modules to be interfaced to the system. The primary task of the PATRM_PMC is to generate a data array that contains a time tag and detector ID for every detector pulse. Another input channel is used for the VETO signal. In active interrogation mode, a VETO

pulse is used to synchronize data acquisition with the pulsing source, whether it is from a neutron generator or LINAC. The rising edge of the VETO pulse is used to initiate a user selectable veto-time-out period. During this time-out period pulses from the detector channels are not recorded. Also a special sequence is put into the data list to indicate a VETO has occurred.

Although only active interrogation was performed in this measurement set, the PATRM_PMC can be used in either passive or active mode. For a passive assay, the PATRM_PMC records neutron arrival times between the receipt of an external start and stop pulse resulting in a list of increasing clock ticks up to $(2^{32}-1)$ before rollover occurs.

Although the minimum tic time of the PATRM_PMC is 10ns or 100MHz for this data set the clock frequency was set to the following speeds: 10, 5, 2.5, and 1.25 MHz, resulting in time bins (tics of the clock) of 100, 200, 400, 800 ns, respectively. If several pulses arrive on the same tic of the clock, they will be recorded in sequential location with their arrival times the same and the detector ID indicating which channel was hit. A clock speed of 5 MHz, resulting time bins of 200 ns was used for this measurement set.

Two important innovations over the original PATRM have been implemented in the new PATRM_PMC list mode module, i.e., the ability to record arrival time for each individual detector channel and virtually unlimited storage capacity. Individual channel numbers were not needed for this application and therefore the channel information was stripped from the data stream prior to analysis. Development of new analytical techniques using both detector channel and timing data is currently underway. The original CAMAC-based PATRM had a storage limitation of one million words which resulted in taking multiple short measurements in highly multiplying configurations and storing each in a separate data file for analysis. The unlimited storage capacity of the new PATRM_PMC allows data to be taken as long as needed to achieve good statistics for analysis.

DETAILED PATRM_PMC DESCRIPTION

The PATRM_PMC provides time and channel tagging of every detected neutron event. This data is stored to on-board dual-ported memory and is available to the host

computer via the PCI bus. A feature of this module allows data to be analyzed in line using the on-board DSP (digital signal processor). The main components consist of a 1 million-gate XILINX FPGA (field programmable gate array), a 480-MFLOP Analog Devices DSP, 512 MB dual-ported memory and a PCI interface ASIC. The majority of the PATRM_PMC's design is contained in the FPGA. The design is static RAM based and is downloaded under software control; this allows hardware designs to be changed under program control. For example a different input configuration could be configured based on operator input. Also the program running in the DSP is RAM based and can also be changed under program control.

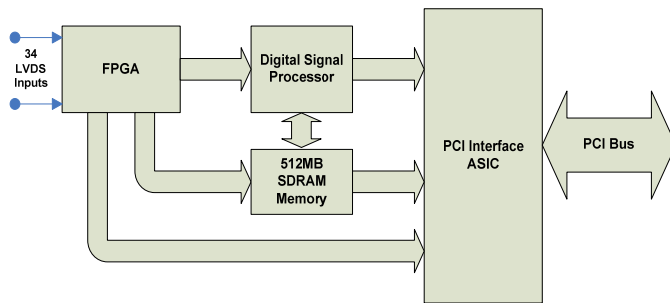


Fig. 2. PATRM_PMC Block Diagram



Fig. 3. Photograph of PATRM_PMC

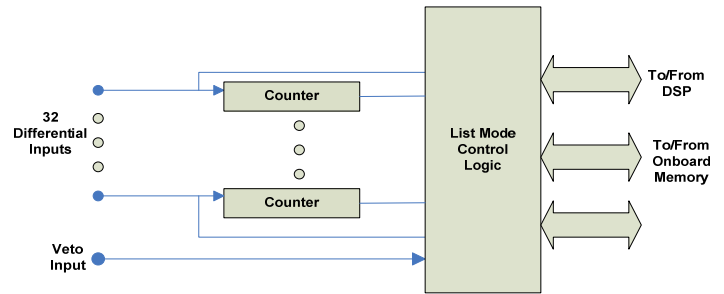


Fig. 4. FPGA Block Diagram

RESULTS

Validation and verification measurements were performed at the DAF and Los Alamos. The results were then compared with legacy data. We are currently working on firmware upgrades to provide a more robust passive mode capability.

The Design and Application of the Pulse Arrival-Time Module for Passive and Active Subcritical Neutron Measurements

G. Arnone, J. Hutchinson, S. Melton,
W. Myers, A. Sood

Los Alamos National Laboratory
N-2 (Advanced Nuclear Technology) and
XCP-7 (Transport Applications)

Outline

- What is List-Mode Data Acquisition?
- History of List mode hardware designs at LANL
- Description of current PATRM_PMC Hardware and Software Design
- Description of Complete Data Acquisition System
- Conclusion

What is List Mode Data Acquisition?

Recording a data set that includes the following information for each detection event

- Timing information
- Detector channel number

Benefits

- Original data is not converted or destroyed
- Several types of data analysis can be performed

Passive and Active Data Lists

Passive Data List

| | |
|------------|--------------------|
| 0x00000000 | 32 Bit Time Tag |
| 0x00000001 | 32 Bit Detector ID |
| 0x00000012 | 32 Bit Time Tag |
| 0x00001000 | 32 Bit Detector ID |
| 0x00000251 | 32 Bit Time Tag |
| 0x01000000 | 32 Bit Detector ID |
| 0x00012478 | 32 Bit Time Tag |
| 0x00100000 | 32 Bit Detector ID |
| 0x00043223 | 32 Bit Time Tag |
| 0x00000001 | 32 Bit Detector ID |

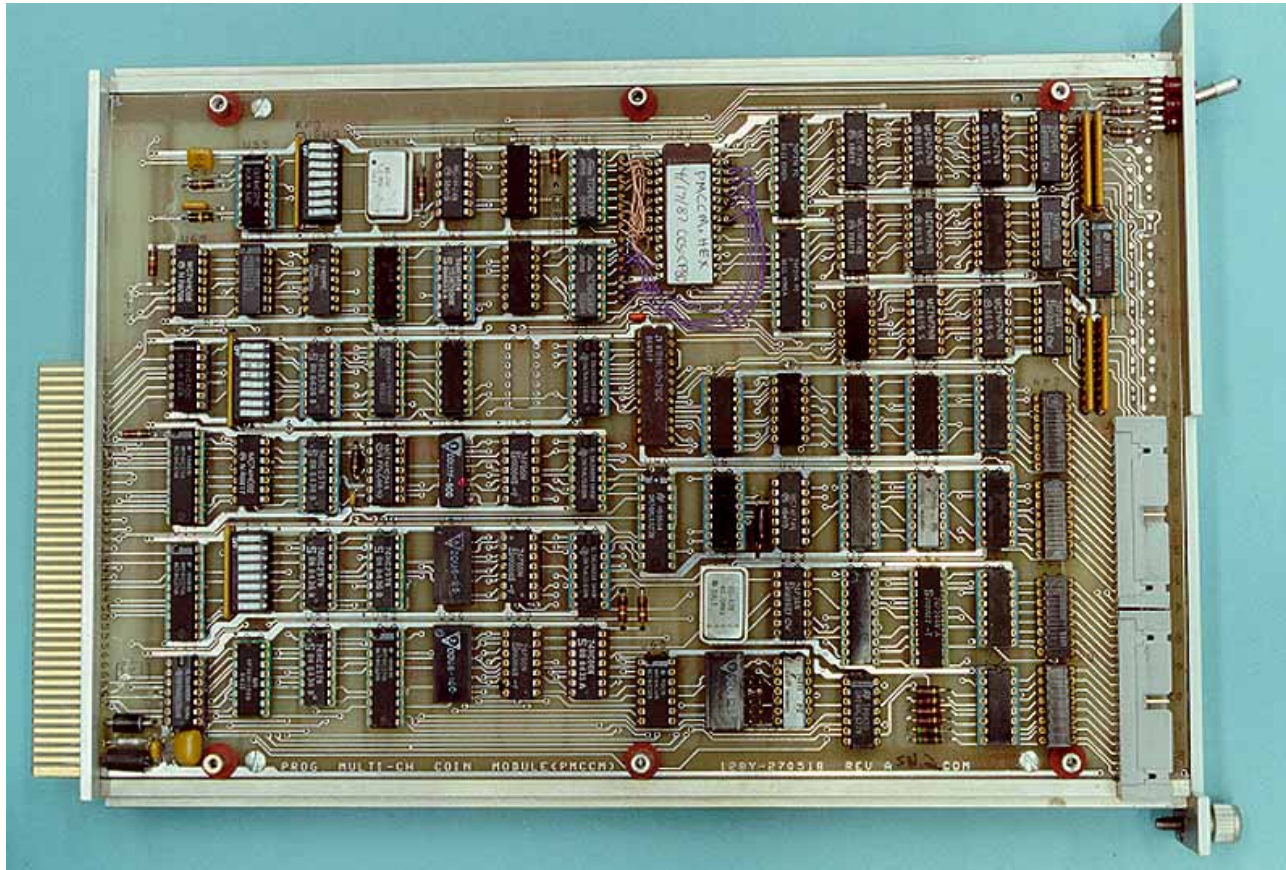
Active Data List

| | |
|------------|--------------------|
| 0x00000000 | 32 Bit Time Tag |
| 0x00000001 | 32 Bit Detector ID |
| 0x00000012 | 32 Bit Time Tag |
| 0x00001000 | 32 Bit Detector ID |
| 0x00000000 | Veto Mark |
| 0x00000001 | Veto Mark |
| 0x00000000 | 32 Bit Time Tag |
| 0x00100000 | 32 Bit Detector ID |
| 0x00000223 | 32 Bit Time Tag |
| 0x00000001 | 32 Bit Detector ID |

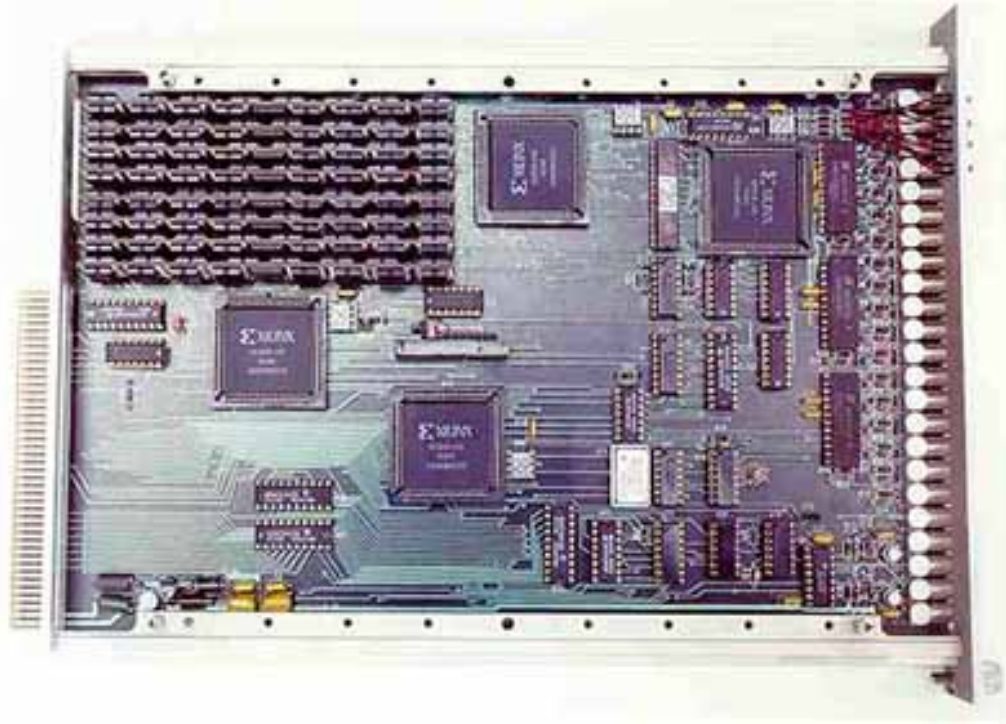
History of List Mode Hardware at LANL

- PMCCM (Programmable Multi-Channel Coincidence Module) CAMAC Standard
- PATRM I (Pulse Arrival Time Recoding Module) CAMAC Standard
- PATRM/PMC (Pulse Arrival Time Recoding Module) PMC (PCI Mezzanine Card)

PMCCM Photograph Circa 1987



Photographs of PATRM I Camac Based Circa 1991



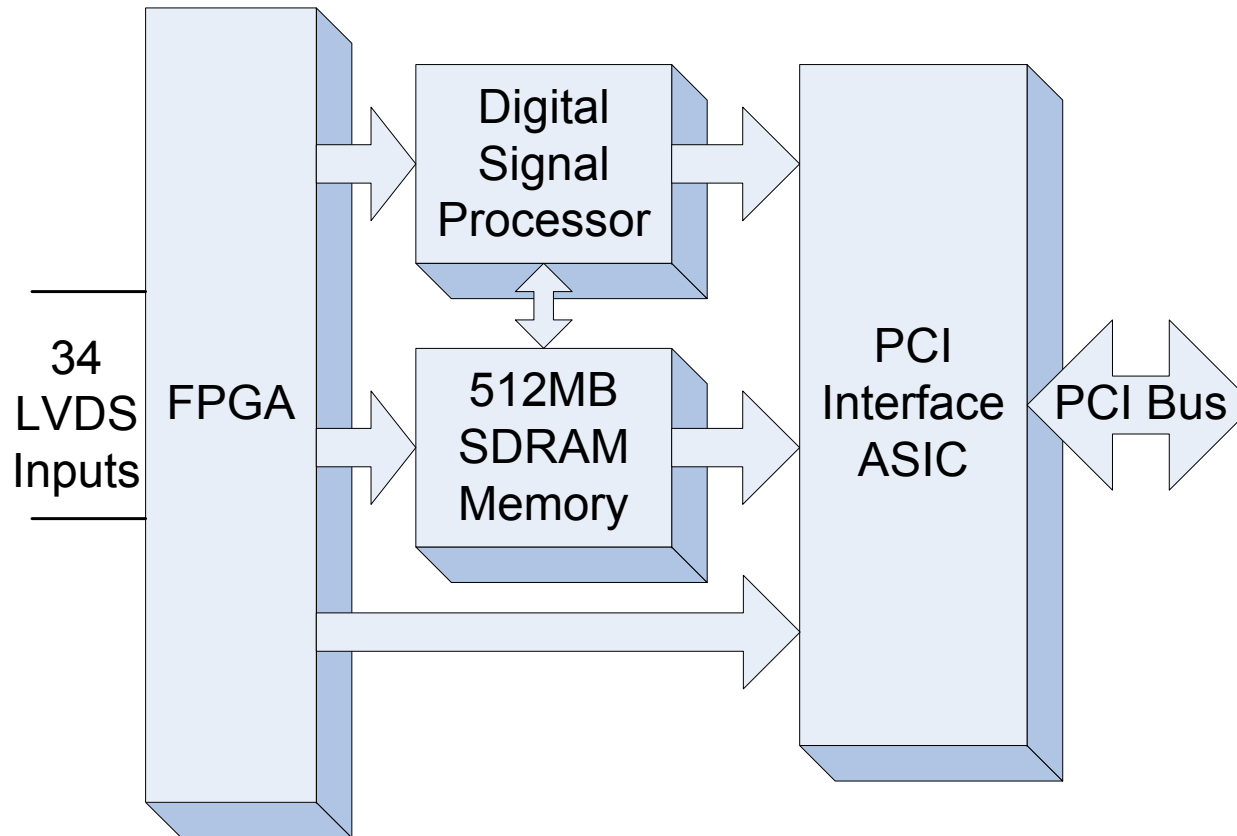
Photograph of PATRM_PMC



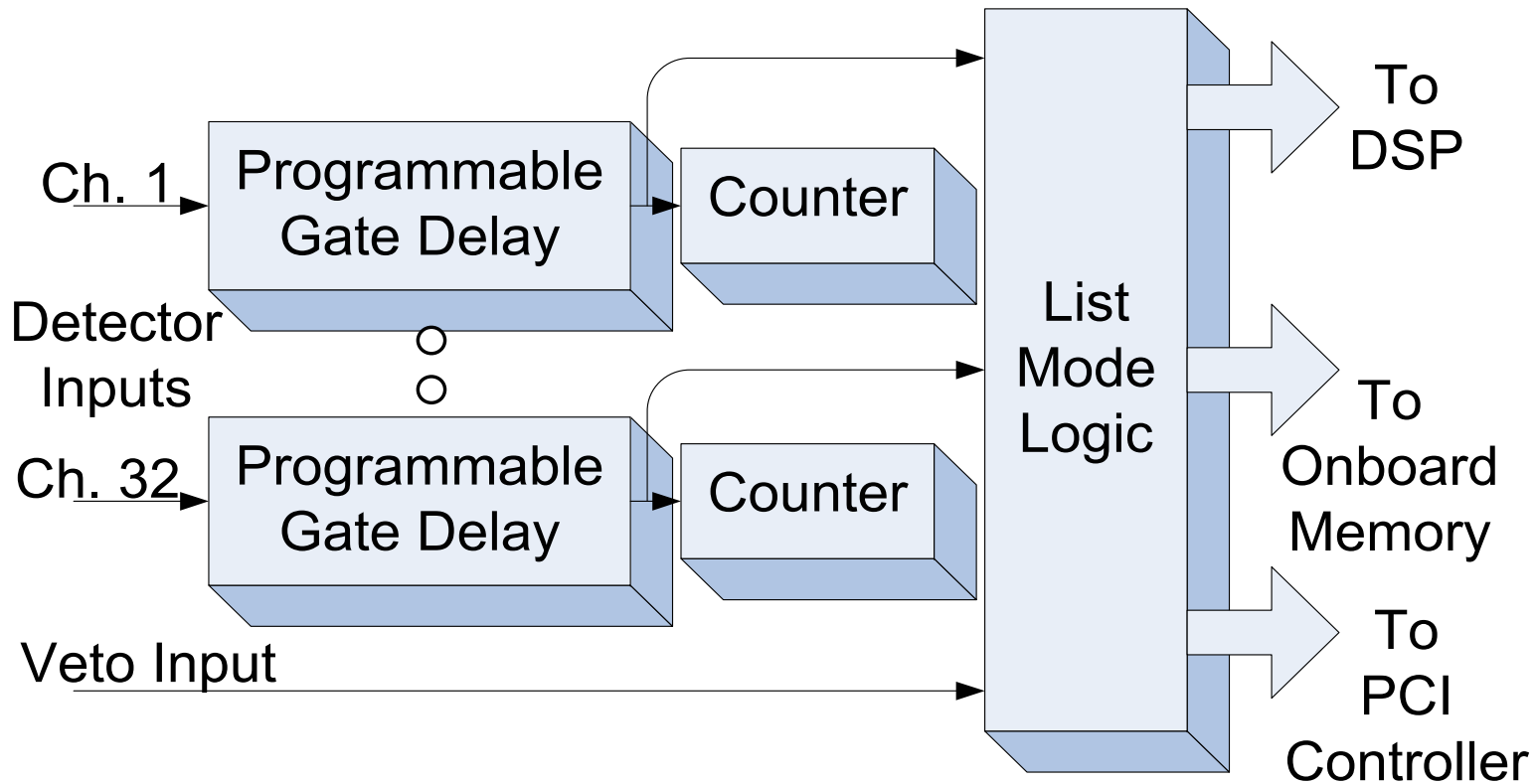
PATRM_PMC Features

- DSP (digital signal processor) (480 MFLOPS)
- 64-bit 66 MHz PCI interface (Rev. 2.2 compliant)
- 1 million-gate FPGA (field programmable gate array)
- FPGA reconfiguration “on-the-fly” from either the host or the DSP.
- 512 MB SDRAM (standard 144-pin SODIMM)
- 34 LVDS (Low-Voltage Differential Signals) inputs accessible via standard 68-pin SCSI-II type connector.
- Small PMC (PCI Mezzanine Card) form factor (74mm x 149mm).

PATRM_PMC Block Diagram



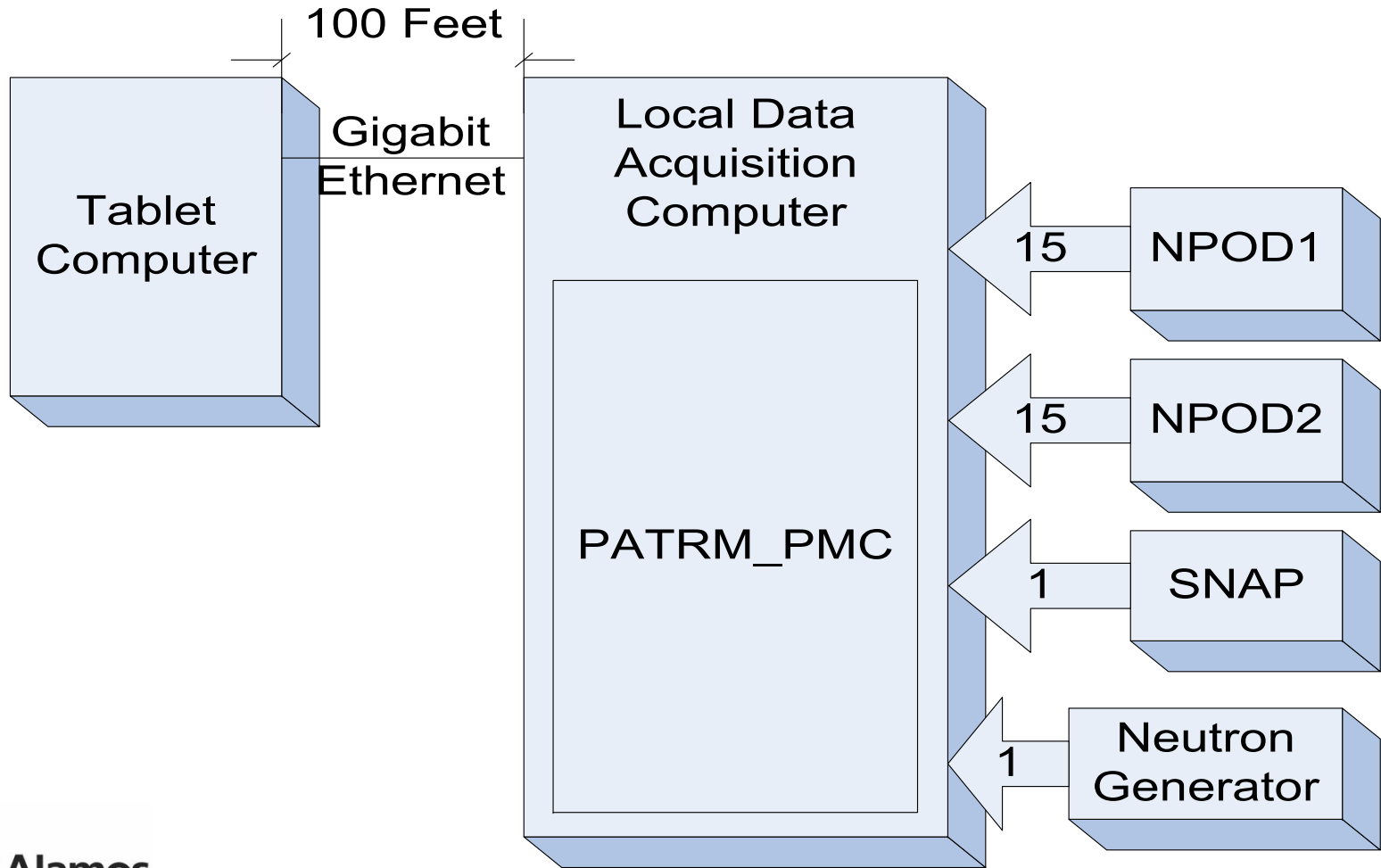
FPGA Block Diagram



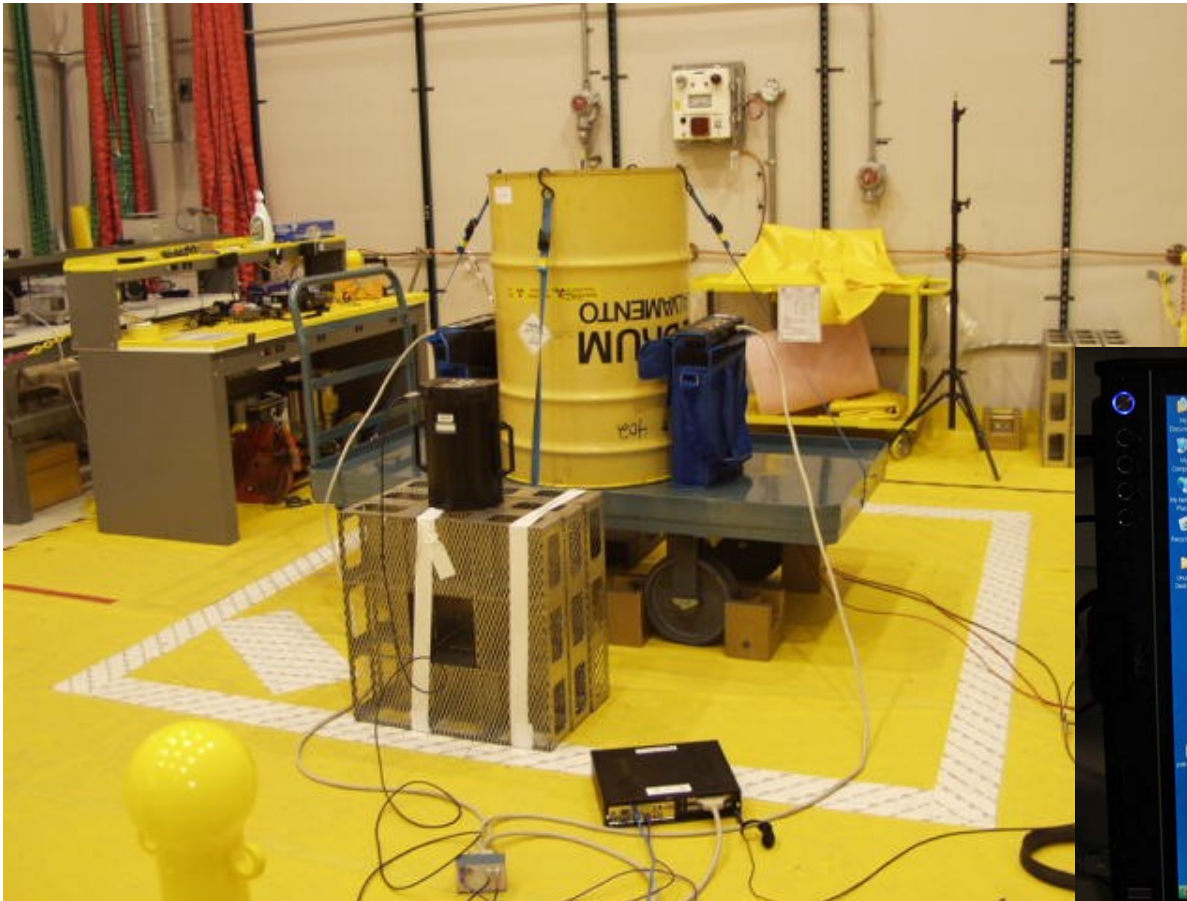
Local Data Acquisition Computer with Remote Tablet Computer



PATRM_PMC Data Acquisition System Block Diagram



Photograph of Data Acquisition System During Test



Remote Tablet Computer

Host Software Functions

- Overall control of PATRM_PMC
- Downloads hardware design into FPGA
- Downloads programs into DSP
- Human Interface
- Reads on-board memory and writes files to disk

Screenshots of Host Computer

PATRM NPOD MAIN

Ch NPOD1 Ch

| | | |
|----|-------|-------------|
| 0 | 0 | 0 |
| 1 | 0 | 1 |
| 2 | 0 | 2 |
| 3 | 0 | 3 |
| 4 | 0 | 4 |
| 5 | 0 | 5 |
| 6 | 0 | 6 |
| 7 | 0 | 7 |
| 8 | 0 | 8 |
| 9 | 0 | 9 |
| 10 | 0 | 10 |
| 11 | 0 | 11 |
| 12 | 0 | 12 |
| 13 | 0 | 13 |
| 14 | 0 | 14 |
| 15 | 0 | 0 |
| 16 | 0 | 1 |
| 17 | 0 | 2 |
| 18 | 0 | 3 |
| 19 | 0 | 4 |
| 20 | 0 | 5 |
| 21 | 0 | 6 |
| 22 | 0 | 7 |
| 23 | 0 | 8 |
| 24 | 0 | 9 |
| 25 | 0 | 10 |
| 26 | 16384 | 11 |
| 27 | 0 | 12 |
| 28 | 0 | 13 |
| 29 | 0 | 14 |
| 30 | 0 | Veto In |
| 31 | 0 | Snap In |
| 32 | | |
| 33 | | |
| 34 | 0 | NPOD1 Sum |
| 35 | 16384 | NPOD2 Sum |
| 36 | 0 | Hit Counter |

Ch NPOD2 Ch

Run Number: 0 Hit Count: 0

Data File Written: _____

Passive Mode
 Active Mode

Enable Acquisition (highlighted in green)
Quit (red button)

Veto Timeout (microsec): 800
 Generator Frequency (Hz): 50
 TMC Clock Period (ns): 200
 Acquisition Time: 0

Ch: 34 Frequency: 0

Enable Diagnostics

control0 = 129 status0 = 0 control1 = 0 status1 = 0 /

PATRM NPOD MAIN

Ch NPOD1 Ch

| | | |
|----|-------|-------------|
| 0 | 0 | 0 |
| 1 | 0 | 1 |
| 2 | 0 | 2 |
| 3 | 0 | 3 |
| 4 | 0 | 4 |
| 5 | 0 | 5 |
| 6 | 0 | 6 |
| 7 | 0 | 7 |
| 8 | 0 | 8 |
| 9 | 0 | 9 |
| 10 | 0 | 10 |
| 11 | 0 | 11 |
| 12 | 0 | 12 |
| 13 | 0 | 13 |
| 14 | 0 | 14 |
| 15 | 0 | 0 |
| 16 | 0 | 1 |
| 17 | 0 | 2 |
| 18 | 0 | 3 |
| 19 | 0 | 4 |
| 20 | 0 | 5 |
| 21 | 0 | 6 |
| 22 | 0 | 7 |
| 23 | 0 | 8 |
| 24 | 0 | 9 |
| 25 | 0 | 10 |
| 26 | 16384 | 11 |
| 27 | 0 | 12 |
| 28 | 0 | 13 |
| 29 | 0 | 14 |
| 30 | 0 | Veto In |
| 31 | 0 | Snap In |
| 32 | | |
| 33 | | |
| 34 | 0 | NPOD1 Sum |
| 35 | 16384 | NPOD2 Sum |
| 36 | 0 | Hit Counter |

Ch NPOD2 Ch

Run Number: 0 Hit Count: 0

Data File Written: _____

Passive Mode
 Active Mode

Enable Acquisition (highlighted in green)

Diagnostic Controls

- FPGA Bit File Download
- Start FPGA** (red button)
- DSP Program Download
- Restart DSP Program
- Stop DSP
- Interrupt up
- Interrupt down
- Interrupt1
- Clear Memory
- Stat_0: 0
- Stat_1: 0
- Mode = 0
- Enable Diag** (green button)

Simulation Controls

- Generate Data
- Abort Run** (red button)
- Write Files
- Read File

Veto Timeout (microsec): 800
 Generator Frequency (Hz): 50
 TMC Clock Period (ns): 200
 Acquisition Time: 0

Ch: 34 Frequency: 0

Enable Diagnostics

Data Transfer

- View Limits: 0.01001440000, 0
- Start STD Transfer
- Start DMA Transfer
- Fill List
- Clear List
- Write Data File
- Read Data File

C:\PatrmPMC\pga_bit_files\patrm_npod_main.bit
 C:\PatrmPMC\dsp_sw\Patrm_npod\release\Patrm_npod.exe
 FIFO_WR_COUNTER = 0
 FIFO_RD_COUNTER = 0
 HIT_COUNTER_LSW = 0
 Interrupt count = 0
 FullEmpty = 0
 Interrupt Status = 0
 Feedback = 0
 UpdateCount = 0

control0 = 129 status0 = 0 control1 = 0 status1 = 0 /

Summary of FY10 Activities

- Performed Validation and Verification Measurements at DAF and Los Alamos
- Compared results with legacy data
- Updated hardware and firmware as needed
- Currently working on firmware upgrade to ensure robust passive mode data acquisition capability

Current Capabilities for Generating List-Mode Data for Simulated Subcritical Neutron Measurements using MCNP

Avneet Sood, J.D. Hutchinson, W.L. Myers, and C.J. Solomon

Los Alamos National Laboratory, P.O. Box 1663 MS A143, Los Alamos, NM 87545

INTRODUCTION

The Monte Carlo N-Particle (MCNP) transport code [1] is a standard in the field of computational Monte Carlo radiation transport. One reason MCNP has become such a standard is the extensive benchmark testing and validation it has undergone. This work examines extensions to MCNP that allow descriptions of correlated fission sources and list-mode tally output for comparisons with sub-critical multiplication measurements. Our simulated list-mode results are intended to be compared with recent validation sub-critical multiplication measurements performed at the Nevada Test Site's Device Assembly Facility. Spontaneous fission and (α ,n) neutron sources were used in both bare and reflected/moderated configurations.

BACKGROUND

Spontaneous and induced fission sources, (α ,n) sources

Intrinsic sources of neutrons in special nuclear materials (SNM) are usually generated through spontaneous fission emission or through the α decay of the SNM and subsequent neutron production in low-Z materials. Neutrons emitted from spontaneous fission are considered to be born instantaneously and at the same location and are thus correlated. Examples of spontaneous fission nuclides include Cf-252 and Pu-240. The number of neutrons emitted in spontaneous (or induced) fission (neutron multiplicity) can vary from one fission to another according to the distribution of the excitation energy of fission fragments. Terrell's work [2] has shown that the multiplicity distributions for both spontaneous and thermal, neutron-induced fission can be approximated by a Gaussian distribution, centered at $\bar{\nu}$. The Gaussian widths that describe the neutron multiplicity distribution exist in several tabulated data sets. Delayed neutrons originate from some of the isotopes that are produced during beta decay of the fission fragments and appear characteristically with the half-lives of their precursors. Alpha particles produced by SNM decay with subsequent absorption in low-Z materials can produce neutrons with intensities comparable with spontaneous fission. This is especially true if isotopes with high alpha decay rates (e.g. U-233, U-234, Pu-238, or Am-241) are present near low-Z targets like O-18, F-19, Be-7, and Li-6. Typical nuclear fuel cycle materials are PuO₂, UF₆, and PuF₄. Common commercial neutron sources include AmBe, AmLi, PuBe, PuC.

Coincidence (multiplicity) counting

The amount of SNM present in bulk samples can be assayed by neutron coincidence (multiplicity) counting. Coincidence counting exploits the fact that neutrons emitted from spontaneous or induced fission are emitted essentially simultaneously and from the same location. A unique signature for a particular nuclear material can be measured even in the presence of background neutrons or (α ,n) because these sources of neutrons are random (not coincident) in their arrival times. While passive neutron counting of spontaneous and induced fission is most routinely performed, (α ,n) induced fissions can also be measured by discrimination against the uncorrelated source. The typical procedure begins with recording the time of a neutron capture event in a neutron detector (He-3 embedded in polyethylene) over a large collection time (e.g. 300 seconds). These data are grouped into capture times in a larger number (e.g. 1 million) smaller time sub-intervals (e.g. 250 μ sec). These time sub-intervals are larger than typical neutron detection and lifetimes which are of the order of 50 μ sec. A multiplicity histogram, called a Feynman histogram, with these characteristics can be constructed from the measured data. The resulting Feynman histogram obeys Poisson distribution if the system is non-multiplying (i.e. neutrons are emitted randomly in time). Deviations from the Poisson distribution indicates a correlated (spontaneous or induced fission) source. The measured data, time of absorption and (detector) location, is called list-mode data.

MCNP Simulations

MCNP is well suited for numerical simulations of sub-critical multiplication because of the three-dimensional geometry representations and continuous-energy nuclear cross section data. Extensive verification and validation documentation exists for a variety of fixed-source and eigenvalue problems. While simulated results are on average correct, MCNP does not represent the spontaneous and induced fission process microscopically correct. For example, the user can define source location, direction, energy, time, and intensity of a spontaneous fission or (α ,n) neutron source but cannot define a fission event (e.g. sample the number of neutrons emitted from $\bar{\nu}$, nor define correlated (time, location) neutron sources. MCNP cannot (easily) record the time and location of detection (Note this may be possible using MCNP's PTRAC capability and user-created external scripts to extract this information but it is not straight-forward). Accurate comparisons of simulation of spontaneous or induced fission neutrons must account for

the correlated fission time, location, and number and produce list-mode data for comparisons. Standard MCNP is not microscopically correct enough to compare with current sub-critical measurements.

RESULTS

MCNP Extensions

An internally-developed “multiplication” patch to MCNP was developed over 25 years ago [3] and was routinely used for comparison with sub-critical multiplication measurements. This patch extended MCNP to use Terrell’s method to statistically sample the actual number of neutrons (rather than $\bar{\nu}$) released when fixed source and induced fissions occurred, have a fixed-source problem that starts fission events, and write a special output file that contained the time at which each neutron was captured in the He-3 gas of the detector tubes. We have updated this work by creating user-defined SOURCE and TALLYX subroutines that are independent of MCNP and can be used with any previous or future version of the code. Our SOURCE subroutine modifies the definition of starting particles to be a starting reaction (e.g. spontaneous fission) and samples starting particles from that reaction. Our TALLYX subroutine modifies a type 4, track length-based tally, to produce a file of absorption times in a tally cell (a.k.a. list-mode data). Our tally output can be processed to analyze inferred multiplication using any available technique (e.g. Feynman analysis, CSDNA, etc).

Sub-critical Validation Measurements

In FY10, we began a series of validation measurements at the Nevada Test Site’s DAF using a variety of well-characterized neutron source and shielding configurations. The series of measurements included weapons grade plutonium (WGPu) (e.g. Berp ball), highly enriched uranium (HEU) (e.g. Rocky Flats shells), spontaneous fission and (α,n) sources (e.g. Cf-252, AmBe), and active interrogation sources (e.g. 14 MeV D-T generator). List-mode data was recorded for WGPu and HEU sources using multiple moderators and reflectors using passive and active neutron sources. The numerical simulations of these measurements are in progress.

Preliminary Benchmark Comparison

One series of recent measurements was performed by Sandia National Laboratory in January 2009 and submitted to RSICC’s Shielding Integral Benchmark Archive and Database (SINBAD). Figure 1(a) shows the experimental configuration measuring the WGPu source (Berp ball) using LANL’s SNAP and NPOD neutron detector and a 140% HPGe detector. Figure 1(b) shows a histogram of the simulated list-mode data for the SNL measurement. Figure 2 shows the calculated and

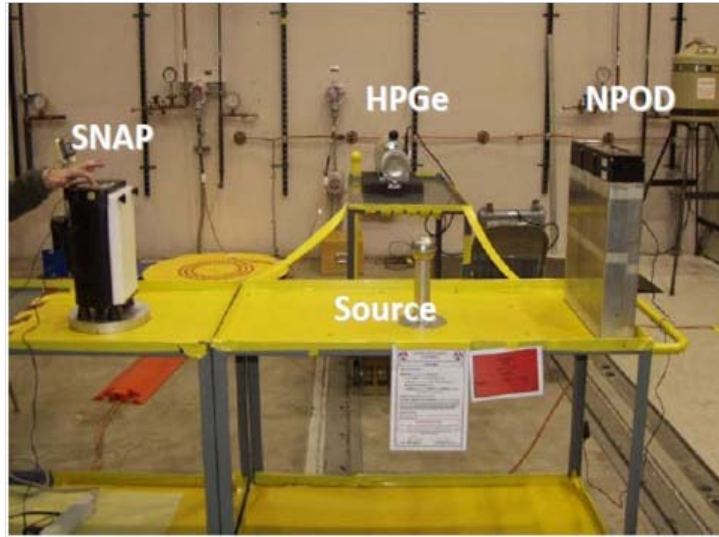
measured counts for the SNAP and NPOD neutron detectors. The predicted and count rates are within 15

CONCLUSION

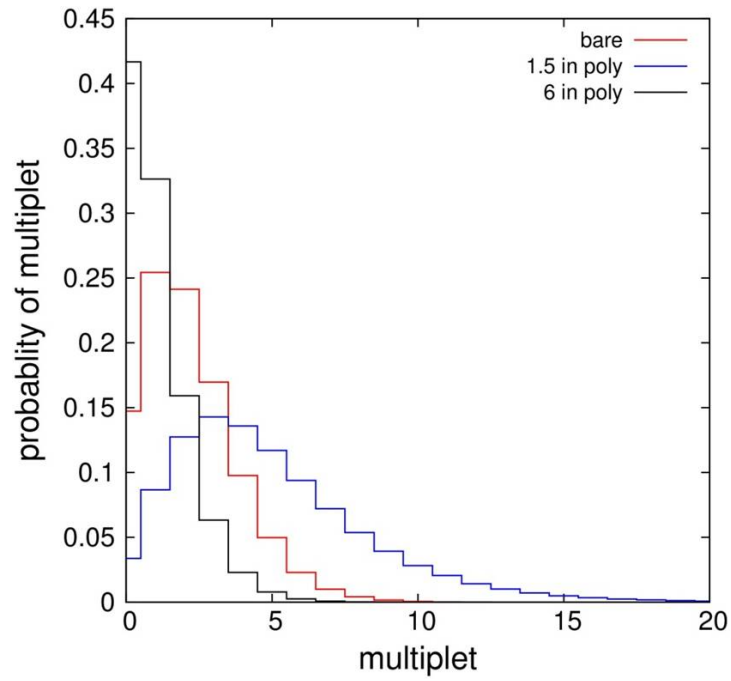
Standard MCNP is not microscopically correct enough to produce list-mode data ready for comparison with subcritical multiplication measurements. We have upgraded an existing capability to produce user-defined source and tally subroutines that can be readily compiled with existing or previous versions of MCNP to provide list-mode comparisons. Our initial comparisons are encouraging. Further improvements in our models and comparisons with other measurements are expected to decrease the systematic difference in our existing computed results.

REFERENCES

- [1] X-5 Monte Carlo Team, *MCNP—A General Monte Carlo N-Particle Transport Code, Version 5*, 2003.
- [2] James Terrell, Distributions of fission Neutron Numbers,, *Physical Review*. **108**, 783-789 (1957).
- [3] H. Grady Hughes and Robert G. Schrandt Gaussian Sampling of Fission Neutron Multiplicity, Los Alamos National Laboratory memorandum X-6:HGH-86-264 (1986).
- [4] J. Mattingly Polyethylene-Reflected Pu metal Sphere, SAND2009-5804

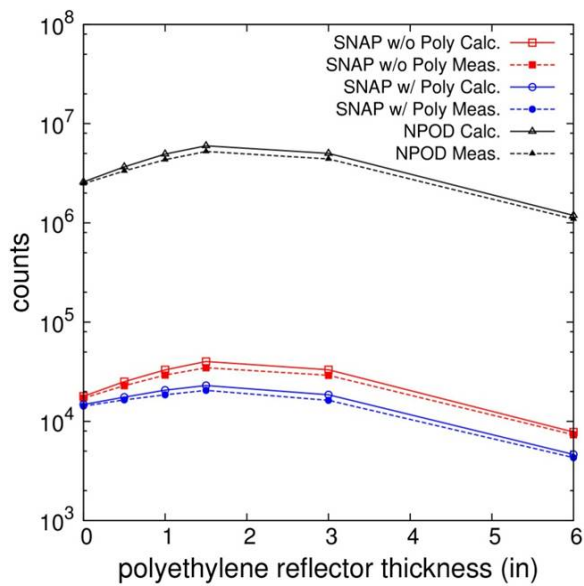


(a)

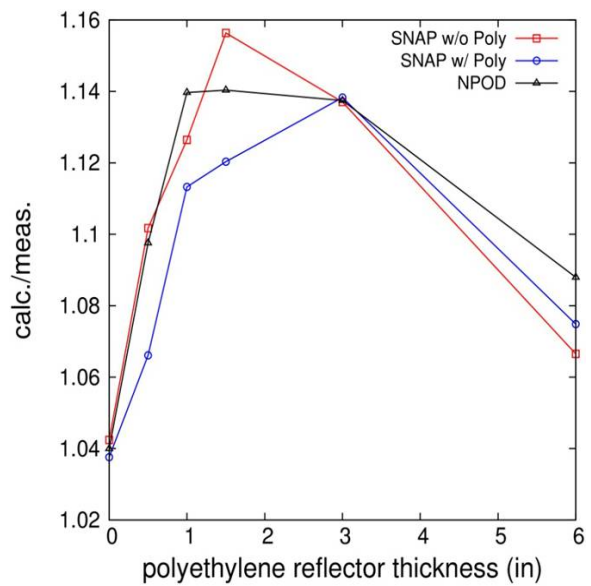


(b)

Fig. 1. (a) NTS DAF measurement of polyethylene-reflected Pu Metal Sphere (b) Simulated list-mode data for bare Berp ball



(a)



(b)

Fig. 2. (a) Comparison of measured and simulated SNAP and NPOD counts for bare and polyethylene reflected Berp ball (b) calculated/measured ratio of measured and simulated counts

Current Capabilities for Generating List-Mode Data for Simulated Subcritical Neutron Measurements Using MCNP

**Avneet Sood, J. Hutchinson, W. Myers,
C.J. Solomon**

Los Alamos National Laboratory

Los Alamos, NM 87545



UNCLASSIFIED

Operated by Los Alamos National Security, LLC for NNSA



Abstract

- **This presentation briefly describes the following topics:**
 - Review of sub-critical multiplication and measurements,
 - Current MCNP simulation capabilities,
 - MCNP modeling needs for comparisons with sub-critical multiplication measurements
 - Summary of FY10 work, Progress on FY11 work

Relevant Physics for Sub-Critical Multiplication

- **(Source) Passive neutrons from fissionable material emitted from:**
 - **Spontaneous fission neutron sources:**
 - Correlated in time and location of fission
 - Examples: Cf-252, Pu-240
 - **(α , n) reactions:**
 - Produced when α particle is absorbed and neutron is emitted
 - Not correlated in time and location
 - Examples: Am-Be
- **(Induced) Neutron multiplication dominated by two physical processes:**
 - **(n,2n)**
 - Occurs mostly above 7 MeV
 - Does not contribute significantly to most scenarios
 - **Neutron-induced Fission**

Simulations need to be “microscopically” correct for comparisons with measured data.

Sub-critical Measurements

- **Neutron multiplication measurements (passive and active) designed to separate the multiple neutron emission events from the (α,n) background neutrons.**
 - Record time of neutron capture in a neutron detector over a large collection time (e.g. 300 sec)
 - Group these capture times in a large number (e.g. 1 M) smaller time sub-intervals (e.g. 250 μ sec)
 - These time sub-intervals are larger than typical neutron detection and lifetimes (~50 μ sec)
 - Multiplicity histogram is constructed
 - Obeys Poisson statistics if system is non-multiplying (i.e. neutrons are emitted randomly in time)
 - Data analysis begins...Feynman Variance-to-Mean, CDNA, etc

Data recorded is neutron detector location and time: list-mode data

Simulations need to produce list-mode data for comparisons

MCNP Simulations of Sub-Critical Measurement

- **MCNP – well suited for comparing results of sub-critical measurements**
 - Calculates relevant quantities for fixed-source, eigenvalue problems
 - How faithfully is MCNP simulating fission process and what we measure?
 - Correct for averaged values but not microscopically correct
- **MCNP simulation of neutron sources**
 - User can define location, direction, energy, time, and intensity of SF, (α,n) neutron sources
 - User **cannot** define fission events
 - e.g. sample number of neutrons emitted from ν_{bar}
 - User **cannot** define correlated (time, location) neutron sources
 - MCNP samples these values from user's input
 - User **cannot** (easily) record location and time of detection.
 - Possible using MCNP's PTRAC capability and a user-created external script to extract this information

Standard MCNP is not microscopically correct enough to compare with current sub-critical measurements:

FY10 Proposal to NCSP

■ Upgrade an existing (unreleased) capability for MCNP

- Use of Terrell data to statistically sample the actual number of neutrons ν released when **induced fissions** occurred in a calculation.
 - MCNP 5.1.40 can do this for induced fissions, but not starting sources
- Add capability to have a fixed source problem that started fission events (correlated) rather than individual neutron histories (independent samples),
- Add capability to allow for a non-fissioning interrogating source (eg. AmBe), and
- Add capability to write a special output file that contained the time at which each neutron was captured in the He-3 gas of the detector tubes (list-mode data)
- Resulting list-mode data can be evaluated by any analysis technique
- **Capability has existed separately for over 25 years (internally V&V'd)**
- **Difficult to maintain separately**
 - Make use of MCNP's user-defined subroutines SOURCE/TALLYX
 - Compare to existing benchmarks

■ FY10 proposal leveraged on-going experiments and equipment to record list-mode data (e.g. PATRM/PMC)

Deliverables for FY10

- **(1) Update the list-mode multiplication capability to MCNP5.1.51.**
 - Implement this capability as a routine that can be applied to any future version of MCNP through the SOURCEX and TALLYX routines provided with MCNP.
 - Produce MCNP5.1.51 executable (sequential, OpenMPI) with standard features plus correlated sources and list-mode capability.
- **(2) Compare and document simulated results with previous experimental results performed at LANL.**
- **(3) Compare and document simulated results with experiments to be performed at LANL or other ICSBEP experiments**
 - (a,n) sources with poly, SS shells, etc
 - SUB-PU-MET-FAST-001,002,and 003
- **(4) Begin R&D for application of variance reduction techniques to accelerate convergence of problems (current simulations are performed in analog mode)**
- **(5) Compare and document our simulation results using currently available codes MCNP-DSP and MCNP-Polimi (code-to-code verification)**
 - UNLV sub-task

FY10 Q4 Results

- **Internally-developed multiplication patch to MCNP has been updated to MCNP5.1.51**
 - Coding existed in internal version of MCNP
 - Initial testing indicates code is working as expected. Comparison with experiments began
 - Still working on developing an independent SOURCE and TALLYX subroutine
- **Validation experiments performed at NTS/DAF**
 - Diagnostics included 2 NPODS, SNAP, 140% HPGe.
 - List-mode data taken, MCNP models developed/improved
 - **May 2010:** BeRP ball (bare), BeRP ball moderated with increasingly thick shells, BeRP ball moderated with fixed outer dimension and variable thickness
 - BeRP ball supported with hemi-shell – no longer a 1-D problem!
 - Two different moderators
 - **July 2010:** BeRP with different moderator, Active interrogation with D-T source
 - **September 2010:** Rocky Flat Shells (HEU) with Cf-252 source and multiple poly configurations

FY11 Q1 - progress

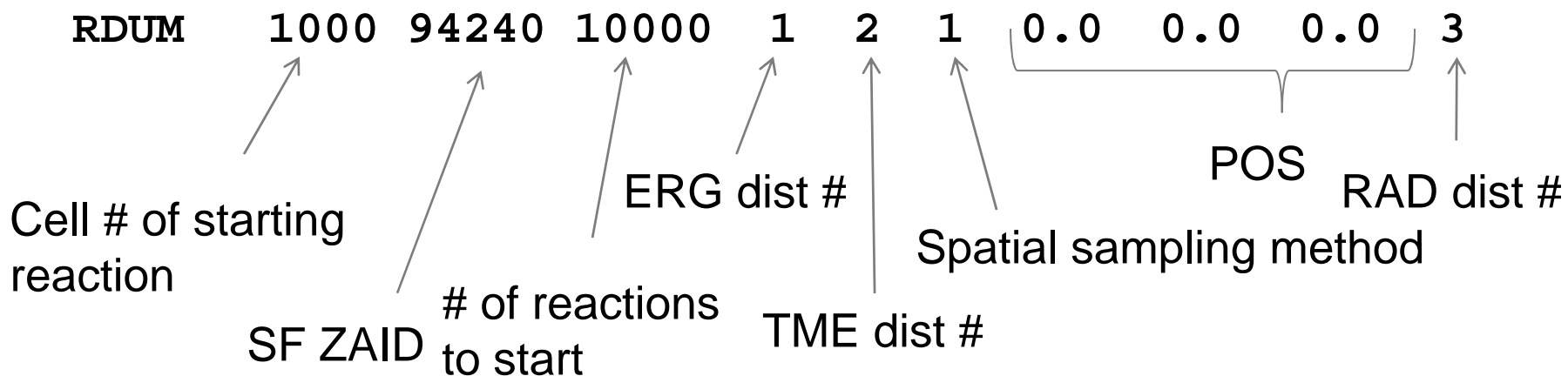
- **SOURCE/TALLYX subroutines written**
 - Subroutines intended for user-defined source and tally
 - Independent of MCNP – no modification of MCNP is required
- **SOURCE—modifies definition of starting particle to be a starting reaction, e.g., spontaneous fission, samples starting particles from that reaction**
- **TALLYX—modifies a type 4 tally to produce a file of absorption times in tally cell, a.k.a. list-mode data**
- **Tally output can be processed to analyze inferred multiplication**

We plan to submit SOURCE/TALLYX routines to MCNP code development team for adaptation into MCNP6 with documentation, validation benchmarks, etc

SOURCE Input Uses RDUM Card

- Input for the source is specified on the RDUM card

EXAMPLE:



- Multiple cells and SF ZAID combinations may be specified—sampled based on the # of starting reactions

Tally Modification Requires FU Card

- The FU card modifies the tally to score captures

- Requires analog simulation

- Sample fission multiplicity

```
phys:n 4j 1 or phys:n 4j 2
```

- Turn off default implicit capture

```
cut:n 2j 0
```

- **EXAMPLE:**

```
F4:n 1001 $ Tally on cell 4
```

```
FU4 2003 $ Score captures by ZAID 2003 (He-3)
```

Example Tally List-Mode Output

| | |
|------|-------------------|
| 3050 | 2902347683.93636 |
| 3049 | 25617701923.43888 |
| 3052 | 28074609346.68214 |
| 3050 | 20857333210.41721 |
| 3052 | 16140211088.86106 |
| 3053 | 24770874466.83554 |
| 3047 | 24759462750.29287 |
| 3049 | 15567786730.17038 |
| 3052 | 21217419855.78508 |
| 3052 | 21217402172.59257 |
| 3061 | 21217406407.25473 |
| 3048 | 21217404433.38023 |
| 3049 | 5437041302.96633 |

Ongoing Validation Measurements at DAF

■ WGPu

- Berp ball with different moderators
- Measurements are done, simulations are in progress

■ HEU

- Rocky Flats shells with different moderators and interrogating sources (SF, (a,n))
- Measurements are done, simulations are in progress

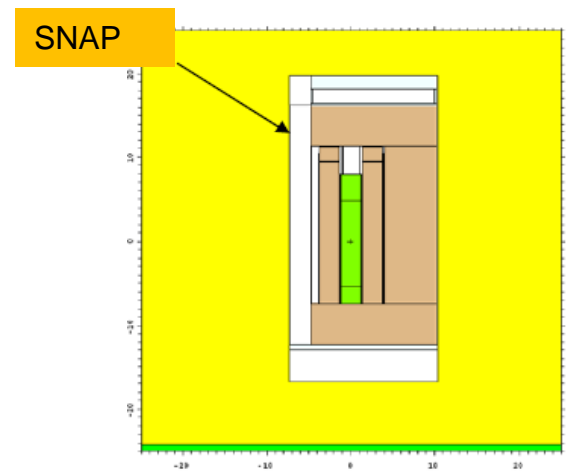
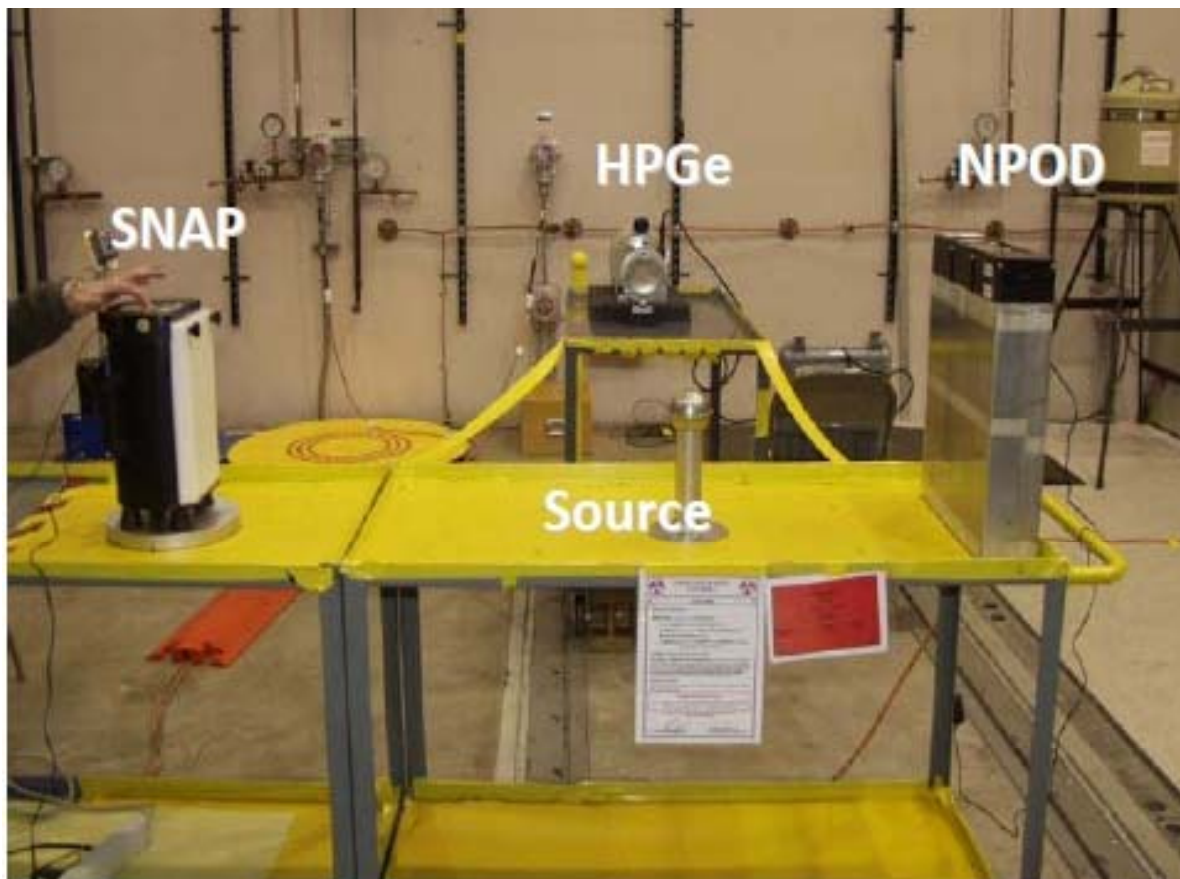
■ SF and (a,n) Sources:

- Multiple moderators

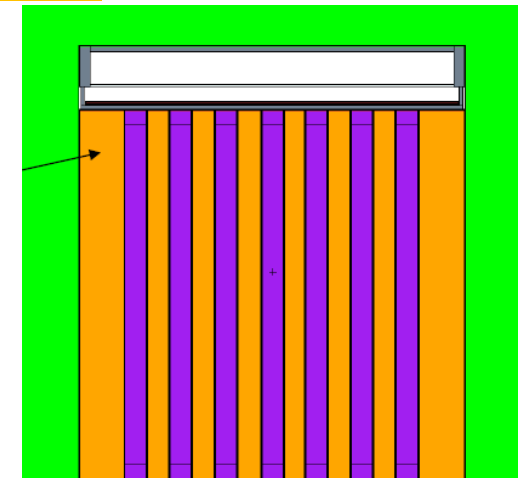
■ Active Sources

- D-T generator source
- WGPu, HEU
- Measurements are done, simulations are in progress

1st “Benchmark” Comparison: SNL - SINBAD

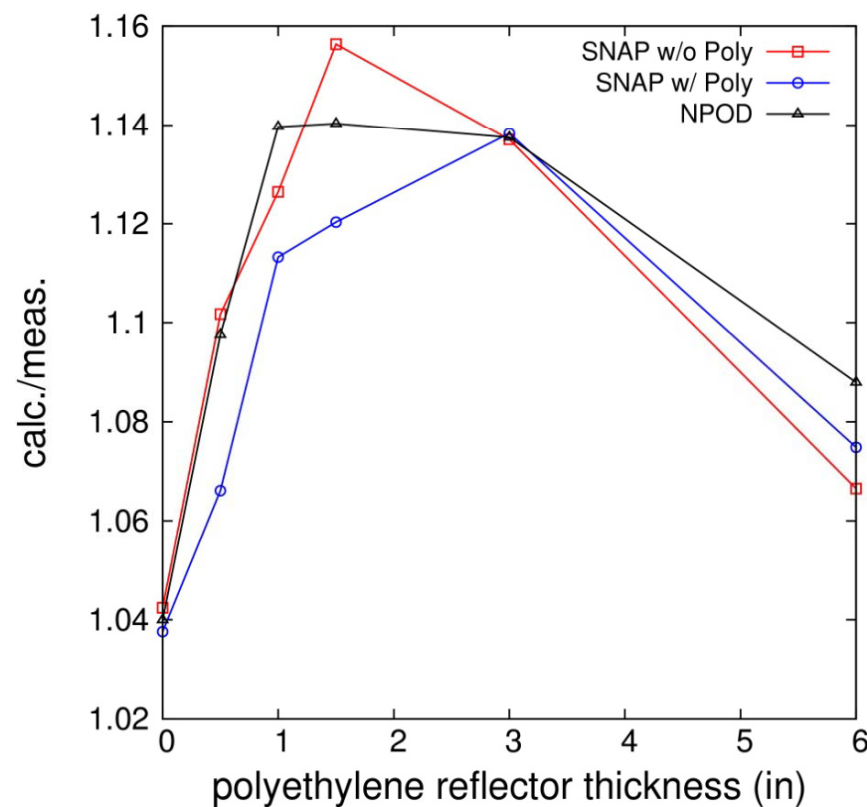
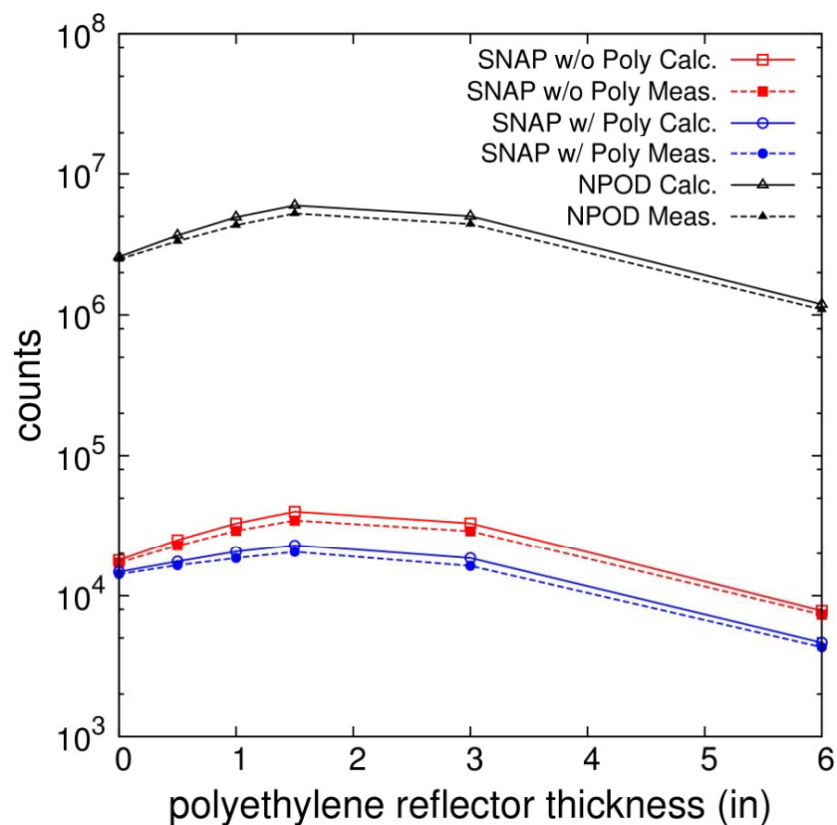


NPOD-3



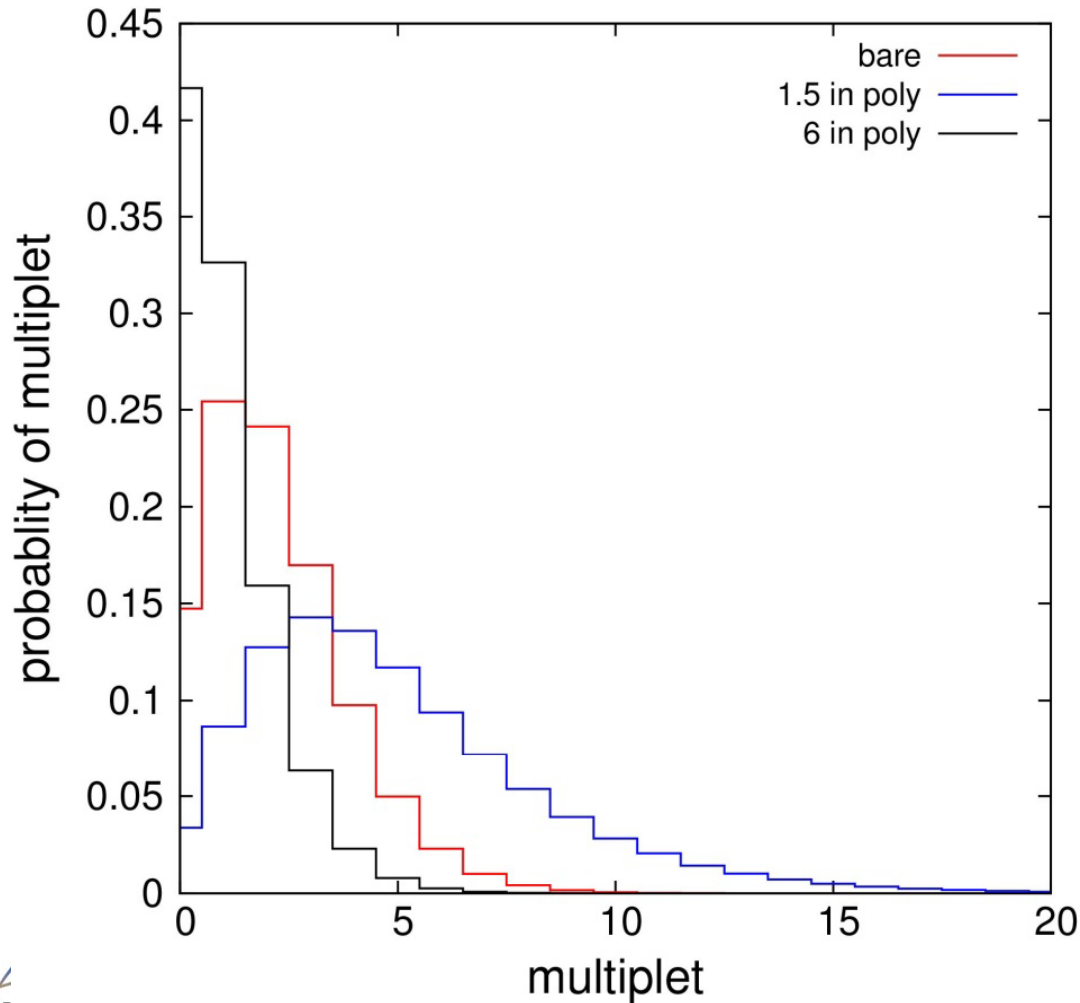
• J. Mattingly, “Polyethylene-Reflected Pu metal Sphere,” SAND2009-5804

SNAP Detector Results: Berp ball



SNAP detector count rates compare well with Berp ball (bare and polyethylene reflected)

NPOD Multiplicity Distributions: Simulated List Mode Data



- **Bare**
 - M1 = 2.1527
 - M2 = 7.3891
- **1.5" Polyethylene**
 - M1 = 4.9551
 - M2 = 36.2336
- **6" Polyethylene**
 - M1 = 0.9905
 - M2 = 2.2611

Status and Future of NCSP Work

■ FY11 proposed work:

- Continue comparison of MCNP simulations' list-mode output to relevant sub-critical benchmark experiments for code validation
- Simultaneously we wish to perform neutron leakage and neutron spectra measurements for additional points of comparison for our MCNP list-mode simulations.
 - Comparison of non-integral results for same neutron sources/scattering environments will give further confidence in the MCNP simulation results
 - Additional measurements will allow us to characterize room return as well as determine neutron detector efficiency.

Analysis Software for Active and Passive Subcritical Neutron Measurements

S. Melton, G. Arnone, J. Hutchinson, W. Myers, A. Sood

Los Alamos National Laboratory, MS-B228, Los Alamos, New Mexico 87545

INTRODUCTION

Statistical fluctuations in the neutron population in zero-power systems can be attributed largely to the variation in the number of neutrons produced per fission. In reactor theory, calculations of large neutron populations use a value that has been averaged over the neutron multiplicity distribution. Fluctuations in the time between nuclear reactions (absorption, fission, and scattering) and in the probability for these reactions lead to variations in the lengths of neutron chains. This in turn introduces fluctuations in the number of counts above the Poisson fluctuations that usually occur from random sources and the detection process.¹

The underlying statistical theory of chain neutron populations was developed by Feynman, de Hoffman, and Serber in experiments performed in 1944 using the variance-to-mean technique.² By 1946, Feynman had developed the theory for the Rossi-alpha technique which was later used to measure decay constants of fast metal assemblies at Los Alamos, Argonne, and Oak Ridge^{3,4} Due to their origins and subsequent applications, the Rossi-alpha and Feynman techniques are still closely associated with reactor noise analysis, but they have also proved useful in coincidence measurements in subcritical systems. Both of these techniques, which originally operated on passive data have been extended to include data from active interrogation and implemented in analysis routines using list mode data generated by the PATRM_PMC (Pulse Arrival-Time Recording Module/(PCI Mezzanine Card).

DESCRIPTION OF WORK

List mode acquisition is accomplished by routing up to 32 independent detector signals into the PATRM_PMC. The primary task of the PATRM_PMC is to generate a data array that contains the time tag and detector ID for every detector pulse, thus recording the arrival time of all neutron detections signals in a sequential list format. During an active interrogation, a VETO pulse is used to synchronize data acquisition with the pulsing source. Neutron arrival times are recorded sequentially with respect to the start of each burst. For a passive assay, the PATRM_PMC records neutron arrival times between the receipt of an external start and stop

pulse resulting in a list of increasing clock ticks up to $(2^{32}-1)$ before rollover occurs.

The LIST_LIB software is comprised of a series of functions designed for reading and analyzing binary data from list mode electronics with the latest version being the PATRM_PMC module. The functions operate on both active and passive data lists and can be divided conceptually into four categories:

- File I/O Functions
- Filtering Functions
- Sorting Functions
- Analyzing Functions

Due to the large size of list mode files, raw data from the PATRM_PMC is stored in binary format with relevant measurement information such as count times, time of measurement, number of VETOs, etc. stored in the form of a header which precedes the actual data list. Since multi-scale or Rossi-alpha spectra can be generated from the list data, the routines also include read and write functions for ASCII files. Input functions for the list mode files read the data into an integer array that can be called by either filtering or sorting functions. Filtering functions remove unwanted events from the data list such as generator/accelerator noise or cosmic-ray events. Other simple filtering functions count the number of VETOs (active) or rollovers (passive). Regardless of the particular filter used, these functions return a modified list stored in an integer array.

Sorting functions operate on the modified list, such as multiple data lists merged into one, or create neutron timing distributions such as the Feynman or Rossi-Alpha. These distributions can be generated on either active or passive lists. Multi-scale spectra can also be generated. These timing distributions are in turn called by the analyzing functions to calculate various parameters such as moments, dieaway times, multiplicity distributions, correlation ratios, and Hanson-Dowdy parameters such as cbar, cbar2 and YY. In addition to the raw binary data read from the PATRM_PMC, the analysis programs also read ASCII input files that allow the user to set analysis parameters such as co-window, maximum multiplicity, maximum event time, bin width, etc. If not set by the user, default values listed in the comment section of the input files are used.

The LIST_LIB software has been developed for a range of applications from large fixed facility systems to the most recent small portable neutron generator based system. The techniques have been used on ²³⁹Pu, ²³⁵U,

^{238}U , ^{237}Np from milligram to multi-kilograms quantities with measurement configurations ranging from bare SNM to SNM surrounded by large amounts of moderators and/or absorbers. The most recent application is the analysis of subcritical benchmark experiments.

RESULTS

In many cases, neutronic information about material surrounding a fissile source is needed in order to determine basic critical parameters. Both material type and configuration may be unknown and therefore “matrix corrections” must be applied. For these applications, the source is externally pulsed from varying distances from the system under study. As an example of this application, Fig. 1 shows the Feynman time distribution for an active interrogation of a bare 228 mg ^{239}Pu foil in a closed cavity system using a neutron generator as the pulsing source with 10% efficient neutron detectors.

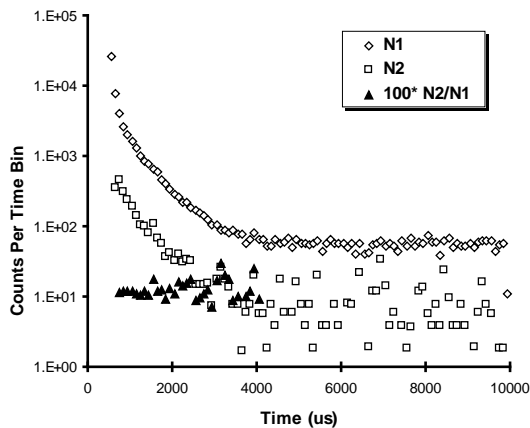


Fig. 1. Feynman time distributions for singles (N1) and correlated neutrons (N2) for a bare 228 mg ^{239}Pu metal foil located in the center of a 55-gallon metal drum.

Both time distributions, singles (N1) and correlated neutrons (N2) show exponential dependence during the thermal time window with dieaway times corresponding to that of the thermal interrogating flux. Prior to 800 μs , the cadmium-shielded detectors are still responding to the epithermal flux from the neutron generator burst. Correlations measured after about 4,000 μs are due to spontaneous fission, cosmic ray bursts, or random coincidences. The active correlated ratio is the ratio of correlated neutrons, which is essentially double coincidence for a 10% efficient detector, to single neutrons and thus depends linearly on the detection efficiency of the system. In the active mode, this ratio has meaning only during the thermal interrogation time region. A linear relationship is observed between the correlated ratio and transmission. Thus the active

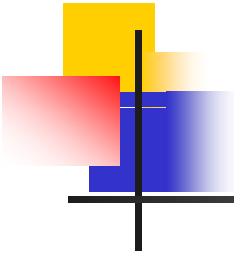
correlated ratio can be used to predict transmission in unknown matrices surrounding SNM.

FUTURE WORK

The basic techniques discussed here been adapted for a wide range of applications. Future work includes adapting these techniques to enable other subcritical analytical techniques such as source jerk. In addition, a user manual describing both the physics and the software operation will be generated in the coming months.

REFERENCES

1. M.M.R. Williams, *Random Processes in Nuclear Reactors*, (Pergamon Press Inc., New York, 1974), pp. 15-22.
2. R.P. Feynman, F. D. Hoffman, and R. Serber, “Dispersion of the Neutron Emission in ^{235}U Fission,” *Journal of Nuclear Energy*, Volume 3, pp. 64-69 (1956).
3. J. D. Orndoff, “Prompt Neutron Periods of Metal Critical Assemblies,” *Nuclear Science and Engineering*, Volume 2, No. 4, pp. 450-460 (1957).
4. G.S. Brunson, R. N. Curran, et.al., “Measuring the Prompt Period of a Reactor”, *Nucleonics*, Volume 15, No. 11, pp. 132-141 (1957).



Analysis Software for Active and Passive Subcritical Neutron Measurements

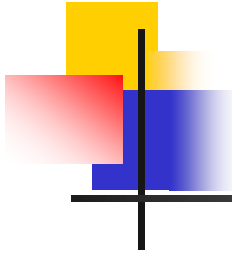
S. Melton, G. Arnone, J. Hutchinson, W. Myers, A. Sood
Los Alamos National Laboratory
N-2 (Advanced Nuclear Technology) and
XCP-7 (Transport Applications)

Nuclear Criticality Safety Program (NCSP) Technical
Seminar

March 1-2, 2011

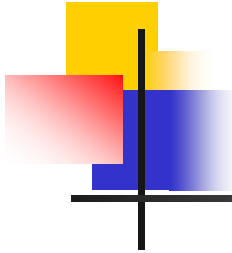
Oak Ridge National Laboratory





List Mode Analysis Software

- Library of functions designed to read and analyze binary data from list mode modules.
- Functions can be used in either active or passive mode and are divided into 4 categories:
 - File I/O Functions
 - Filtering Functions
 - Sorting Functions
 - Analyzing Functions

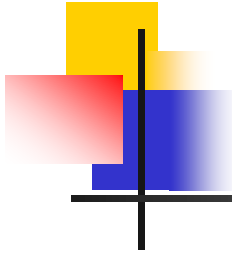


List Mode Analysis Functions

File I/O Functions:

Read and write binary and ASCII files generated as a result of either active or passive measurements using PATRM-PMC.

- Reads/writes legacy data files
 - CAMAC-PATRM
 - PATRM-PCI
 - GuideTech Card
- Reads/writes PATRM-PMC

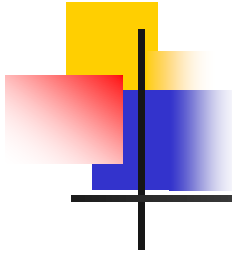


List Mode Analysis Functions

Filtering Functions:

Remove unwanted events from data list and return modified list stored in integer array.

- Zetatron Noise
- Cosmic-Ray Events
- Vetos (Active)
- Rollovers (Passive)

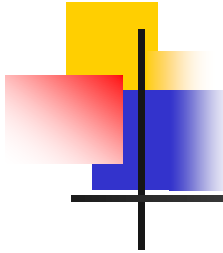


List Mode Analysis Functions

Sorting Functions:

May either return a modified list or create timing distributions (Passive and Active)

- Merge multiple data lists
- Feynman distributions
- Rossi-Alpha
- Multi-scale spectra

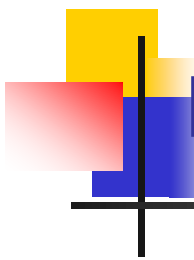


List Mode Analysis Functions

Analyzing Functions:

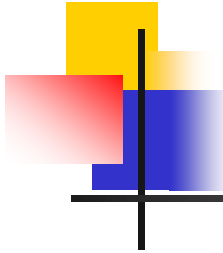
Timing distributions can be called to calculate parameters (Active and Passive)

- Multiplicity distributions
- Distribution moments
- Dieaway times – Cavity and Detector
- Correlation factors
- Hanson-Dowdy parameters
- Correlated ratios



Range of Application for List Mode Analysis

- Active or Passive Measurement
- Interrogating Sources: Accelerator or Neutron Generator
- Neutron Detector Efficiency ranging from 1 to 40%
- Closed cavity or open air geometry
- Large Fixed Facility or Small Portable Systems
- ^{239}Pu , ^{235}U , ^{238}U , ^{237}Np from mg to multi-kg quantities
- Measurement configurations ranging from bare SNM to SNM surrounded by large amounts of moderators and/or absorbers
- Analysis of subcritical benchmark experiments

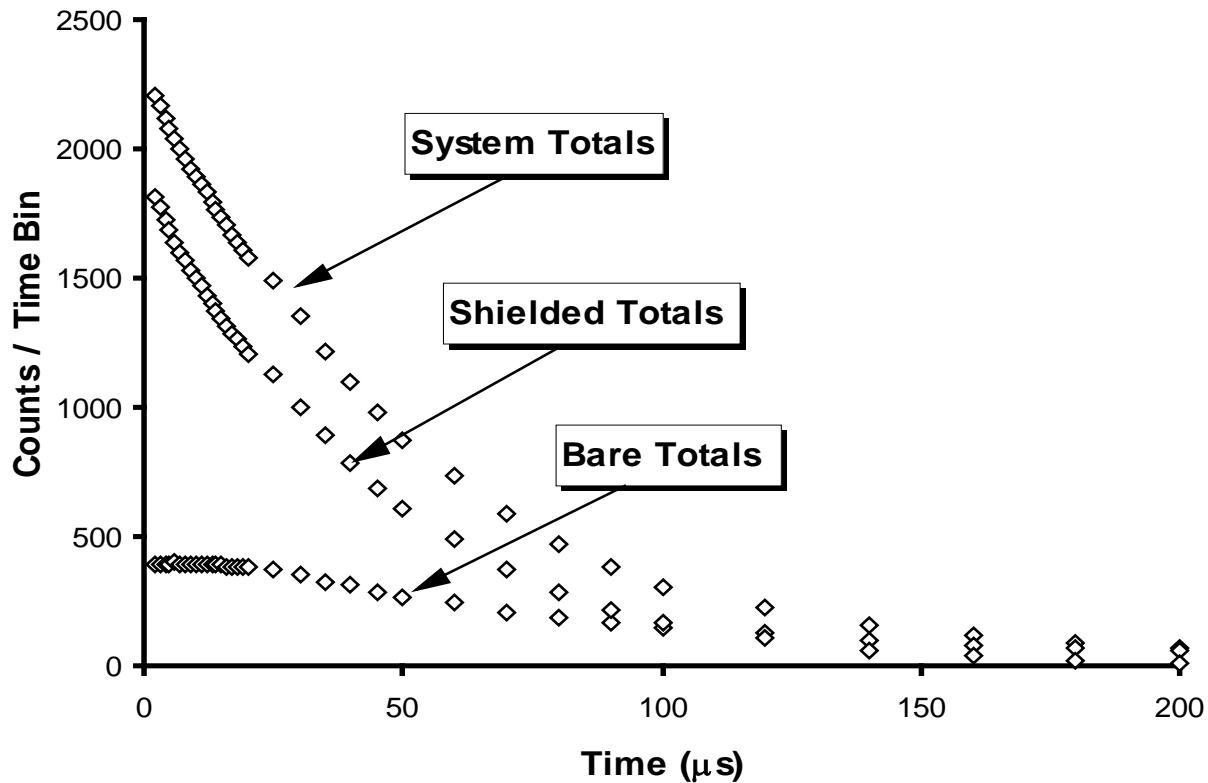


Rossi Alpha Distribution

- Calculates a Rossi Alpha distribution for a total time span of 1000 microseconds with individual time intervals set by the user.
- Time difference between each event and successive events within the 1000 microsecond time span was calculated and appropriate time bins incremented.

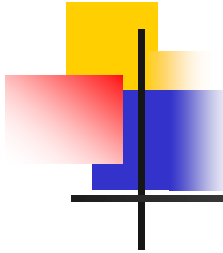
Rossi-Alpha Distribution – Passive

100 g Pu metal cylinder



Calculation of Detector Dieaway - Rossi-Alpha

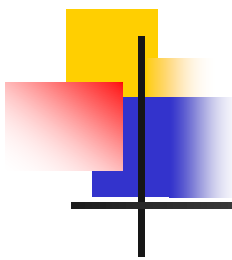
- List Mode data generated in the passive mode using a 100 g Pu metal source
- Dips in the smooth exponential in the first few microseconds are due to dead time losses
- Detector dieaway time is extracted from the fit of data to a single exponential plus a constant from the time span from 20 to 200 microseconds



Detector Dieaway Comparison

Comparison of measured and MCNP-calculated detector dieaway times for a 100-g plutonium metal source centered in empty drum

| Detector Package | Detector Dieaway Time (μs) | | Difference ($\Delta / \sigma_{\text{measured}}$) |
|------------------|---|---------------------------------|---|
| | Measured $\pm \sigma_{\text{measured}}$ | MCNP $\pm \sigma_{\text{MCNP}}$ | |
| Shielded Totals | 40.55 \pm 0.90 | 40.76 \pm 0.25 | -0.23 |
| Bare Totals | 83.18 \pm 2.01 | 81.60 \pm 1.81 | +0.79 |
| System Totals | 47.60 \pm 0.93 | 47.84 \pm 0.88 | -0.26 |

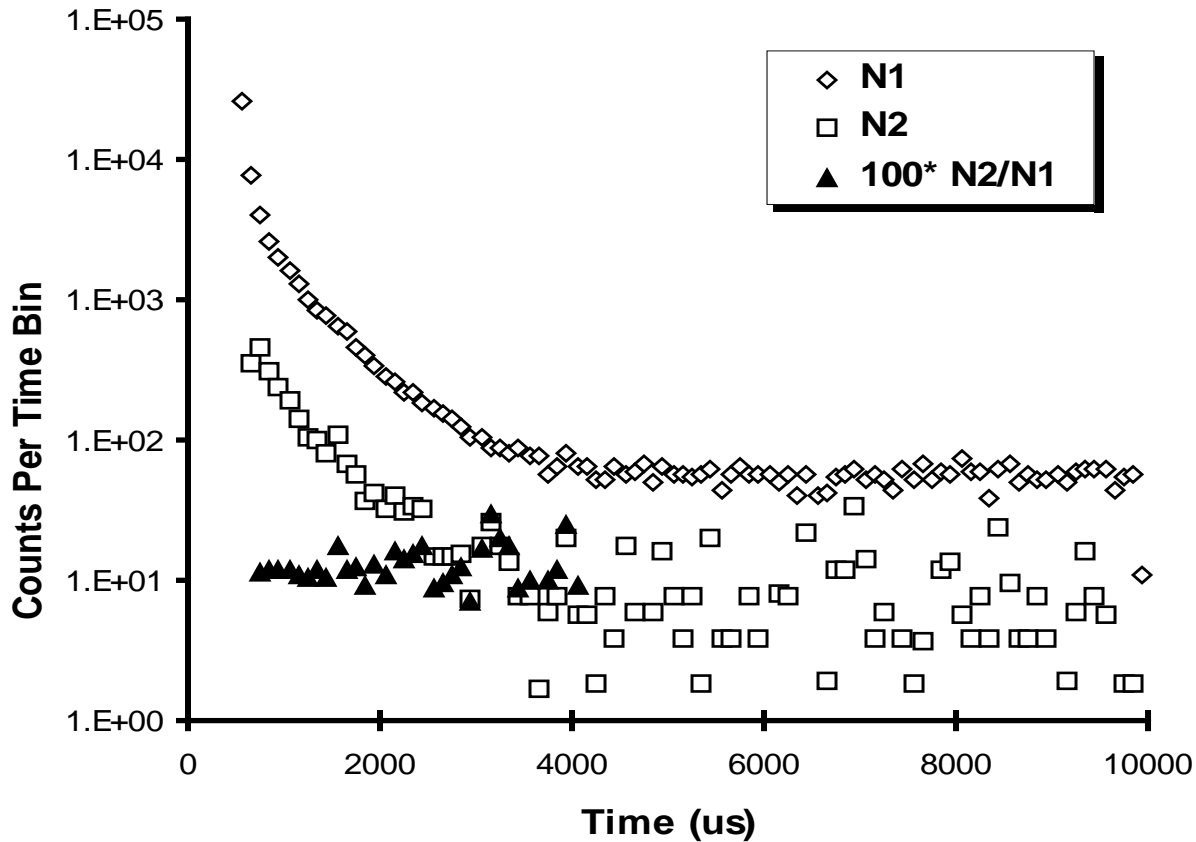


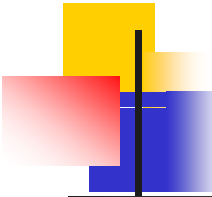
Feynman Histograms – Moments and Variance to Mean Parameters

- Formed by counting the number of times 0, 1, 2, up to 99 events (user selectable) events are observed in consecutive observation windows.
- In active mode, time is referenced from each source pulse (veto markers) so that distributions can be summed over number of pulses.
- First, second, and third moments and the Hage Cifarelli and Hanson Dowdy parameters are calculated from these histograms.

Feynman Time Distribution - Active

228 mg Pu foil





Feynman Variance-To-Mean Technique

From the Feynman distribution, both the first moment about zero (mean) and the second moment about the mean can be calculated

$$\bar{C} = \sum_{i=1}^m i \cdot P_i,$$

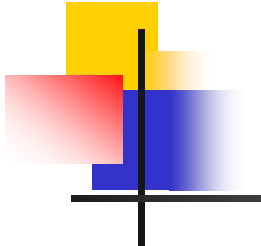
$$\overline{C^2} = \sum_{i=1}^m i^2 \cdot P_i, \quad \text{and}$$

$$\overline{(C - \bar{C})^2} = \overline{C^2} - \bar{C}^2,$$

\bar{C} = first moment about zero,

$\overline{C^2}$ = second moment about zero, and

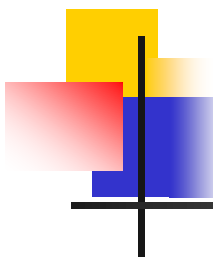
$\overline{(C - \bar{C})^2}$ = second moment about the mean; Variance.



Feynman Variance-To-Mean Technique

- For a purely random source such as an (α, n) source, the probability distribution is Poisson and the variance is equal to the mean.
- For a fission source such as ^{240}Pu , where neutrons are correlated as to location and time due to the fission process, the ratio of the variance to mean is greater than unity. Feynman symbolized this excess variance caused by neutron chain fluctuations as Y given by

$$\frac{\overline{C^2} - \overline{C}^2}{\overline{C}} = 1 + Y$$



Variance-To-Mean Parameters- Active Rocky Flats Shells ~1.5kg 93.1% HEU

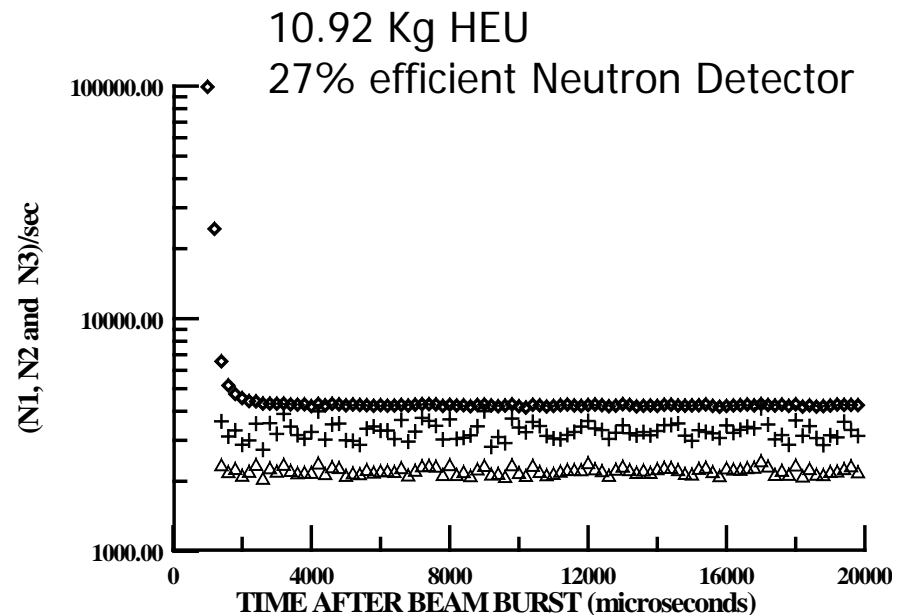
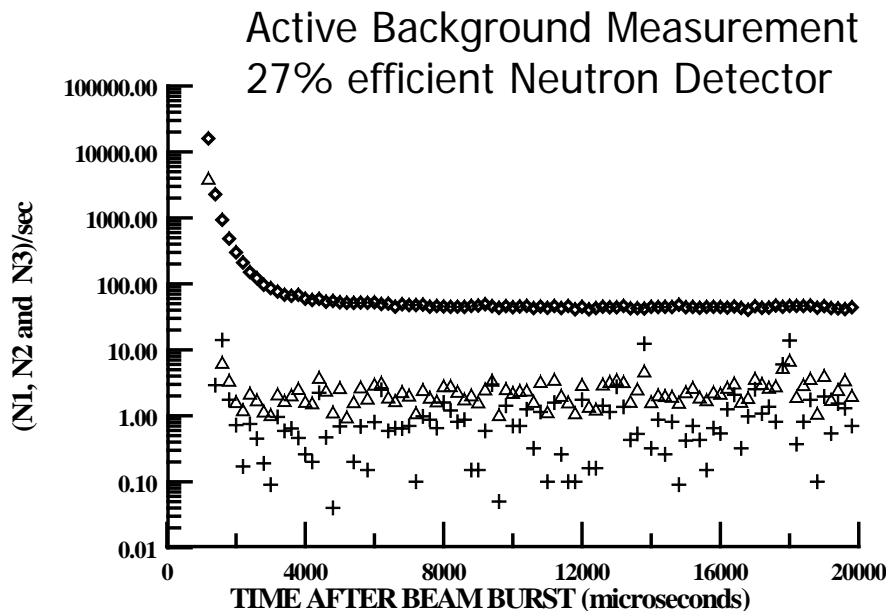
Hage Cifarelli Feynman Variance-To-Mean

| | Mean | Std Deviation | % Error |
|-----------------|---------|---------------|---------|
| Singles Rate | 177.664 | 0.702 | 0.395 |
| Doubles Rate | 5.866 | 0.182 | 3.106 |
| Triples Rate | 0.505 | 0.057 | 11.273 |
| Doubles/Singles | 0.033 | 0.001 | 3.019 |
| Triples/Singles | 0.003 | 0.000 | 11.342 |
| Triples/Doubles | 0.084 | 0.008 | 9.606 |

Hansen Dowdy Feynman Variance-To-Mean

| | Mean | Std Deviation | % Error |
|-------|-------|---------------|---------|
| Cbar | 0.044 | 0.000 | 0.395 |
| Cbar2 | 0.049 | 0.000 | .0572 |
| YY | 0.066 | 0.002 | 3.019 |

Pulsed Neutron HEU Measurements

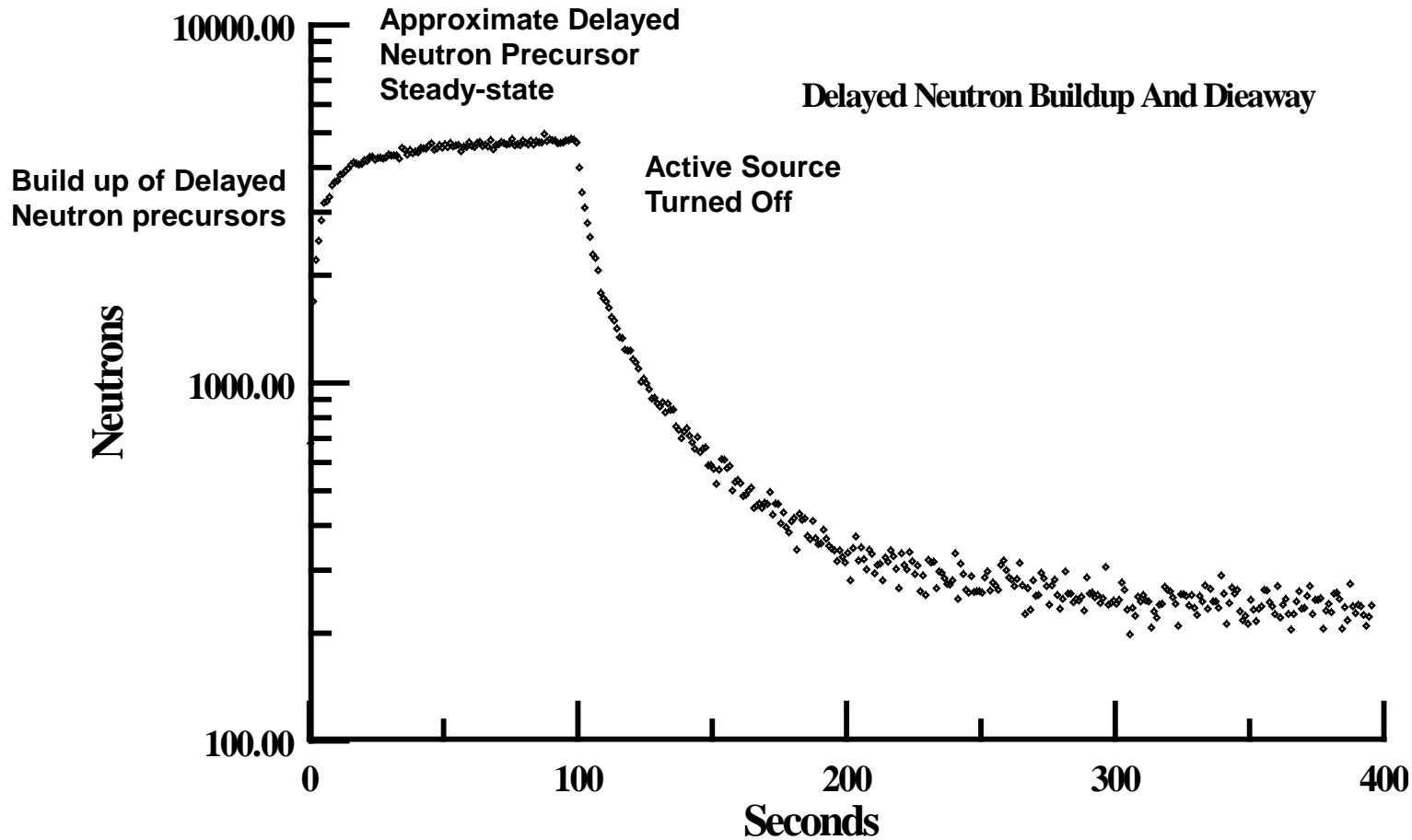


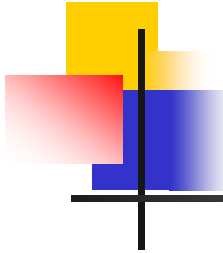
Diamonds-singles rate Triangles-second moment Crosses-third moment

Time Dependence of Neutron Response

14 MeV Neutron Interrogation

91% ^{235}U Oxide Sample





Future Work

- Create software for enabling other subcritical analytical techniques such as source jerk
- Generate a user manual for data analysis techniques and software operation